Targeted Application of Biochar in the Palouse: Modeling Hydrologic Processes in Undulating Topographies

A Thesis
Presented in Partial Fulfillment of the Requirements for the
Degree of Master of Science
with a
Major in Chemical and Biological Engineering
in the
College of Graduate Studies
University of Idaho
by
Adam O'Keeffe

Major Professor: Dev Shrestha, Ph.D., P.E.
Committee Members: Erin Brooks, Ph.D.; Armando McDonald, Ph.D.
Department Administrator: Dev Shrestha, Ph.D., P.E.

August 2021

Authorization to Submit Thesis

This thesis of Adam O'Keeffe submitted for the degree of Master of Science with a Major in Chemical and Biological Engineering and titled "Targeted Application of Biochar in the Palouse: Modeling Hydrologic Processes in Undulating Topographies" has been reviewed in final form. Permission, as indicated by the signatures and dates below, is now granted to submit final copies to the College of Graduate Studies for approval.

Major Professor: _____ Date: _____
Dev Shrestha, Ph.D., P.E.

Committee Members: _____ Date: _____
Erin Brooks, Ph.D.

_____ Date: _____
Armando McDonald, Ph.D.

Department Administrator: _____ Date: _____
Dev Shrestha, Ph.D., P.E..

Abstract

The use of biochar as a soil amendment has gained a great interest among academics, researchers, and private industry over the recent years. Biochar is a carbon-rich substance that is made from thermochemical conversion of biomass. It is rich in carbon and nitrogen, two components of soil organic matter, that when introduced into the soil has shown to be beneficial to soil fertility, water retention, and crop yields. Currently, biochar is cost-prohibitive for indiscrete applications in large fields. This thesis hypothesizes integrating biochar into precision agriculture technologies by applying biochar in a targeted manner to increase soil health, water retention, and crop yield. A combination of laboratory experimentation and hydrologic modeling was employed to determine biochar's potential for integration into precision agriculture. A finite element analysis model was developed and implemented in MATLAB to simulate how moisture is redistributed in an undulating topography. Two types of biochar were amended to a standard Palouse silt loam soil at two different concentrations to measure how biochar affects the matric potential, hydraulic conductivity, and diffusivity of a silt loam soil. The developed model utilizes the measured soil hydraulic properties to simulate the effects of biochar on water redistribution. This model is driven by evaporation off the simulated soil profile. A novel equation for modeling evaporation/evapotranspiration was developed analogous to convective heat transfer theory, which is utilized in the model. This work then proceeded to validate the model output by comparing simulated and measured soil moisture data. The developed model yielded positive results. Amending Palouse silt loam soil with biochar showed increased retention across both amendment types and concentrations. The simulation showed that more moisture was retained in and around the amendment area. This is likely due to biochar increasing the soil's water retention in wet conditions and an apparent reduction in hydraulic conductivity in saturated conditions. Finally, this work culminated in the exploration of biochar amendment on the greater hydrologic processes in the region. In the Palouse, argillic and fragipan horizons form restrictive layers in the soil profile that drive subsurface hydrology. A soil moisture routing (SMR) model, based on water balance principles, was developed to explore biochar amendment in a more complex soil profile. This model showed biochar was able to increase the ET from the profile while reducing runoff. The results from this work are promising for integrating biochar into precision agriculture and promote the need for further refinement and model development.

Acknowledgments

I would like to first and foremost thank my advisor, Dr. Dev Shrestha, for his continued support and commitment to this project. His responsibilities are many, but he was always available when needed and provided guidance and support when I needed it. In particular, he was able to provide me with the right balance of support when required, and the freedom to make mistakes, fail, and figure things out by myself. This balance taught me valuable lessons on how to conduct research and trust myself. When I needed support, he gave me his full attention and enthusiasm towards the project, for which I am grateful. I also would like to thank Chad Dunkel, the research support scientist at James Martin Lab (JML). He was a constant presence throughout this work. His advice, guidance, enthusiasm, and support throughout this entire process was immense. This work would not resemble what it is without him.

I received two and a half years of support and funding through the Department of Energy's Industrial Assessment Grant and the USDA National Institute of Food and Agriculture, Hatch project 1009342. I worked closely with students in the Industrial Assessment Center (IAC) to provide energy auditing services to manufacturing companies throughout the region. This is an apprenticeship program through the Department of Energy (DOE) that trains undergraduate and graduate students to have an energy efficiency mindset and to be energy engineers. My time spent in this program has been of great value. From the people I have met to the lessons learned, my involvement in the IAC was memorable.

Dedication

This work is dedicated to all the people who have helped me and supported me in my academic career over the years. I could not have made it here without your support in my life. I specifically would like to thank my parents, grandparents, and brothers – I would not be who I am today without you.

Table of Contents

Authorization to Submit Thesis ii

Abstract iii

Acknowledgments iv

Dedication v

Table of Contents vi

List of Tables x

List of Figures xi

Chapter 1: Introduction and Background 1

The Palouse Region 1

Precision agriculture and the Palouse 5

Biochar & its use in the soil 6

Biochar's effects on soil hydraulic properties 8

Need for development of new model 9

Study Objectives 9

Literature Cited 11

Chapter 2: Modeling moisture redistribution from the selective non-uniform application of biochar on Palouse Hills 17

Abstract 17

Introduction 17

Study Site 19

Objectives of this study 19

Materials and Methods 20

Theory: Vadose Zone Transport Model 20

Darcy's Law 21

Boundary Conditions 22

Finite element analysis with MATLAB PDE solver 23

Sample composition and preparation 25
Experimental setup for determining soil hydraulic properties 26
Initial conditions and model setup 29
Results and Discussion 29
Biochar's effects on silt loam soil hydraulic properties 29
Model output 33
Conclusion 37
Literature Cited 38
Chapter 3: Validation of MATLAB soil moisture redistribution model with laboratory experimentation 44
Abstract 44
Introduction 44
Methods 45
Calibration Theory 45
Experimental Setup 46
Statistical Testing 48
Results and Discussion 49
Statistical analysis 51
Model Limitations and concerns 53
Conclusion 53
Literature Cited 55
Chapter 4: Soil Moisture Routing (SMR) Modeling of Targeted Biochar Amendment in Undulating Topographies: An Analysis of Biochar's Effects on Streamflow 56
Abstract 56
Introduction 56
Objectives of the study 57
Site Description 58

Model development 58
Materials and Methods 62
Sample Measurement 62
Initial Conditions 63
Model Calibration: Statistical testing and sensitivity analysis 64
Results 66
Model Calibration and Sensitivity analysis 66
Targeted Biochar amendment 68
Discussion 71
Limitations to the model 73
Conclusion 73
Literature Cited 75
Chapter 5: Conclusion 78
Site-Specific water management 78
The case for biochar 78
Literature Cited 81
Chapter 6: Future Work 82
Next step for the overall research 82
Chapter 2: Model future work 83
Chapter 3: Refining the current evaporation equation 83
Chapter 4: 5 cell SMR model Future Work 87
Literature Cited 88
Appendix A - Research Pathway 89
Brief overview of the theory of water movement, retention, and key soil hydraulic properties 89
Model development: Theory and parameter requirements 91
Diffusivity Experiment 1: The box setup 93
Diffusivity Experiment 2: 1-dimensional soil column 98

Hydraulic Conductivity Experiment 1: Constant head permeability 100

Hydraulic Conductivity Experiment 2: Falling head method 101

Chosen Approach – HYPROP from METER Group 101

Lessons learned from the HYPROP 101

Literature Cited 103

List of Tables

Table 1: Proximal analysis and surface area analysis (BET) of biochar samples 25
Table 2: Key soil properties for each of the samples. This table displays the bulk density (BD), pH, Electric conductivity, Organic matter (OM), and Cation Exchange Capacity (CEC) of the soil samples. Porosity was estimated by the HYPROP and displayed the average and standard deviation of the four replicates 26
Table 3: Bulk density (BD in g/cm^3) obtained from the HYPROP for each of the samples. The values shown in the table are the averaged values from each of the runs with standard deviation 30
Table 4: Compiled VG parameters obtained from HYPROP and WP4C measurements. The values displayed are the averages across the four replicates with standard deviation displayed. This table also includes biochar's effects on the field capacity (FC) and permanent wilting point (PWP) estimated from the HYPROP 31
Table 5: Statistical analysis from the simulated SM data with the measured SM data from sensor 7 (top sensor) 52
Table 6: Statistical analysis from the simulated SM data with the measured SM data from sensor 6 (middle sensor) 52
Table 7: Statistical analysis from the simulated SM data with the measured SM data from sensor 5 (bottom sensor) 52
Table 8: Physical properties of each of the samples measured by the HYPROP and WP4C devices. Values reported in this table are averaged between the four replicates and displayed with the standard deviation. It is important to note that the field capacity (FC) is displayed at two different tensions, and similarly, the Plant available water (PAW) is also shown. PAW_{low} is the PAW over the FC_{-33kPa} to PWP while the PAW_{high} is for the range of FC_{-6kPa} to PWP. While PAW_{low} is more traditionally used PAW_{high} is important. Van Genuchten parameters are displayed in the bottom portion of the table. Lateral K_{sat} is scaled as the % change that was observed in the vertical K_{sat}. 63
Table 9: Summary of streamflow statistics for the water years of 2013 to 2019. Simulated Restricted and non-restrictive soil profiles vs. measured streamflow from Palouse River. 67
Table 10: Sensitivity equations for each influential model parameter. Displayed are the linear equations for each parameter 67
Table 11: Potential bu/acre increase from amendment area from restricted and non-restricted soils at 6 kPa FC 72
Table 12: Regression coefficients obtained from two iterations of regression analysis 85

List of Figures

Figure 1: Classification of % erosion depending on hill direction and location on the hill for a typical hillslope in the Palouse region (USDA et al., 1979) 2
Figure 2: Yield map showing the variation in yield with topographical variation. 4
Figure 3: Cross-section of a typical Palouse hill. Adapted from (Kaiser, 1967) 4
Figure 4: Model of the Palouse hill as a sinusoidal curve. The top surface has Neumann boundary condition; no moisture movement is assumed in the lateral direction. 21
Figure 5: Finite Element mesh of the hillslope. The biochar application area covers 5% of the hillslope and is displayed in black. The units are in meters. 24
Figure 6: Matric potential, hydraulic conductivity, and diffusivity curves for all samples. The matric potentials (blue axes) are displayed in positive values but are inherently negative values. a) denotes the matric potential and hydraulic conductivity (in log scale) vs. moisture content. b) displays the matric potential and hydraulic conductivity (in normal scale) vs. moisture content. c) shows the diffusivity vs. moisture content. a) and b) are included to highlight hydraulic conductivity changes in both dry and wet conditions. The generated curves are the averages of the four sample replicates. 32
Figure 7: Simulated moisture difference plots at the end of the simulated growing season. All amendment samples are shown, which display areas of increased and decreased moisture. The black contour line indicates the zero-contour line, which displays no change in moisture between the Control and the biochar amendment 34
Figure 8: Moisture difference plot (BC amendment vs. Control) for one node throughout the duration of the simulation 36
Figure 9: Soil column schematic 47
Figure 10: Measured SM, temperature, and RH obtained from the laboratory experiment 50
Figure 11: Measured moisture content (averaged between the three sensors) vs. Simulated moisture content 51
Figure 12: Conceptual model depicting the hydrologic fluxes, taken from (Frankenberger et al., 1999) 61
Figure 13: Streamflow hydrographs for the years 2013 to 2019 (cm/day) 66
Figure 14: % change from control with biochar amendment, non-restricted soil profile and FC set to 33 kPa. 68
Figure 15: % change from control with biochar amendment, non-restricted soil profile, and FC set to 6 kPa. 69
Figure 16: % change from control with biochar amendment, restricted soil profile, and FC set to 33 kPa. 70

Figure 17: % change from control with biochar amendment, restricted soil profile, and FC set to 6 kPa 70
Figure 18: Regression analysis for both the higher and lower order regression equations. One-to-one plots for each respective equation are plotted against the Penman-Monteith model..... 86
Figure 19: Early-stage design for the experimental setup. This drawing, while rudimental, provides a good visualization for the methods and potential sensor placement throughout the soil profile..... 94
Figure 20: Layout of the Diffusivity box and sensor placement evenly distributed throughout the box, a) Side view. b) Rear view. c) Top View. d) Angled view. The blue circle indicates the point where water was introduced into the soil profile, and green circles indicate the presence of a soil moisture sensor..... 95
Figure 21: Constructed experimental setup. Box filled with soil and sensors dispersed throughout the box according to figure 19. Water reservoir filled and float sensor inserted at depth for minimal constant head pressure. Saturation zone on right picture is isolated to the level of the water pipe and below indicating that gravity is primarily driving water down into the soil profile..... 96
Figure 22: Completed setup of 1-dimensional soil column experiment. Sensors are inserted and float sensor maintains constant head pressure 99

Chapter 1: Introduction and Background

The Palouse Region

The Palouse is rich fertile farmland that is found in the inland northwest of the United States. Spanning from southeastern Washington to west-central Idaho, the Palouse consists of over 2 million acres of rich agricultural land (Hartmans & Michalson, 2000). It is well known for its' unique topography, consisting of rolling hills throughout the region. Many years ago, high winds of the drier southwest region of Washington blew loess into the Palouse, which settled, forming the rolling hills (Bryan, 1926). The loess deposits have led to the primary soil being classified as silt loam soil (Palouse silt loam). The Palouse follows precipitation patterns similar to the Mediterranean climates with cold, wet winters and warm, dry summers (McCool et al., 2001). Roughly 60% of the annual precipitation accumulates from November through March, while roughly 5% occurs between July and August (Kaiser, 1967). The precipitation pattern brings about wet springs that the crops use to thrive and dry summers, extending throughout the growing season. The Köppen climate classification denotes the Palouse as a humid continental climate with dry, cool summers (PlantMaps, 2021). There are many agronomic zones throughout the inland northwest US; however, the Palouse is categorized as cool/moist (Hagerty et al., 2019).

Further, these areas generally receive sufficient winter precipitation to fill deep (more than 40 inches) soil profiles each year and have a near-optimum growing season for winter crops (Hagerty et al., 2019). There are nine distinct topographies recognized throughout the Palouse and, while distinct, they do have some commonalities between them (Kaiser et al., 1951). The unique undulating topography creates site-specific microclimates of unique patterns of sunlight exposure, snowmelt, and wind (Brooks et al., 2012). These microclimates directly influence crop growth and production in the region. The Palouse is a dryland cropping system, which relies on stored water (provided by the wet spring season) deep into the summer months. The crops grown throughout the region rely heavily on the stored water or additional irrigation for growth. Stored water is key to dryland agriculture and the patterns of stored water (where it is stored in the soil profile) has been linked to the topography (Beven & Kirkby, 1979; Wilson et al., 2005), cropping sequences (Schlegel et al., 2017), and tillage practices (Fuentes et al., 2003; Jin et al., 2007; Kühling et al., 2017). Throughout the year, stored soil water will fluctuate spatially (Eagleson, 1978) due to climatic changes (Brown et al., 2021), vegetation (Eagleson, 1978), topography (Burt & Butcher, 1985), and heterogeneous soil profiles (Sheets & Hendrickx, 1995).

The Palouse has consistently been a productive dryland farming region, supporting significant crop yields of winter wheat, canola, spring wheat, and hay. Palouse soils provide some of the highest dryland white wheat yields worldwide (WWC, 2009). Cultivation of the Palouse land began around 100 years ago and yields valuable and plentiful crops today. However, the Palouse is not devoid of unique problems that agronomists, researchers, and farmers have attempted to mitigate over the last 40 years. Since cultivation of the region began, all of the original topsoil has been lost from 10% of the region, and one-fourth to three-fourths of the original

topsoil has been lost from another 60 percent of the cropland (USDA, 1978). From 1939 to 1977, the average annual erosion rate was 9.2 tons/acre of available cropland (USDA, 1978). A study in Whitman county found an average annual erosion rate over 26 years of 0.7 tons of soil for each bushel of wheat raised, and in some places, the figure was as high as 2.3 tons of topsoil lost per bushel of wheat (Kaiser, 1967). Till erosion, water erosion, and wind erosion were significant forms of erosion that contributed to this high rate (USDA, 1978).

Water erosion is a significant concern in areas where the annual precipitation is greater than 300 mm (McCool et al., 2001). Conventional till methods and the use of the moldboard plow turn over the topsoil, which loosens the soil structure, increasing these soils' susceptibility to erosion from high winds or water (Johnson & Moldenhauer, 1979. Excess water throughout the region runs down the hills and settles into the gullies at the toe slopes. As the water moves downward, it removes soil that has been dislodged due to tilling or wind erosion, causing sedimentation to be deposited in the lower regions. This process continually affects the top two-thirds of the hillslopes throughout the region (USDA, 1978), and erosion will vary based on the region's topography. Figure 1 shows a classification of the different regions of a general hill in the Palouse and the percentage erosion (of the total soil lost to erosion over the entire hillslope) depending on the direction the region is facing and the location on the hillslope.

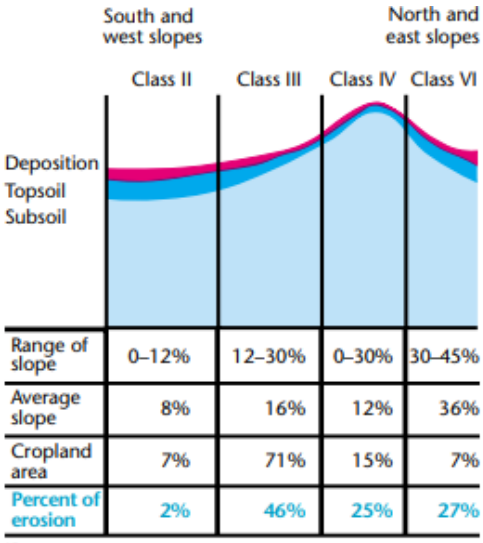

	Class II	Class III	Class IV	Class VI
Range of slope	0–12%	12–30%	0–30%	30–45%
Average slope	8%	16%	12%	36%
Cropland area	7%	71%	15%	7%
Percent of erosion	2%	46%	25%	27%

*Source:
Idaho, Oregon, and Washington Agricultural Experiment Stations and Agricultural Research Service, USDA. Economics of cropping systems and soil conservation in the Palouse. Bulletin No. 2. August 1961.

Figure 1: Classification of % erosion depending on hill direction and location on the hill for a typical hillslope in the Palouse region (USDA et al., 1979)

Classes III, IV, and VI have a significant erosion potential with 46%, 25%, and 27%, respectively. The direction of the hillslope is important, with the erosion potential varying by nearly 20% between south/west facing slopes and north/east-facing slopes, with the south/west slopes contributing more to erosion. The topsoil is deeper in class II categorization and reduces further up the slope. Erosion has contributed to significant variation in topsoil depth throughout the undulating region. From the '70s until the late 2000s, most of the research

pertaining to farming in the area dealt with ways to mitigate or reduce erosion. The outcomes from this research changed the way the region had farmed. Currently, farmers more frequently use no-till or minimum-till practices coupled with direct seeding throughout the region (Yourek, 2016). Switching from conventional till practices to no-till or minimum-till allows for the preservation of the soil structure (Brown et al., 2021). Leaving 30% of the soil surface covered with harvest residue post-harvest has shown to reduce the erosion of the soil by half as compared with bare fallow soil; leaving 50% to 100% of the surface covered throughout the year (no-till practices), reducing soil erosion dramatically (Huggins & Reganold, 2008). Crop rotation between years is also used to restore some of the soil nutrients, soil properties and prevent erosion from wind and water (Langdale et al., 2014). Significant adoption of conservation tillage practices and cover cropping to increase infiltration and decrease soil surface erodibility has led to greatly reduced erosion throughout the region, and stream sediment loads are declining (Brooks et al., 2010; Ebbert & Roe, 1998; Kok et al., 2009; McCool et al., 2001). Despite a significant reduction in erosion rates, the effects of erosion on an ecosystem and farmland can be long-lasting.

Areas with less topsoil, the tops, and steeper hillslopes, have low organic matter, poor water retention, and poor nutrient use/cycling, which has been linked to the shallow topsoil depth (Kaiser, 1967). These soil characteristics can be caused by erosion, directly impacting the crop yields from these areas. Topsoil and soil organic matter loss impairs the soil's water-storage capacity, reduces the soil's natural fertility, and requires increased use of fertilizers to maintain yields (Hartmans & Michalson, 2000). The shallow topsoil cannot retain much of the water that infiltrates during rainfall events, which is then forced further down the slope. Accumulation of water may begin at the bottom of the hillslopes or in the gullies between hills, which may not drain adequately. Waterlogging can occur in these areas, creating poor conditions for crop growth, hindering gas exchange between the roots and the atmosphere, oxygen levels, and ATP synthesis (Tian et al., 2021). The oxygen in waterlogged soils is rapidly exhausted, resulting in the roots changing from aerobic respiration to anaerobic fermentation, which will affect crop growth (Tian et al., 2021). Poor drainage also increases nitrous oxide emissions, a potent greenhouse gas that is 310 times more potent than CO_2 (Hougton et al., 2001). Agricultural soil management contributed 75% of all the anthropogenic nitrous oxide emitted to the atmosphere in 2012, up from 70% in 1990 (EPA, 2014).

Additionally, the complexities of the Palouse region extend to the hydrologic processes that drive water retention and movement in soils. At the top of the hills, argillic and fragipan horizons in north-facing hillslopes lead to perched water tables in the winter months, which drives rapid subsurface lateral flows and accelerates the eluviation of clays in albic Esoil horizons (Brooks et al., 2012; McDaniel et al., 2001, 2008). The impermeable fragipan layers can be relatively shallow in the soil, ~0.65 m, and along with the formation of perched water tables, drive the hydrologic processes of these areas (Brooks et al., 2004). The argillic/fragipan layers reduce the storage capacity of the soil by restricting the soil depth. Topography-based surface and subsurface lateral flow is an influential determinant of water movement and storage in the winter and spring months (Western et al., 2002; Zhu et al., 2010). Work by Brooks et al. 2004 details more information regarding

the argillic and fragipan horizons and is a good source for more information regarding their effects on hydrologic processes in the Palouse (Brooks et al., 2004).

The topographical complexities, erosion factors, and complex surface/subsurface hydrology culminate in significant variation in crop yields throughout the Palouse. Crop yields of winter wheat can vary from 5 bushels/acre to as high as 110 bushels/acre in the same field (Shrestha, 2021). Figure 2 displays a heat map of a typical crop yield in a single field in the Palouse, showing significant variation in crop productivity. Areas highlighted in red are poor yield areas, green is good yield, and yellow is mild yielding areas.

Figure 2: Yield map showing the variation in yield with topographical variation.

The variability within Palouse fields is high. Combined with diverse management legacies, irregular weather patterns create heterogeneous growing conditions (Weddell et al., 2017), contributing to variable crop yields throughout a field. The 1967 Kaiser Whitman county study showed that wheat yield was directly affected by soil erosion, and eroded soil on hilltops and steep slopes produced only 32 percent of the yields of non-eroded soil (Kaiser, 1967). A recent data analysis obtained from a wheat field in the Palouse region confirmed a statistically significant correlation between wheat yield and both slope and elevation. In this study, the winter wheat yield varied in a typical field at a magnitude of over 20-fold. Locations with higher slopes and elevations had a negative impact on wheat yield, confirming findings from the 1967 study (Yang et al., 1998). Figure 3 displays a cross-section of a typical Palouse hill.

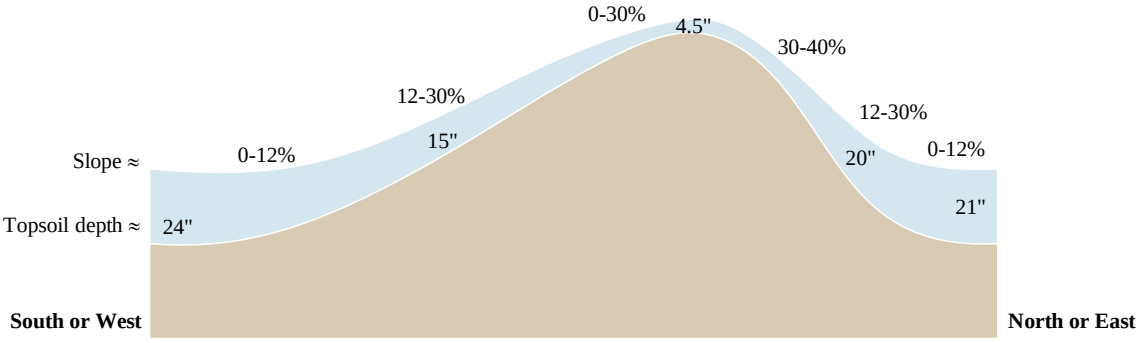

Figure 3: Cross-section of a typical Palouse hill. Adapted from (Kaiser, 1967)

Changes in topography and soil properties will influence water distribution; however, these changes are site-specific (Corwin & Lesch, 2003, 2005). Geostatistical analyses showed that the spatial patterns of variability in wheat yields differed from one field to another and from one region to another within a single field (Yang et al., 1998). The same study showed through regression analysis that the topographic attributes, including elevation, slope, and aspect, had significant effects on wheat yield; which could explain 13 to 35% of the variability in wheat yield for the whole fields, though 49 to 84% of the yield variability could be explained by topography in some regions within the five fields (Yang et al., 1998). Due to the inherent variability associated with Washington dryland crop production, a one-size-fits-all recommendation for management is of little value (Koenig, 2005).

This thesis aims to explore integrating soil restoration practices into precision agriculture methods to reduce soil health and fertility variability, crop yield, and aid in sustainable farming in the Palouse. More specifically, this thesis explores the potential use of biochar as a precision agriculture technique and understanding the effects of targeted application of biochar on eroded soils. It focuses on the complexities of farming in the Palouse and the role that soil water plays in soil fertility. Further, it attempts to provide support for the use of biochar in the Palouse by analyzing how biochar amendment changes soil water redistribution. Using numerical modeling, a new model was developed to be used as a precision agriculture tool for biochar amendment throughout the region and to assess biochar's impact on soil fertility. From laboratory testing, measured soil hydraulic properties are input into the numerical model, which, along with weather data, simulates the change in soil moisture over time under evaporation and redistribution. This work utilizes this developed model to understand the effectiveness of biochar amendment (both in biochar type and amendment concentration) would have on the Palouse's eroded soils. The developed model operates under a new evaporation equation derived from heat transfer theory, and this work presents the equation, assesses its performance, and provides future work for the equation. This work expands further beyond the numerical model with exploration on the greater hydrologic processes in the Palouse by developing a 5-cell soil moisture routing (SMR) model based on Brooks et al. (2007) and Frankeberger et al. (1999). Lastly, future work and the larger direction of this work is presented.

Precision agriculture and the Palouse

The underlying objective of precision agriculture is site-specific management of land by matching the site-specific needs in a field with resource inputs that respond to those needs. Investing in site-specific management technologies makes more sense when significant variation occurs within a field which may require multiple different management strategies. Consequently, the higher the field variability, the higher the potential savings from precision agriculture practices. Some techniques are already utilized and employed throughout the Palouse region. Remote sensing has been used to identify areas of high erosion down to layers of paleosols (Frazier & Cheng, 1989). Sensors can predict the level of water stress plants are under at any point in the growing season (Adamchuk et al., 2004). Proximal sensing and remote sensing have been used to measure physical properties of the soil and the vitality of the crops either on the ground or from aircraft and using satellite imaging (Yourek, 2016). Electromagnetic induction, a proximal sensing technique, can infer various soil properties by measuring

the electroconductivity of the soil (Adamchuk et al., 2004). These methods allow for a more precise understanding of what is occurring at specific sites within a single field or entire farmland. Steps can then be taken to address issues throughout the field that are potentially harmful to soil health and crop yields. As technology continues to develop and advance, other precision agriculture techniques will become more accessible to be used by farmers throughout the Palouse and country, making farming more sustainable and efficient. Given the soil and hydrologic complexities of the Palouse and the impacts of biochar in the soil, biochar shows promise to be integrated into precision agriculture techniques in eroded areas. This thesis aims to evaluate the use of biochar as a precision agriculture technique to ease the challenges farmers face, increase crop yields, and restore soil fertility in eroded areas. Blanket application of biochar is cost-prohibitive (Garcia-perez et al., 2019), which reinforces the notion for targeted application of biochar to maximize impact while minimizing cost. Understanding the effects of targeted application of biochar on soil health and water retention in highly eroded areas would increase sustainable farming in the Palouse.

Biochar & its use in the soil

Biochar has been a heavily researched topic in the fields of soil health, soil restoration, and climate change mitigation in recent years. Biochar is the carbon-rich solid product from thermochemical conversion of biomass, usually manure, wood, leaves, and crop residues, and is generally enclosed in an oxygen-deprived environment, intended for use as a soil amendment as a means of improving soil productivity and health (Lehmann & Joseph, 2009a). The common types of thermochemical conversion are pyrolysis, liquefaction, and gasification, of which pyrolysis and gasification are the most common for biochar production. Biomass that undergoes thermochemical conversion is subjected to heating to reasonable temperatures (roughly 300 to 1,000 degrees C) in the absence of oxygen. Process parameters for thermochemical conversion will vary based on which conversion process is desired and feedstock inputs. Oxygen deprivation prevents traditional combustion from occurring, which prompts the volatile matter in the biomass to decompose, leaving solid residue behind; biochar. More information regarding biochar production and the complexities and factors associated with production, application, and composition can be found in the comprehensive work by Lehmann and Joseph (2009b).

Biochar is rich in carbon and nitrogen (two elements that make up the organic matter of soils), which have been shown to positively affect soil fertility and water retention characteristics in the soil (Aller et al., 2017; Dokoohaki et al., 2017). The properties of biochar are highly variable and dependent on the conditions of pyrolysis (cook temperature, residence time, type of reactor, etc.) and the feedstock used (woody biomass, crop residue, manure, etc.) (Agegnehu et al., 2017; Bhogal et al., 2009; Chowdhury et al., 2016; El-naggar et al., 2019; Jeffery et al., 2019; Mukherjee et al., 2014; Palansooriya et al., 2019; Razzaghi et al., 2020; Verheijen et al., 2010). In general, the primary characteristics that make biochar desirable for use in soils are the high porosity, high surface area, low density, and high organic matter content (Lehmann & Joseph, 2009b). Biochar is full of micro and macro pores that generate a large internal surface area and high porosity. This high internal porosity contributes to the low density of biochar by reducing the weight of the solid material. The porosity and

the bulk density are linked. When adding biochar to the soil, the high porosity tends to reduce the bulk density of the soil, depending on the soil type and physical properties of the soil. Biochar-specific surfaces, being generally higher than sand and comparable to or higher than clay, will therefore cause a net increase in the total soil-specific surface when added as an amendment (Lehmann & Joseph, 2009b). The porous structure of biochar shows an affinity for charged particles (Keech et al., 2005). The interactions with the charged particles can facilitate interactions with biological and physical components in the soil (Glaser et al., 2002), affecting the larger macro ecosystem in which biochar application occurs (Hammes & Schmidt, 2009). Given the complex nature of biochar, the effects of biochar on soil can be varied (Razzaghi et al., 2020). The amendment's effectiveness depends significantly on the physiochemical characteristics of the biochar and the properties (such as structure, soil type, nutrient concentration, and particle size) of the soil (Edeh & Buss, 2020). However, research has shown that the results of biochar amendment in soil have largely been positive, and a comprehensive meta-analysis regarding the impacts of biochar application on plant growth conducted by Jeffery et al. (2011) showed that amending soils with biochar largely helped the soil fertility and crop yields, outweighing the neutral results and one negative result.

Further, this analysis showed an average positive effect of 10% on crop yield across soil types. The amendment of biochar to the soil has further demonstrated positive impacts on water retention and plant available water (Liu, 2016; Rawls et al., 2003), which are two prime indicators of soil fertility and crop growth. A meta-analysis, performed by Razzaghi et al., 2020, of recent research involving biochar and its effects on soil properties. Biochar on average decreased the soil BD by 9%, field capacity (FC) and permanent wilting point (PWP) increased for coarse-textured soils (a 51% increase and a 47% increase, respectively), and moderately for medium-textured soils (by a 13% increase and a 9% increase respectively). The same study found that there was minimal effect on the FC of the soil for fine-textured soil, but PWP decreased by roughly 5% (Razzaghi et al., 2020). Furthermore, despite variability in climate conditions, amending soils with biochar resulted in an average increase in aboveground productivity, crop yield, soil microbial biomass, and nutrient retention compared to non-amended soils (Biederman & Stanley Harpole, 2013). The mechanism in which biochar impacts crop yield is generally a combination of the nutrient effects and structural effects that affect the soil's water-holding capacity and soil biota (Jeffery et al., 2019).

A key aspect of this research involves assessing biochar's impact on soil fertility. Soil fertility involves many components, including and not limited to nutrient cycling, water retention, plant available water (PAW), physical stability/structure, and biodiversity. The greater questions surrounding soil fertility and inter-field management of soil fertility are broad. Therefore, this study addresses research questions that encompass water and soil interactions when biochar is applied. A significant aspect of this pursuit is biochar's effects on PAW and the soil water range (from FC water content to PWP water content). Biochar's effect on PAW is variable, and the mechanism in which biochar changes PAW in the soil is not well documented or researched (Masiello et al., 2019). Plant available water is defined as the difference between two soil parameters: FC and PWP. FC is

defined as the water content of a soil profile after the excess gravitational water, or the water held by gravitational forces as opposed to capillary forces, has drained out of the system, and the downward movement of water has decreased. This occurs at soil tensions of -0.1 kPa, -6 kPa, or -33 kPa, dependent upon the soil texture and physical properties (Richards & Weaver, 1944). PWP is defined as the minimum amount of water that plants require before plants permanently wilt (occurs at a soil tension of -1,500 kPa for most plants). Below this range (i.e., at more negative pressures), plants cannot uptake water from the root zone and wilt. The difference between FC and PWP is considered water that is available to plants, or PAW. Both field capacity and wilting coefficient depend on the soil's physical characteristics, like soil texture or organic matter (OM).

Increasing the soil's water retention can increase PAW, and one method that has been shown to help is increasing the OM content of the soil. Research in 1994 showed a positive correlation between organic matter (OM) and available water content (AWC) for sand ($R^2 = 0.79$), silt loam ($R^2 = 0.58$), and silty clay loam ($R^2 = 0.76$); in all texture groups when OM increased from 0.5% to 3% available, water content doubled (Hudson, 1994). Lehmann et al. further noted that organic matter contributes to soil fertility by retaining plant-available water and nutrients or promoting soil structure formation (Lehmann & Kleber, 2015). Applying manure to soil showed an increase in topsoil porosity and plant available water capacity and a decrease in bulk density of 0.6%, 2.5%, and 0.5% with every 10 t ha^{-1} applied to the soil (Bhogal et al., 2009). Another study determined that increasing the organic carbon content of already low organic carbon soils lead to a higher sensitivity (or greater effect) in sandy soils; At the same time, there was an increase in water retention across all soil types when they initially had a high organic carbon content (Rawls et al., 2003). These findings support the notion that amending soil with biochar, high in OM, may positively affect degraded soils.

Biochar's effects on soil hydraulic properties

Soil hydraulic properties, matric potential, hydraulic conductivity (K), and diffusivity (D), dictate the ability for moisture to move through a soil profile. Further, soil moisture is a key component of soil fertility and soil health. Understanding biochar's effects on soil moisture and soil hydraulic properties is key to understanding water movement and this study. The matric potential of the soil is influenced by the soil water content, size and number of pores in the soil matrix, surface tension of soil water, and surface properties of the soil particles (Whalley et al., 2013). The hydraulic conductivity of a soil is affected by many factors, including density, water contents, degree of saturation, void ratio, particle size distribution, particle structure, tortuosity, soil texture, and size shape and abundance of pores (Campbell et al., 2021; Chung et al., 2018). Biochar has been shown to decrease the bulk density and increase the porosity of the soil (Basso et al., 2013). The changes in the soil structure showed an enhancement in soil water retention (Castellini et al., 2015) and the hydraulic conductivity of the soil (Devereux et al., 2013; Lim et al., 2016). The changes to the physiochemical properties influenced by the amendment of biochar leads to changes in the soil hydraulic properties. Therefore, it is critical that experimentation is designed in such a manner to understand the effects of biochar on soil hydraulic properties.

Need for development of new model

Numerical models are used throughout subjects of hydrology, environmental systems, farming, precision agriculture, and other fields. They are important tools that can provide stakeholders and decision-makers information to make informed decisions. The Soil & Water Assessment Tool (SWAT) model and the Environmental Policy Integrated Climate (EPIC) model are two standard hydrologic models used to aid decision-makers with adequate information regarding hydrologic and agriculture systems. The SWAT model is a small watershed to river basin-scale model used to simulate the quality and quantity of surface and groundwater and predict the environmental impact of land use, land management practices, and climate change (Arnold et al., 2012). SWAT is widely used in assessing soil erosion prevention and control, non-point source pollution control, and regional management in watersheds. The EPIC model is a cropping systems model that was developed to estimate soil productivity as affected by erosion as part of the Soil and Water Resources Conservation Act analysis for 1985. EPIC simulates approximately eighty crops with one crop growth model using unique parameter values for each crop. These models, SWAT and EPIC, are suitable for macro-level analysis regarding larger watersheds and areas. These larger-scale analyses are important but did not provide the finer resolution and greater flexibility that this research required. To obtain a model with finer resolution to provide analysis regarding small-scale application sites, the development of a new model was required. This new numerical model was developed in MATLAB and relies on finite element analysis to simulate water redistribution in a soil profile under the forces of evaporation.

Looking back, two models that could potentially be used are CropSyst and Decision-Support System for Agro-technology Transfer (DSSAT). CropSyst is a daily time-step model used as an analytical tool to study the effects of crop management on productivity and the environment. The model is flexible and can simulate the soil water budget, the soil-plant nitrogen budget, crop canopy and root growth, dry matter production, yield, residue production and decomposition, and erosion (Stöckle et al., 2003). DSSAT is a crop-based model that simulates the growth, development, and yield of crops as a function of the soil-plant-atmosphere-management dynamics. This model requires daily weather data, soil information, generic crop information, and detailed crop management as its inputs (Hoogenboom et al., 1999). These models show promise and could, in all likelihood, have been used. However, at the time of model development, these models were not evaluated. Additionally, there are benefits in developing a model-specific to one's primary research question. The benefit of new model development lies in a greater understanding of the components and inner workings of the model, which can lead to a greater understanding of the system that researchers are trying to model. Additionally, new models can be tailored to evaluate specific research questions pertaining to ones work.

Study Objectives

The purpose of this work is to analyze one primary research question: Can biochar be integrated into precision agriculture technologies to target areas of farmland that need it most. The hypothesis is narrowed to evaluate biochar amendment on the tops of hillslopes in the Palouse region, which are some of the more eroded areas in the area. The work presented here follows this hypothesis and the developed models involve changes to the soil

induced by biochar when applied to the tops of the hills. Answering this question consists of analyzing the different ways biochar affects soil, either through effects on water, effects on nutrients, and/or effects on the soil biota. While the interactions of biochar in the soil are complex and will likely affect all three considerations, this work analyzes the effects of biochar through the lens of soil water and primarily water retention and redistribution. This work primarily analyzes the effects of biochar on soil physical and hydraulic properties, which are important properties for how water moves through the soil. This work then presents modeling for how those changes in soil properties affect water retention and redistribution in a soil profile. Analyzing the water movement and retention in the soil is important for analyzing the potential increases in crop yields from a farmer's intended investment in biochar. The return on investment for a farmer will either come from an increase in crop yield because of the amendment and/or the reduction in overhead with an amendment.

Literature Cited

Adamchuk, V. I., Hummel, J. W., Morgan, M. T., & Upadhyaya, S. K. (2004). *On-the-go soil sensors for precision agriculture*. *44*, 71–91. https://doi.org/10.1016/j.compag.2004.03.002

Agegnehu, G., Srivastava, A. K., & Bird, M. I. (2017). The role of biochar and biochar-compost in improving soil quality and crop performance: A review. *Applied Soil Ecology*, *119*, 156–170. https://doi.org/10.1016/j.apsoil.2017.06.008

Aller, D., Rathke, S., Laird, D., Cruse, R., & Hatfield, J. (2017). Impacts of fresh and aged biochars on plant available water and water use efficiency. *Geoderma*. https://doi.org/10.1016/j.geoderma.2017.08.007

Arnold, J Kiniry, Srinivasan, R., Williams, Haney, (2012). *Soil & Water Assessment Tool, Texas Water Resources Institute-TR-439.*

Basso, A. S., Miguez, F. E., Laird, D. A., Horton, R., & Westgate, M. (2013). Assessing potential of biochar for increasing water-holding capacity of sandy soils. *GCB Bioenergy*, *5*(2), 132–143. https://doi.org/10.1111/gcbb.12026

Beven, K. J., & Kirkby, M. J. (1979). A physically based, variable contributing area model of basin hydrology. *Hydrological Sciences Bulletin*, *24*(1), 43–69. https://doi.org/10.1080/02626667909491834

Bhogal, A., Nicholson, F. A., & Chambers, B. J. (2009). Organic carbon additions: Effects on soil bio-physical and physico-chemical properties. *European Journal of Soil Science*, *60*(2), 276–286. https://doi.org/10.1111/j.1365-2389.2008.01105.x

Biederman, L. A., & Stanley Harpole, W. (2013). Biochar and its effects on plant productivity and nutrient cycling: A meta-analysis. *GCB Bioenergy*, *5*(2), 202–214. https://doi.org/10.1111/gcbb.12037

Brooks, E

Brown, M., Heinse, R., Johnson-Maynard, J., & Huggins, D. (2021). Time-lapse mapping of crop and tillage interactions with soil water using electromagnetic induction. *Vadose Zone Journal*, *November 2020*, 1–16. https://doi.org/10.1002/vzj2.20097

Bryan, K. (1926). The " Palouse Soil " Problem. *Contributions to Geography of the United States*, *5*, 287–296. https://pubs.usgs.gov/bul/0790b/report.pdf

Burt, T. ., & Butcher, D. P. (1985). Topographic controls of soil moisture distributions. *Journal of Soil Science*, *36*(3), 469–486. https://doi.org/10.1111/j.1365-2389.1985.tb00351.x

Castellini, M., Giglio, L., Niedda, M., Palumbo, A. D., & Ventrella, D. (2015). Soil & Tillage Research Impact of biochar addition on the physical and hydraulic properties of a clay soil. *Soil & Tillage Research*, *154*, 1–13. https://doi.org/10.1016/j.still.2015.06.016

Chowdhury, Z. Z., Karim, M. Z., Ashraf, M. A., & Khalid, K. (2016). Influence of Carbonization Temperature on Physicochemical Properties of Biochar derived from Slow Pyrolysis of Durian Wood (Durio zibethinus) Sawdust. *Bioresources*, *11*(2), 3356–3372.

Chung, C.-K., Kim, J.-H., Kim, J., & Kim, T. (2018). Hydraulic Conductivity Variation of Coarse-Fine Soil Mixture upon Mixing Ratio. *Advances in Civil Engineering*, *2018*, 1–11. https://doi.org/10.1155/2018/6846584

Corwin, D. L., & Lesch, S. M. (2003). Application of Soil Electrical Conductivity to Precision Agriculture. *Agronomy Journal*, *95*(3), 455. https://doi.org/10.2134/agronj2003.0455

Corwin, D. L., & Lesch, S. M. (2005). Apparent soil electrical conductivity measurements in agriculture. *Computers and Electronics in Agriculture*, *46*(1-3 SPEC. ISS.), 11–43. https://doi.org/10.1016/j.compag.2004.10.005

Devereux, R. C., Sturrock, C. J., & Mooney, S. J. (2013). The effects of biochar on soil physical properties and winter wheat growth. *Earth and Environmental Science Transactions of the Royal Society of Edinburgh*, *103*(1), 13–18. https://doi.org/10.1017/S1755691012000011

Dokoohaki, H., Miguez, F. E., Laird, D., Horton, R., & Basso, A. S. (2017). Assessing the Biochar Effects on Selected Physical Properties of a Sandy Soil: An Analytical Approach. *Communications in Soil Science and Plant Analysis*, *48*(12), 1387–1398. https://doi.org/10.1080/00103624.2017.1358742

Eagleson, P. (1978). Introduction to Water Balance Dynamics. *Water Resources Research*, *14*(5), 705–712.

Ebbert, J., & Roe, D. (1998). Soil erosion in the Palouse River basin: indications of improvement. *US Department of Agriculture*, 7(445,000), 1–700. http://wa.water.usgs.gov/pubs/fs/fs069-98/

Edeh, I. G., & Buss, W. (2020). *Science of the Total Environment A meta-analysis on biochar ' s effects on soil water properties – New insights and future research challenges*. *714*. https://doi.org/10.1016/j.scitotenv.2020.136857

El-naggar, A., Soo, S., Rinklebe, J., Farooq, M., & Song, H. (2019). Geoderma Biochar application to low fertility soils : A review of current status , and future prospects. *Geoderma*, *337*(May 2018), 536–554. https://doi.org/10.1016/j.geoderma.2018.09.034

EPA, U. S. E. P. A. (2014). *Inventory of U.S. GHG Emissions and Sinks 1990-2012*, *in Annex 3*.

Frazier, B. E., & Cheng, Y. (1989). Remote sensing of soils in the Eastern Palouse region with landsat thematic mapper. *Remote Sensing of Environment*, *28*(C), 317–325. https://doi.org/10.1016/0034-4257(89)90123-5

Fuentes, J. P., Flury, M., Huggins, D. R., & Bezdicek, D. F. (2003). Soil water and nitrogen dynamics in dryland cropping systems of Washington State, USA. *Soil and Tillage Research*, *71*(1), 33–47. https://doi.org/10.1016/S0167-1987(02)00161-7

Glaser, B., Lehmann, J., & Zech, W. (2002). *Ameliorating physical and chemical properties of highly weathered soils in the tropics with charcoal – a review*. 219–230. https://doi.org/10.1007/s00374-002-0466-4

Hagerty, C., Fickas, K., & Wysocki, D. (2019). *Agronomic Zones of the Dryland Pacific Northwest*. https://catalog.extension.oregonstate.edu/pnw354/html

Hammes, K., & Schmidt, M. W. I. (2009). Changes of Biochar in Soil. In J. Lehmann & S. Joseph (Eds.), *Biochar for Enviornmental Management* (First Edit, pp. 169–178). Earthscan.

Hartmans, M. A., & Michalson, E. L. (2000). *Evaluating the Economic & Environmental Impacts of Farming Practices on the Palouse Using PLANETOR*.

Hougton, J. T., Din, Y., Griggs, D. ., & Noguer, M. (2001). *Third Assessment Report: Climate Change 2001(TAR): The Science Basics*.

Hudson, B. (1994). Soil organic matter and available water capacity. *Soil and Water Conservation*, *April*, 189–194.

Huggins, B. D. R., & Reganold, J. P. (2008). No-Till : The Quiet Revolution. *Scientific American*, *July*, 71–77. https://www.ars.usda.gov/ARSUserFiles/20902500/DavidHuggins/NoTill.pdf

Jeffery, S., Spokas, K. A., & Verheijen, F. G. A. (2019). Biochar effects on crop yield. In J. Lehmann & S. Joseph (Eds.), *Biochar for Environmental Management* (Second, pp. 1–2). https://doi.org/10.4324/9780203762264-19

Jin, K., Cornelis, W. M., Schiettecatte, W., Lu, J., Yao, Y., Wu, H., Gabriels, D., De Neve, S., Cai, D., Jin, J., & Hartmann, R. (2007). Effects of different management practices on the soil-water balance and crop yield for improved dryland farming in the Chinese Loess Plateau. *Soil and Tillage Research*, *96*(1–2), 131–144. https://doi.org/10.1016/j.still.2007.05.002

Kaiser, V. (1967). Soil Erosion and Wheat Yields in Whitman County, Washington. *Northwest Science*, *41*(2), 85–91.

Kaiser, V., Starr, W., & Johnson, B. (1951). Types of Topography as Related to Land Use in Whitman County, Washington. *Northwest Science*, *XXV*(2).

Keech, O., Carcaillet, C., & Nilsson, M. (2005). *Adsorption of allelopathic compounds by wood-derived charcoal : the role of wood porosity*. 291–300. https://doi.org/10.1007/s11104-004-5485-5

Koenig, R. T. (2005). *Dryland Winter Wheat : Eastern Washington Nutrient Management Guide*. http://pubs.cahnrs.wsu.edu/publications/wp-content/uploads/sites/2/publications/eb1987e.pdf

Kok, H., Papendick, R. I., & Saxton, K. E. (2009). STEEP: Impact of long-term conservation farming research

and education in Pacific Northwest wheatlands. *Journal of Soil and Water Conservation*, *64*(4), 253–264. https://doi.org/10.2489/jswc.64.4.253

Kühling, I., Redozubov, D., Broll, G., & Trautz, D. (2017). Impact of tillage, seeding rate and seeding depth on soil moisture and dryland spring wheat yield in Western Siberia. *Soil and Tillage Research*, *170*, 43–52. https://doi.org/10.1016/j.still.2017.02.009

Langdale, G. W., Karlen, D., Mccool, D., & Nearing, M. A. (2014). Cover crop effects on soil erosion by wind and water. In *Wind and Water Erosion* (Issue February 2014, pp. 15–40). https://www.researchgate.net/profile/Mark_Nearing/publication/238089979_Cover_crop_effects_on_soil_erosion_by_wind_and_water/links/0f3175304f163cf485000000/Cover-crop-effects-on-soil-erosion-by-wind-and-water.pdf

Lehmann, J., & Joseph, S. (2009a). Biochar for Environmental Management : An Introduction. In J. Lehmann & S. Joseph (Eds.), *Biochar for Environmental Management Science and Technology* (1st ed., Vol. 1, pp. 1–12). Earthscan.

Lehmann, J., & Joseph, S. (2009b). *Biochar for Environmental Management* (First). Earthscan.

Lehmann, J., & Kleber, M. (2015). The contentious nature of soil organic matter. *Nature*, *528*(7580), 60–68. https://doi.org/10.1038/nature16069

Lim, T. J., Spokas, K. A., Feyereisen, G., & Novak, J. M. (2016). Predicting the impact of biochar additions on soil hydraulic properties. *Chemosphere*, *142*, 136–144. https://doi.org/10.1016/j.chemosphere.2015.06.069

Liu, Z. (2016). *Interactions between Biochar, Soil, and Water*. https://search.proquest.com/pqdtglobal/docview/1999348435/83940BAE4E3E42FEPQ/1?accountid=15115

Masiello, C. A., Dugan, B., Brewer, C. E., Spokas, K. A., Novak, J. M., Liu, Z., & Giovambattista, S. (2019). Biochar effects on soil hydrology. In J. Lehmann & S. Joseph (Eds.), *Biochar for Environmental Management* (Second, pp. 543–562). https://doi.org/10.4324/9780203762264-26

McCool, D. K., Huggins, D. R., Saxton, K. E., & Kennedy, A. C. (2001). Factors affecting agricultural sustainability in the Pacific Northwest , USA: An overview. *Sustaining the Global Farm. Selected Papers from the 10th International Soil Conservation Organization Meeting Held May 24-29, 1999 at Purdue University and the USDA-ARS National Soil Erosion Research Laboratory*, 255–260.

McDaniel, P. A., Gabehart, R. W., Falen, A. L., Hammel, J. E., & Reuter, R. J. (2001). Perched Water Tables on Argixeroll and Fragixeralf Hillslopes. *Soil Science Society of America Journal*, *65*(3), 805–810. https://doi.org/10.2136/sssaj2001.653805x

McDaniel, P. A., Regan, M. P., Brooks, E., Boll, J., Barndt, S., Falen, A., Young, S. K., & Hammel, J. E. (2008). Linking fragipans, perched water tables, and catchment-scale hydrological processes. *Catena*, *73*(2), 166–173. https://doi.org/10.1016/j.catena.2007.05.011

Mukherjee, A., Lal, R., & Zimmerman, A. R. (2014). Effects of biochar and other amendments on the physical properties and greenhouse gas emissions of an artificially degraded soil. *Science of the Total Environment*, *487*(1), 26–36. https://doi.org/10.1016/j.scitotenv.2014.03.141

Palansooriya, K. N., Ok, Y. S., Awad, Y. M., Lee, S. S., Sung, J. K., Koutsospyros, A., & Moon, D. H. (2019). Impacts of biochar application on upland agriculture: A review. *Journal of Environmental Management*, *234*, 52–64. https://doi.org/10.1016/j.jenvman.2018.12.085

PlantMaps. (2021). *Interactive United States Köppen Climate Classification Map*. https://www.plantmaps.com/koppen-climate-classification-map-united-states.php

Rawls, W. J., Pachepsky, Y. A., Ritchie, J. C., Sobecki, T. M., & Bloodworth, H. (2003). Effect of soil organic carbon on soil water retention. *Geoderma*, *116*(1–2), 61–76. https://doi.org/10.1016/S0016-7061(03)00094-6

Razzaghi, F., Bilson, P., & Arthur, E. (2020). Geoderma Does biochar improve soil water retention ? A systematic review and meta- analysis. *Geoderma*, *361*(October 2019), 114055. https://doi.org/10.1016/j.geoderma.2019.114055

Schlegel, A. J., Assefa, Y., Haag, L. A., Thompson, C. R., Holman, J. D., & Stone, L. R. (2017). Yield and soil water in three dryland wheat and grain sorghum rotations. *Agronomy Journal*, *109*(1), 227–238. https://doi.org/10.2134/agronj2016.07.0387

Sheets, K. R., & Hendrickx, J. M. H. (1995). Noninvasive Soil Water Content Measurement Using Electromagnetic Induction. *Water Resources Research*, *31*(10), 2401–2409. https://doi.org/10.1029/95WR01949

Shrestha, D. (2021). *Precision Agriculture*. https://www.webpages.uidaho.edu/~devs/Research/Agriculture.html

Tian, L. X., Zhang, Y. C., Chen, P. L., Zhang, F. F., Li, J., Yan, F., Dong, Y., & Feng, B. L. (2021). How Does the Waterlogging Regime Affect Crop Yield? A Global Meta-Analysis. *Frontiers in Plant Science*, *12*(February), 1–9. https://doi.org/10.3389/fpls.2021.634898

USDA. (1978). *Palouse cooperative river basin study.* //catalog.hathitrust.org/Record/000302437

USDA, Service, S. C., & Service, F. (1979). *Erosion in the Palouse : A Summary of the Palouse River Basin Study*. United States Department of Agriculture.

Verheijen, F., Jeffery, S., Bastos, A. C., Van Der Velde, M., & Diafas, I. (2010). Biochar Application to Soils: A Critical Scientific Review of Effects on Soil Properties, Processes and Functions. In *Environment* (Vol.

8, Issue 4). https://doi.org/10.2788/472

Weddell, B., Brown, T., & Borrelli, K. (2017). Precision Agriculture. In G. Yorgey & C. Kruger (Eds.), *Advances in Dryland Farming in the Inland Pacific Northwest* (pp. 319–352). http://pubs.cahnrs.wsu.edu/wp-content/uploads/sites/2/2017/06/em108-ch8.pdf

Western, A. W., Grayson, R. B., & Blöschl, G. (2002). Scaling of soil moisture: A hydrologic perspective. *Annual Review of Earth and Planetary Sciences*, *30*, 149–180. https://doi.org/10.1146/annurev.earth.30.091201.140434

Whalley, W. R., Ober, E. S., & Jenkins, M. (2013). *Measurement of the matric potential of soil water in the rhizosphere*. *64*(13), 3951–3963. https://doi.org/10.1093/jxb/ert044

Wilson, D. J., Western, A. W., & Grayson, R. B. (2005). A terrain and data-based method for generating the spatial distribution of soil moisture. *Advances in Water Resources*, *28*(1), 43–54. https://doi.org/10.1016/j.advwatres.2004.09.007

WWC. (2009). *Washington Wheat Facts 2008-2009*. http://admin.aghost.net/images/E0177801/2008WF4WebSmHomepage.pdf

Yang, C., Peterson, C. L., Shropshire, G. J., & Otawa, T. (1998). *41*(1), 17–27.

Yourek, M. A. (2016). *An Investigation of Crop Senescence Patterns Observed in Palouse Region Fields Using Satellite Remote Sensing and Hydrologic Modeling A Thesis Presented in Partial Fulfillment of the Requirements for the Degree of Master of Science with a Major in Environ* (Issue January). University of Idaho.

Zhu, Q., Lin, H., & Doolittle, J. (2010). Repeated Electromagnetic Induction Surveys for Determining Subsurface Hydrologic Dynamics in an Agricultural Landscape. *Soil Science Society of America Journal*, *74*(5), 1750–1762. https://doi.org/10.2136/sssaj2010.0055

Chapter 2: Modeling moisture redistribution from the selective non-uniform application of biochar on Palouse Hills

Abstract

Precision agriculture is most effective in areas where significant intra- and inter-field variation occurs. The Palouse region of the Pacific Northwest in the US, a vast area of undulating fertile farmland, has relatively high in-field variation in water retention and crop yield. The rainfed Palouse agriculture depends on the soil at or near field capacity towards the end of wet spring for the next few months of little rain, creating the need for management of soil water retention. Uniform application of biochar to improve water retention is cost-prohibitive. A finite element vadose zone transport model was developed and used to understand the benefits of targeted application of biochar on water redistribution in a hillslope and potential crop yield improvement. A Redwood Sawdust (RSD) and Wheat Straw (WS) biochar was amended at 4% and 7% concentrations by mass (m/m). The biochar amendment soils showed an increase in water retention at lower matric potentials. Biochar amendment showed an apparent reduction in unsaturated hydraulic conductivity as the soil approached saturated conditions (moisture contents > 0.35 or 35%). This was consistent for all samples. After two months of bare field evaporation, the model showed that RSD application did affect the redistribution of water in the soil profile. Biochar amendment was able to retain more moisture in and around the amendment area, although the magnitude between samples varied, with several samples showing minimal effectiveness. Despite the differences in magnitude with biochar amendment, these results indicate that biochar can be used to change the redistribution of water in a soil profile. Additionally, the developed model shows promise as a tool to inform stakeholders about the integration of biochar into precision agriculture technologies.

Introduction

Feeding a growing population and climate change are two significant problems that are imminent in the foreseeable future. For generations, overuse of resources and continued population growth has stressed global environmental systems, creating a need for progressive, sustainable solutions to these stressors. Addressing the difficulties surrounding agriculture on a local and global level is an integral part of mitigating these issues directly. Creating sustainable and efficient agricultural systems entails addressing the deficiencies in agriculture that are detrimental to local, regional, and global soil health and crop yields. These issues promote the need for agriculture to foster more sustainable practices to meet generational needs. Precision agriculture can aid in this pursuit.

Integrating precision agriculture into agricultural systems allows for site-specific management of areas to create a more uniform crop yield in a field. The return on investment for precision agriculture is more significant with higher in-field variability in crop yields. Precision agriculture practices/technologies are becoming increasingly common throughout the United States. Remote sensing has been used to identify areas of high erosion down to layers of paleosols (Frazier & Cheng, 1989). Sensors can predict the level of water stress plants are under at any point in the growing season (Adamchuk et al., 2004). Proximal sensing and remote sensing have been used to

measure the physical properties of the soil and the vitality of the crops either on the ground or from aircraft and using satellite imaging (Yourek, 2016). Electromagnetic induction, a proximal sensing technique, can infer various soil properties by measuring the electroconductivity of the soil (Adamchuk et al., 2004). These methods can be used in proactive or reactive ways to aid farmers in operation. Soil restoration can be employed in precision agriculture techniques similarly. Targeting soils that require restoration falls under the scope of precision agriculture. The primary purpose of this work is to evaluate the feasibility of site-specific soil restoration, using biochar, and analyzing the effects on soil-water relationships.

Biochar has been a heavily researched topic in the fields of soil health, soil restoration, and climate change mitigation in recent years. Biochar is defined as charred organic matter produced with the intent to be applied to soil to improve soil productivity and health (Lehmann & Joseph, 2009). This substance is rich in carbon and nitrogen (two elements that make up the organic matter of soils), which can positively affect soil fertility and water retention characteristics in the soil (Aller et al., 2017; Dokoohaki et al., 2017). Research in 1994 showed a positive correlation between organic matter (OM) and PAW for sand ($R^2 = 0.79$), silt loam ($R^2 = 0.58$), and silty clay loam ($R^2 = 0.76$); in all texture groups when OM increased from 0.5% to 3% available water content doubled (Hudson, 1994). Lehmann et al. further noted that organic matter contributes to soil fertility by retaining plant-available water and nutrients or promoting soil structure formation (Lehmann & Kleber, 2015). A comprehensive meta-analysis regarding the impacts of biochar application on plant growth conducted by Jeffery et al., 2011 showed that amending soils with biochar largely helped the soil fertility and crop yields, outweighing the neutral results and one negative result (S. Jeffery et al., 2011). Further, this analysis showed an average positive effect of 10% on crop yield across soil types. Despite the documented positive effects of the biochar amendment on soils, the amendment's effectiveness depends significantly on the physiochemical characteristics of the biochar and the properties (such as structure, soil type, nutrient concentration, and particle size) of the soil (Edeh & Buss, 2020). This is primarily due to the differences in biochar characteristics and soil properties in which the amendment occurs. The physiochemical characteristics of biochar largely vary depending on the conditions of thermochemical conversion and the feedstock used in the processing (Agegnehu et al., 2017; Bhogal et al., 2009; Chowdhury et al., 2016; El-naggar et al., 2019; S. Jeffery et al., 2011; Lehmann & Joseph, 2009; Palansooriya et al., 2019). The amendment of biochar to the soil has further shown positive impacts on water retention and plant available water (Z. Liu, 2016; Rawls et al., 2003), which are two prime indicators of soil fertility and crop growth.

Furthermore, the impacts from biochar are linked to soil hydraulic properties. Soil hydraulic properties, like matric potential and hydraulic conductivity, are influenced by differences in the physiochemical properties of the soil. The matric potential of the soil is affected by the soil water content, size and number of pores in the soil matrix, surface tension of soil water, and surface properties of the soil particles (Whalley et al., 2013). The hydraulic conductivity of soil is affected by many factors, including density, water content, degree of saturation, void ratio, particle size distribution, particle structure, tortuosity, soil texture, and size/shape/number of pores

(G. Campbell et al., 2021; Chung et al., 2018). The changes in the soil structure showed an enhancement in soil water retention (Castellini et al., 2015) and the hydraulic conductivity of the soil (Devereux et al., 2013; Lim et al., 2016). This study hypothesizes that biochar's effects on water retention and redistribution in areas throughout the Palouse could benefit the region considerably.

Study Site

This study utilizes a generic hillslope in the Palouse region. No specific location is defined within the Palouse; however, the characteristics used in this study are representative of the greater Palouse region. The Palouse area of the Pacific Northwest United States spans from southeastern Washington to west-central Idaho and consists of over 2 million acres of rich agricultural land (Hall et al., 1999; Hartmans & Michalson, 2000). The soil throughout the region is dominated by Palouse Silt Loam that is classified as fine-silty, mixed, superactive, mesic Pachic Ultic Haploxerolls (Soil Survey Staff, 2021). This area, while fertile, has some of the fastest eroding topsoil in the United States. Since this land was first cultivated about 100 years ago, all of the original topsoil has been lost from about 10% of Palouse cropland, and one-fourth to three-fourths of the original topsoil has been lost from another 60% of cropland (USDA, 1978). Topsoil and soil organic matter loss impairs the soil's water-storage capacity, reduces the soil's natural fertility, and requires increased fertilizer use to maintain yields (Hartmans & Michalson, 2000). Portions of the Palouse are a dryland agricultural system. Stored water is key to dryland agriculture, and the patterns of stored water (where and when it is stored in the soil profile) has been linked to the topography (Beven & Kirkby, 1979; Wilson et al., 2005), cropping sequences (Schlegel et al., 2017), and tillage practices (Fuentes et al., 2003; Jin et al., 2007; Kühling et al., 2017). Throughout the year, stored soil water will fluctuate spatially (Eagleson, 1978) due to climatic changes (Brown et al., 2021), vegetation (Eagleson, 1978), topography (Burt & Butcher, 1985), and heterogeneous soil profiles (Sheets & Hendrickx, 1995). A study in Whitman county in Washington, USA, found an average annual erosion rate over 26 years of 0.7 tons of soil for each bushel of wheat raised, and in some places, the figure was as high as 2.3 tons of topsoil lost per bushel of wheat (Kaiser, 1967). These eroded areas have shallow topsoil depth, minimal organic matter, and poor water retention properties (Kaiser, 1967) and can consistently be found at the tops or steeper sections of the hillslopes. At the top of the hills, argillic and fragipan horizons in north-facing hillslopes lead to perched water tables in the winter months, which drives rapid subsurface lateral flows and accelerates the eluviation of clays in albic Esoil horizons (Brooks et al., 2012; McDaniel et al., 2001, 2008). The impermeable fragipan layers can be relatively shallow in the soil, ~0.65 m, and along with the formation of perched water tables, drive the hydrologic processes of these areas (Brooks et al., 2004). This reduces the amount of water that is stored in the already shallow topsoil, which directly impacts crop yield in these areas. Furthermore, topography-based surface and subsurface lateral flow is an influential determinant of water movement and storage in the winter and spring months (Western et al., 2002; Zhu et al., 2010).

Objectives of this study

Currently, biochar is cost-prohibitive for uniform application of biochar over large areas. Applying biochar in a targeted to eroded areas in the region would, theoretically, allow for specific eroded areas to benefit from

biochar amendment without significant cost to a farmer. This study aims to provide support for integrating biochar into precision agriculture, primarily analyzing biochar amendment to improve water retention in poor yielding areas. It focuses on the complexities of farming in the Palouse to ascertain valuable information regarding the impact of biochar amendment on water retention characteristics and local agriculture. Using numerical modeling and finite element analysis, a vadose zone transport model was developed with the partial differential equation toolbox in MATLAB to estimate the redistribution of water throughout an undulating topography. The model utilizes laboratory measurements (of soil hydraulic properties) and meteorological data to simulate water redistribution over the dry summer months of the Palouse. This study aims to determine a) the effectiveness of biochar as a precision agriculture technique, b) the impact of biochar amendment on the soil hydraulic properties of a Palouse silt loam soil through laboratory measurements, c) an assessment of biochar as a soil restoration technique in the Palouse, and d) the effectiveness and validity of the developed model to simulate water redistribution and retention in a soil profile.

Materials and Methods

The experiment was divided into two sections: laboratory experimentation and vadose zone transport modeling. The laboratory experimentation provides realistic data for the different soil sample properties throughout the entire soil moisture range, while the vadose zone transport modeling provided the larger impact of biochar over a specified period of time.

Theory: Vadose Zone Transport Model

In its current form, this model is intended to evaluate water retention and redistribution on an hourly time scale as soil dries throughout a simulated growing season. It is a bare soil vadose zone transport model that is open strictly to evaporation off the surface and percolation out of the bottom of the geometry. The vadose zone transport model developed throughout this work is the preliminary baseline development that could eventually be expanded to more complex applications. The initial model would simulate a small catchment in a watershed, and more specifically, it would simulate one small hillslope in a catchment. The use of finite element analysis (FEA) is important because it provides flexibility and scalability that is desired for larger watershed applications. It was desirable to incorporate the simulation of hourly changes in moisture in two dimensions (both laterally on the surface of the profile and vertically into the profile).

Additionally, FEA allows for the simulation of the soil water inside a specified geometry, which is important for understanding how biochar amendment affects soil close to the surface and further into the profile. FEA utilizes a mesh (and node) approach. To simulate the moisture redistribution, each node in the geometry will have values of matric potential, hydraulic conductivity, and diffusivity associated with the current water content of that node. As the water content changes, the soil properties of that node change, creating the need for soil property characteristics throughout the entire water content range obtained from the lab experimentation. After analyzing existing groundwater flow models (SWAT and EPIC models), it was determined that those models did not directly accomplish the desired field level moisture distribution, and a much finer resolution was

needed. CropSyst and DSSAT models were not evaluated for use. A MATLAB model provides a finer resolution (0.01 m mesh size) to smaller areas, while pre-existing models look at larger-scale watersheds.

To model the redistribution of water in a vadose zone, a representative model geometry is required. Given the significant variation in the topography of the Palouse region, a simplified "generic" hillslope is most effective for showing biochar application across a broad application of typographies. An idealized hillslope was created using a sinusoidal wave from -π/2 to 3π/2 (Figure 4). The sinusoidal curve serves as the hillslope profile with concave and convex sections, which resembles a generic hillslope. Initially, the base thickness of the hillslope was set to be 2 m, and the height of the sloped region was set to be 1 m. The length of the hillslope is 10 m wide. Theoretically, if the mechanics of the model are validated and functioning appropriately, the model geometry could change to an actual hillslope that is found in the region. The dimensional parameters used to model the hillslope are shown in Figure 4.

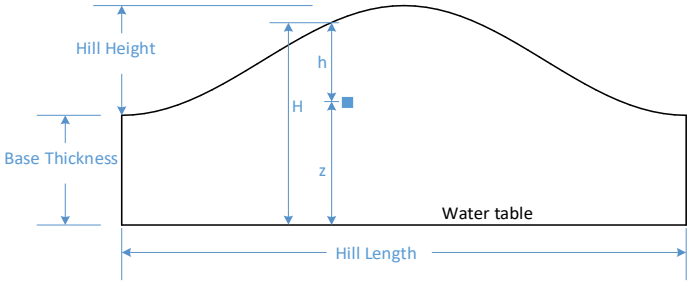

Figure 4: Model of the Palouse hill as a sinusoidal curve. The top surface has Neumann boundary condition; no moisture movement is assumed in the lateral direction

The primary forces that drive the moisture throughout the hillslope are the gradient of the hydraulic head and the capillary action or diffusion process. Henry Darcy first developed this notion and has since become Darcy's Law (Hubbert, 1957).

Darcy's Law

For saturated soil, the water flow rate Q per unit cross-section area is proportional to the forces producing flow, given by Darcy's Law:

$$Q = K\frac{d\phi}{dl} \quad [1]$$

Where K [LT^{-1}]is hydraulic conductivity at moisture content θ, and $d\phi/dl$ is hydraulic potential gradient in the direction of flow. Darcy's Law is valid only for laminar flow, which occurs for Reynold's number (Re) less than 1. Most practical applications of groundwater flow have Re < 1 and thus can be modeled with Darcy's Law. Darcy's Law summarizes water flow through a saturated soil column and can be applied to the specified geometry. If θ is the volume of water per unit volume of soil, the time rate of change of moisture θ in a unit soil cube is the divergence of the flow into the soil matrix and is given by:

$$\frac{d\theta}{dt} = Divergence\ of Q = \nabla \cdot K\,\nabla\phi \quad [2]$$

For unsaturated soil, pore space contains both air and water. The hydraulic potential is the sum of pressure head (p), elevation head (z), and soil matric potential (can also be osmotic potential) (ψ). The matric potential is the portion of the water potential that can be attributed to the attraction of the soil matrix for water. The matric potential used to be called the capillary potential because, over a large part of its range, the matric potential is due to capillary action. However, as the water content decreases in a porous material, water held in pores due to capillarity becomes negligibly small compared to the water held directly on particle surfaces. Therefore, the term matric potential covers phenomena beyond those for which a capillary analogy is appropriate (Kirkham, 2005). For unsaturated soil, the hydraulic potential is given by:

$$\phi = p + \psi + z \quad [3]$$

The matric potential(ψ) is a function of moisture content. ψ is zero at saturation and above and is negative for lower moisture. Combining equations 2 and 3,

$$\frac{d\theta}{dt} = \nabla \cdot K\,\nabla\psi + \nabla \cdot K\,\nabla \mathrm{p} + \nabla \cdot K\,\nabla \mathrm{z} \quad [4]$$

But $\nabla\psi = \frac{d\psi}{dl} = \frac{d\psi}{d\theta}\frac{d\theta}{dl} = \frac{d\psi}{d\theta}\nabla\theta.\frac{d\theta}{dl}$ is the change in moisture content between two points in any direction, either in the x,y, or z-direction. The term $K\frac{d\psi}{d\theta}$ is defined as soil diffusivity (D), which is also dependent on the soil moisture content of the soil. Assuming a homogeneous and isotropic soil matrix, the K and ψ are scalar functions of θ. For a saturated soil profile, the pressure head is equal to the height of the saturated layer. For unsaturated soil, the hydraulic head is less than the height of the soil layer. We can assume a linear relationship between pressure head p and moisture content of the soil profile as $p = h\frac{\theta-\theta_{fc}}{\theta_s-\theta_{fc}}$, where h is the depth of the soil element from the surface (Figure 4), and θ_{fc} is the moisture content at field capacity. The linear relationship applies to the saturated layer in the soil. By definition, soil below field capacity is under the force of only gravity, and therefore, pressure head, p, is 0. The gradient of p in the horizontal direction is 0 and hence, $\nabla \cdot K\,\nabla \mathrm{p} = \frac{\partial}{\partial z}K\frac{\theta-\theta_{fc}}{\theta_s-\theta_{fc}} = \frac{K}{\theta_s-\theta_{fc}}\frac{\partial\theta}{\partial z}$. The gradient of elevation in the vertical direction $\frac{\partial z}{\partial z} = 1$ and 0 in the horizontal direction; hence $\nabla^2 z = 0$. Therefore, equation 4 can be written as:

$$\frac{d\theta}{dt} - \nabla \cdot \mathrm{D}\nabla\theta - K\frac{1}{\theta_s-\theta_{fc}}\frac{\partial\theta}{\partial z} = 0 \; if \; \theta > \theta_{FC}$$

$$\frac{d\theta}{dt} - \nabla \cdot \mathrm{D}\nabla\theta = 0 \; if \; \theta \le \theta_{FC} \quad [5]$$

Equation 5 are included for completeness and clarity. The model setup and initial conditions, described in later sections, indicates the soil moisture does not increase beyond θ_{fc}. The second equation, which is applicable for all moisture contents that do not develop positive pressures, is sufficient for the type of modeling and setup that is described in this work.

Boundary Conditions

Equation 5 provides the governing PDE for moisture movement inside the soil matrix. The moisture distribution around the boundary, such as the topsoil surface, depends on boundary conditions, where the soil exchanges moisture with the environment. The theory presented below expands upon research by Wang et al. (2019) and

presents a novel evaporation equation. Research by Wang et al., 2019 used a Kelvin equation under dry conditions to calculate the equilibrium matric potential of the soil surface with atmospheric air is given by:

$$\psi_a = \frac{RT}{Mg}\ln(RH) \quad [6]$$

Where R is the universal gas constant (8.314 J·mol−1·K−1), T (Kelvin) is the absolute temperature, M is the molecular weight of water (0.018015 kg mol−1), g is the gravitational acceleration (9.81 m s−2), and RH is the in-equilibrium relative humidity at the soil surface (Wang et al., 2019). Similar to applying Newton's Law of cooling via convection, we can assume that the rate of evaporation is proportional to the difference between soil potential at the surface and air. Equating the rate of evaporation to the rate of change of moisture content to the surface,

$$\frac{d\theta}{dt} = \varepsilon(\psi - \psi_a) \quad [7]$$

Where ε [$L^{-1}T^{-1}$] is the evaporation constant, similar in meaning to convective heat transfer coefficient in a thermal system, the value of ε depends on soil temperature, wind speed, and other energy sources aiding evaporation. The evaporation rate is defined as the depth of water evaporated per unit of time per unit gradient of matric potential. This has units of T^{-1}. Combining this with equation 5, we get the boundary condition,

$$n.\left(D + K\frac{1}{\theta_s - \theta_{fc}}\right)\nabla\theta = \varepsilon(\psi - \psi_a) \quad [8]$$

Note that instead of divergence, the derivative is taken in the direction normal to the surface. The boundary condition for either side in Figure 4 is assumed to be in equilibrium with its neighbor, and hence no moisture is exchanged. The boundary condition for the bottom is assumed to be at the field capacity. A separate boundary is constructed for the biochar amendment area, which allows for the transmittance of water across the boundary layer.

Finite element analysis with MATLAB PDE solver

Analytic solution to equation 8 with initial boundary conditions is almost impossible. MATLAB's Partial Differential Equation (PDE) Toolbox solves scalar equations of the form shown expressed in equation 8. Since moisture is a scalar quantity and is the only component being considered, a scalar form of the equation can be applied. MATLAB® (Mathworks.com)'s PDE toolbox was used to solve the partial differential equation in equation 5. MATLAB has a standard form of the equation (MathWorks, 2006) for its PDE solver given by:

$$m\frac{\partial^2\theta}{dt^2} + d\frac{\partial\theta}{dt} - \nabla\cdot(c\nabla\theta) + \mathrm{a}\theta = \mathrm{f} \quad [9]$$

For a 3-D representation of the model, MATLAB internally computes $\nabla\cdot(c\nabla\theta)$ as

$$\nabla\cdot(c\nabla\theta) = \begin{bmatrix}\frac{\partial}{\partial x} & \frac{\partial}{\partial y} & \frac{\partial}{\partial z}\end{bmatrix}\begin{bmatrix}c_x & 0 & 0\\ 0 & c_y & 0\\ 0 & 0 & c_z\end{bmatrix}\begin{bmatrix}\frac{\partial\theta}{\partial x}\\ \frac{\partial\theta}{\partial y}\\ \frac{\partial\theta}{\partial z}\end{bmatrix}$$

For an isotropic diffusivity coefficient, equation 5 can be written in matrix form for moisture above field capacity as:

$$\frac{d\theta}{dt} - \begin{bmatrix} \frac{\partial}{\partial x} & \frac{\partial}{\partial y} & \frac{\partial}{\partial z} \end{bmatrix} \begin{bmatrix} D & 0 & 0 \\ 0 & D & 0 \\ 0 & 0 & D + K\frac{1}{\theta_s - \theta_{fc}} \end{bmatrix} \begin{bmatrix} \frac{\partial\theta}{\partial x} \\ \frac{\partial\theta}{\partial y} \\ \frac{\partial\theta}{\partial z} \end{bmatrix} = 0 \quad [10]$$

For moisture contents below field capacity, the middle matrix turns into a unit matrix with scalar multiple D. For a 2-D representation of Palouse hill, comparing equations 9 and 10, $m = 0,\ d = 1,\ a = 0,\ f = 0$. The value of c is computed conditionally:

$c = \begin{bmatrix} D & 0 \\ 0 & D + K\frac{1}{\theta_s - \theta_{fc}} \end{bmatrix} if\ \theta_{fc} < \theta < \theta_s$, Otherwise $c = D$.

Neumann boundary condition is applied in the upper surface where water evaporates. MATLAB specifies the Neumann boundary conditions by the following equation:

$$\vec{n} \cdot (c\nabla u) + qu = g \quad [11]$$

Comparing equation 11 to equation 8 gives, $q = 0$, and $g = \varepsilon(\psi - \psi_a)$. The value of c is the same as shown above.

The theory and FEA approach culminate in the generated mesh for the specified geometry (Figure 4). The FEA mesh is displayed in Figure 5. The geometry is confined on both the left and right sides. The surface is open to evaporation, and the bottom is open to percolation. Additionally, this is a uniform vadose zone profile, which is idealistic. The mesh size was set to 1 cm. The nodes in the black area indicate the biochar amendment area, which will have biochar amended soil characteristics. The blue nodes indicate control nodes (100% soil).

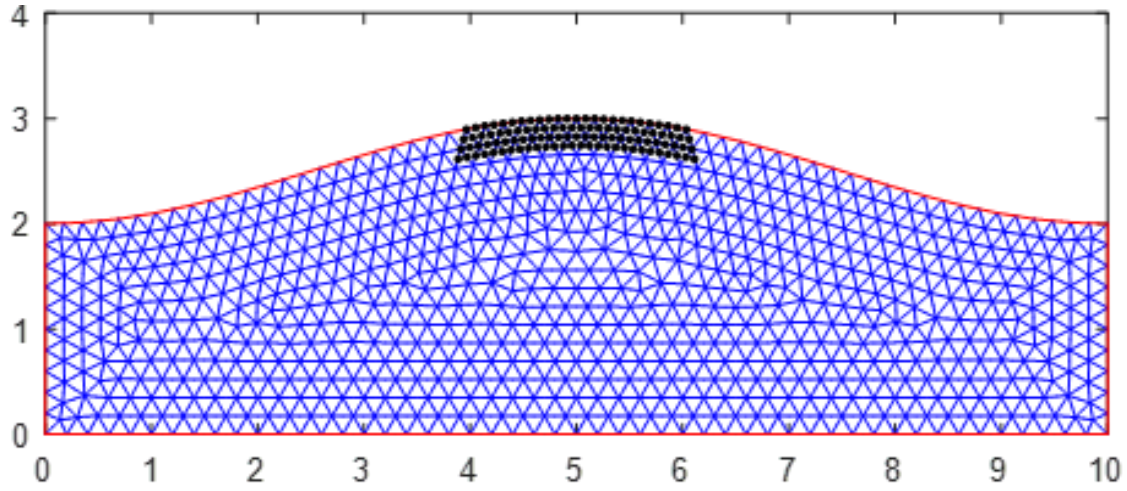

Figure 5: Finite Element mesh of the hillslope. The biochar application area covers 5% of the hillslope and is displayed in black. The units are in meters.

Sample composition and preparation

To assess the effectiveness of biochar in moisture redistribution, samples of soil and biochar were measured for hydraulic properties in a laboratory setting. Disturbed soil was collected at the University of Idaho Parker Farm, outside of Moscow, Idaho. Soil samples were sieved with a No.6 mesh sieve, diameter 3.35 mm, (USA standard testing sieve, ASTM E-11 Specification) to ensure larger aggregates did not create a higher degree of variability during experimentation. Biochar samples were obtained through Carbon Logic LLC (part of Ag-Energy solutions) in Spokane, Washington. A Redwood Sawdust (RSD) and a Wheat Straw (WS) biochar were used, which was produced from gasification. Proximal analysis, corresponding with ASTM proximate analysis procedures, was performed on both biochar samples. Surface area analysis was performed by using the Brunauer–Emmett–Teller (BET) methodology. Proximal and surface area analysis yielded the following table:

Table 1: Proximal analysis and surface area analysis (BET) of biochar samples

Sample	Ash content (% mass)	Volatile matter (% mass)	Fixed Carbon (% mass)	Surface Area (m^2/g)
RSD	1.94	10.10	88.01	47.12
WS	24.34	12.20	63.40	7.08

Biochar samples were added to the soil and manually mixed until a homogenous mixture was formed. Both RSD and WS samples were mixed at 0% (100% soil), 4%, and 7% concentration by dry mass. Each sample was manually mixed using manual stir sticks until a homogenous mixture formed. This was done in bulk and then stored for later testing. This allowed for an understanding of the potential trends for how biochar type and concentration affect the soil's hydraulic and physical properties. Textural analysis and other soil characteristics on the soil and biochar mixtures were outsourced to Best Test Analytics in Moses, Lake, Washington. The external soil lab received disturbed soil samples, which needed to be reconstituted for specific soil tests/analysis, for example, bulk density (BD). To get the BD from a disturbed soil sample, a sample is sieved to 2 mm or smaller particles. The facility takes a settled bulk density based upon a 10 mL volume and the mass needed to fill the 10 mL volume. This process is done on a dry basis. Textural analysis was determined by mechanical analysis hydrometer methodology. The soil textural analysis displayed 26% sand, 58% silt, and 16% clay. This is indicative of a silt loam soil, which is the primary soil in the region. Key soil properties of interest are tabulated below in Table 2. The % organic matter was determined through Walkley-Black OM testing methodology per the USDA and the Department of Sustainable Natural Resources (USDA, 2003).

Table 2: Key soil properties for each of the samples. This table displays the bulk density (BD), pH, Electric conductivity, Organic matter (OM), and Cation Exchange Capacity (CEC) of the soil samples. Porosity was estimated by the HYPROP and displayed the average and standard deviation of the four replicates

Sample	BD (g/cm^3)	pH	EC (dS/m)	% OM	CEC (meq/100g)	Porosity
Control (0% BC)	1.22	5.36	0.68	5.08%	20.3	54.0 ± 2.9
4% BC	1.07	5.34	0.74	5.44%	19.3	59.8 ± 0.5
7% BC	0.94	5.46	0.56	6.43%	18.9	64.5 ± 0.6
4% WS	1.13	6.19	0.84	5.22%	19.3	59.8 ± 0.5
7% WS	1.01	6.87	0.86	5.36%	18.9	63.8 ± 1.0

These samples were then tested for different soil hydraulic properties. An important thing to note regarding the initial soil sample properties in Table 2 is the OM for each of the samples. The initial control sample has an OM value that is high for a Palouse silt loam soil. This deviation from a typical value of 2.9% (National Cooperative Soil Survey, 2021) is likely due to the collection of disturbed soil samples. Disturbed soil lacks the typical structure of observed soil in the field. Furthermore, organic matter was likely introduced when it was disturbed, accounting for the higher initial OM content of the Control. Despite this, the general trend observed between samples is consistent with what is expected with increasing biochar amendment concentration in soil. Increasing the biochar concentration increases the OM in the soil. It is important to note, that intuitively biochar amendment would increase the OM of the soil to a larger value than observed. Upon evaluation, the testing service noted that some biochar in each of the samples floated in the chromate and sulfuric acid solution when testing consistent with Walkley-Black testing methodology. This likely caused the discrepancies between the measured and the expected changes in OM.

Experimental setup for determining soil hydraulic properties

Soil hydraulic properties of matric potential, diffusivity, and hydraulic conductivity (K) were measured using a HYPROP from METER group (G. Campbell et al., 2015) was used. The HYPROP follows the simplified evaporation method developed by Schindler in 1980 (Schindler et al., 2010). This method was further outlined in work by (Bezerra-Coelho et al., 2018) and Schindler et al. (2010). This method measures the matric potential of a confined saturated soil core (saturated from the bottom). As the soil sample dries, the matric potential is measured by two tensiometers at two different heights in the soil column. To account for the disturbed nature of the initial soil samples, each sample was intentionally packed into the soil rings prior to testing. The Control was packed into the soil ring to a common bulk density throughout the region, 1.20 g/cm^3 (National Cooperative Soil Survey, 2021). Each following sample was then packed following the same procedure to ensure that there was no significant variation in compaction between samples. The developed procedure reduces the effects of potential compaction between samples and creates support for the biochar affecting the BD of the samples, consistent with both the samples testing in the external laboratory (Table 2) and literature. Each soil

sample was tested in replicate (4 times per sample). The sample runs' results were averaged and compiled to obtain a representative (average) soil hydraulic property for each of the samples.

The HYPROP allows for the measured values to be fitted to a soil physics model of choosing. For this experiment, the Van Genuchten model (m=1-1/n) (Van Genuchten, 1980) was used and is fitted to the water retention values. Based on the measured values and the fitted curve, the HYPROP estimates the Van Genuchten parameters α, n, θ_r, θ_s, and Ksat using soil tension measurement.

Van Genuchten's 1980 paper provides relationships for converting from the matric potential and water content relationship to unsaturated hydraulic conductivity and diffusivity relationships. To determine the unsaturated K at any given moisture content of a soil, the following relationship was developed by Van Genuchten (Van Genuchten, 1980):

$$K_r(\theta) = \theta^{(1/2)} * \left(1 - \left(1 - \theta^{(1/m)}\right)^m\right)^2 \quad [12]$$

Where $K_r(\theta)$ is the relative hydraulic conductivity of the soil in terms of the water content of the soil, θ (commonly presented as S_e) is the relative moisture content of the soil given by the following relation $\theta = \frac{\theta - \theta r}{\theta s - \theta r}$, and m is a Van Genuchten parameter denoted by the relationship (m = 1 – 1/n). K_r can then be converted to the actual K(θ) of soil by the following relationship.

$$K(\theta) = K_r * K_{sat} \quad [13]$$

Where K(θ) is the hydraulic conductivity of the soil at a given water content, K_r is the relative hydraulic conductivity calculated from equation 12, and K_{sat} is the saturated hydraulic conductivity. Equations 12 and 13 lead to the indirect estimation of K(θ) for different soils. The K_{sat} value in equation 13 is key to the HYPROP accurately estimating unsaturated K of a soil sample. Without a determined K_{sat} (by outside methods) to anchor the conductivity relation in the HYPROP, significant variation in unsaturated K can be common. HYPROP measurements will show the general trend of unsaturated K, but the values may remain inaccurate. The K_{sat} for each soil sample was not directly measured using different methods, and therefore significant variation in both unsaturated and saturated K values was observed. To account for this, Rosetta, a Natural Resources Conservation Service (NRCS) soil tool, was used to estimate the K_{sat} of the samples from known soil properties by using pedotransfer functions (PTFs). Rosetta is found as a neural network inside of HYDRUS-1D, another NRCS soil tool (Šimůnek et al., 2013). Rosetta utilizes a hierarchical approach to estimating the K_{sat} for soil samples. This hierarchical approach gets more specific as more data is input into the system. Three levels of PTFs were used to estimate the K_{sat} values. The first PTF utilized soil texture (% sand, % silt, and % clay) and bulk density (BD) to estimate K_{sat}. The second PTF utilizes the soil texture, BD, and field capacity (FC = θ_v at – 33 kPa). The third PTF in Rosetta utilized soil texture, BD, FC, and PWP (PWP = θ_v at – 1,500 kPa). Biochar amendment is accounted for in the PTF calculations through changes in BD, FC, and PWP when biochar was applied to the soil. Changes to the soil texture, while likely, were ignored. The K_{sat} values obtained from the three PTFs (in Rosetta) were then averaged to achieve the estimated K_{sat} value for the soil. The average K_{sat}

values were then used in equation 13 to determine the unsaturated K for the soil samples. The diffusivity of the soil is the last parameter that is required to be input into the model. Soil diffusivity is the hydraulic conductivity of a soil divided by the flux of water per unit of moisture content. Van Genuchten provides this relation in his 1980 paper (Van Genuchten, 1980). The relationship that Van Genuchten developed is as follows.

$$D(\theta) = K(\theta)\left|\frac{d\psi}{d\theta}\right| \quad [14]$$

Where D(θ) is the diffusivity of the soil at any given water content, K(θ) is the hydraulic conductivity at any given water content calculated from equation 13, dψ is the difference in matric potential between water contents, and dθ is the difference in water contents. The equations above are applicable to the moisture range between the residual (θ_r) and the saturated (θ_s) water contents. In nature, the soil at the surface, and shallow depths below, may go below θ_r if the environment is sufficiently dry or drought conditions occur. To account for the potential drought conditions, there was a need to model soil hydraulic properties beyond θ_r. Campbell and Shiozawa in 1992 illustrated that moisture content below θ_r, film water movement prevails and will decrease linearly with the log-scale matric suction (G. S. Campbell & Shiozawa, 1992). Below θ_r, the matric suction and film water content relationship can be expressed as:

$$\psi = \psi_0 \left(\frac{\psi_{\theta_r}}{\psi_0}\right)^{\frac{\theta}{\theta_r}} \quad [15]$$

As suggested by (Schneider & Goss, 2012), $\psi_0 = 6.25 \times 10^{-9}$ (m) corresponding to air dry moisture of soil. According to Wang et al., 2019, for film flow below θ_r the conductivity of the soil can then be determined by the following (Wang et al., 2019):

$$K = K_{\theta_r}\ \frac{\theta}{\theta_r}\left(\frac{\psi}{\psi_{\theta_r}}\right)^{-\frac{2}{3}} \quad [16]$$

The diffusivity is less complex to model below θ_r. Since the diffusivity is a function of both matric potential and hydraulic conductivity, once both these properties are determined, the diffusivity is also known based on equation 14.

For inputting the soil hydraulic data into the model, the water content increased linearly from 0 to θ_s. The magnitude of each saturation range is unique to each sample due to biochar affecting the θ_s for the samples. The moisture content increases at a rate of 0.5% moisture over the entire range: providing adequate resolution for the model. The data was averaged across all four replicates and compiled for MATLAB.

Lastly, the effects of biochar amendment on plant available water (PAW) were briefly examined. PAW is largely considered to be the difference between FC and PWP. FC is commonly presented at a soil tension of -33 kPa but can also be at -10 kPa or -6 kPa, depending on the soil texture. However, research has shown that water may be available for plant uptake greater than -33 kPa FC (Lier, 2017). Furthermore, this research showed that the uptake beyond FC may represent a significant share of the total water uptake (Lier, 2017). This research presents the importance of including PAW at higher saturation values (lower tensions) when available.

Initial conditions and model setup

Hourly temperature and relative humidity data for the year 2010 were downloaded from NOAA meteorological data (NOAA, 2021) (national weather service data) for Spokane airport outside of Spokane, Washington, to estimate soil evaporation. The downloaded data had an hourly record of dew point and dry bulb temperature. The relative humidity was derived from psychrometric relation based on the August-Roche-Magnus approximation, which implies that saturation vapor pressure changes approximately exponentially with temperature under typical atmospheric conditions. The weather data provides a regional perspective of the climate, humidity, and temperature in the Palouse region, where the simulation is located. The driving forces of the simulation are the redistribution of the water throughout the profile and evaporation from the hillslope surface. The model runs under the assumption that this is a bare hillslope, has no vegetation, and the soil is isometric and uniform. The entire field is held initially at FC_{-33kPa}; positive pressure in the profile is not a factor. The field capacity is set by the soil sample that is applied to the soil, i.e., if biochar amendment occurs, the amendment area is initially at biochar's FC value. This sets the initial conditions for the simulation, and these conditions represent a later spring-early summer field and after a rainfall event. The model is assumed to begin on April 30th and will dry over the next two months, 60 days, under the primary forces of evaporation and water redistribution. To assess biochar's potential use as a precision agriculture technique, an application region was chosen on the hillslope profile. We assumed that the biochar application region covers 5% of the top of the hillslope. Biochar application will be applied to a depth of 30 cm. Each of the biochar types and application concentrations (4% and 7% RSD) will be tested against the control soil sample. It is important to note that biochar was applied to a uniform soil profile. A uniform profile disregards the argillic and fragipan horizons that can form throughout the winter months in the Palouse. These hardpan layers drive subsurface lateral flow in the soil profiles, which are important for understanding stored water and redistribution throughout a hillslope. Applying biochar to a uniform soil profile will still provide valuable insights into how biochar can affect water redistribution in undulating topography.

Finally, the effectiveness of biochar amendment from this model will depend on the initial conditions set for the simulation. The results presented in this research depict one specific scenario and outcome. Changing the initial conditions will change the final output from the model: rendering biochar either effective or ineffective depending on the model inputs. Universal blanket statements regarding the effectiveness of biochar in all scenarios should be avoided.

Results and Discussion

This research has two primary results: 1) the effects of biochar amendment on soil hydraulic and physical properties; 2) the output from the developed model.

Biochar's effects on silt loam soil hydraulic properties

Table 2 displays the soil physical properties analyzed in the lab. Additionally, the BD is estimated by the HYPROP and was compiled for each of the replicates. The BD values (g/cm^3) obtained from the HYPROP is as follows:

Table 3: Bulk density (BD in g/cm^3) obtained from the HYPROP for each of the samples. The values shown in the table are the averaged values from each of the runs with standard deviation

Sample	BD (g/cm^3)
Control (0% BC)	1.22 ± 0.077
4% BC	1.063 ± 0.013
7% BC	0.935 ± 0.017
4% WS	1.065 ± 0.013
7% WS	0.96 ± 0.028

Table 3 displays the bulk density values from the HYPROP. These values were not significantly different from the best test values and therefore were used for T-testing. BD and porosity were the two physical properties that were used in T-testing against the Control with an $\alpha = 0.05$. With biochar amendment, the BD of all samples was reduced. Increasing the concentration of the biochar amendment further increased the BD of the soil. The reduction in BD from all biochar amendments and concentrations was statistically significant. The soil porosity increased when amended with biochar. Furthermore, increasing the concentration of biochar from 4% to 7% further increased the porosity of the soil. The increases in porosity were statistically significant.

Biochar amendment in silt loam soil did influence the soil's hydraulic properties, which is consistent with literature (Biederman & Stanley Harpole, 2013; Caroline A. Masiello, Brandon Dugan, Catherine E. Brewer, Kurt A. Spokas, Jeffrey M. Novak, 2019; El-naggar et al., 2019; Hardie et al., 2014; Simon Jeffery et al., 2019). Compiled in Table 4 shows the averaged Van Genuchten (VG) parameters and water capacity values (permanent wilting point, PWP, and field capacity, FC) for each of the samples. The FC is reported at two tensions, -33 kPa (FC_{-33kPa}) and -6 kPa (FC_{-6kPa}). While the -33 kPa value is more conventionally used, researchers do report FC at -6 kPa as plants can uptake water at tensions lower than -33 kPa (Logsdon, 2019).

Table 4: Compiled VG parameters obtained from HYPROP and WP4C measurements. The values displayed are the averages across the four replicates with standard deviation displayed. This table also includes biochar's effects on the field capacity (FC) and permanent wilting point (PWP) estimated from the HYPROP.

	100% soil	**4% RSD**	**7% RSD**	**4% WS**	**7% WS**
α (1/cm)	0.0069 ± 0.002	0.0097 ± 0.002	0.0172 ± 0.003	0.009 ± 0.002	0.012 ± 0.003
n	1.537 ± 0.14	1.4635 ± 0.09	1.3908 ± 0.05	1.4963 ± 0.06	1.5128 ± 0.07
m	0.345 ± 0.06	0.3149 ± 0.04	0.2803 ± 0.02	0.331 ± 0.03	0.3378 ± 0.03
Θr (%)	5.18 ± 1.51	3.28 ± 1.69	5.73 ± 6.95	3.9 ± 1.01	4.4 ± 0.3
Θs (%)	51.45 ± 1.0	56.4 ± 1.58	54.15 ± 1.48	55.7 ± .44	61.8 ± 3.79
Ks* (cm/day)	49	102	148	101	157
FC_{-33kPa} (%)	33.2 ± 2.3	33.1 ± 2.2	27.2 ± 0.9	32.6 ± 0.7	32.4 ± 1.8
FC_{-6kPa} (%)	48 ± 1.3	50.7 ± 2.1	44.1 ± 0.8	50.3 ± 0.9	53.7 ± 4.2
PWP (%)	9.1 ± 0.5	8.7 ± 0.5	7.1 ± 0.5	8.5 ± 0.1	8.5 ± 0.8

*denotes values estimated from pedotransfer functions

Soil hydraulic properties were tested statistically for significance using a T-test with $\alpha = 0.05$. FC_{-33kPa}, FC_{-6kPa}, $PWP_{-1500kPa}$, residual moisture content (θ_r), and saturated moisture content (θ_s) were all tested for significance. The FC_{-33kPa} p-values were 0.96, 0.021,0.0627, and 0.267 for the 4% RSD, 7% RSD, 4% WS, and 7% WS respectively. This indicates that the 7% RSD did significantly affect the FC_{-33kPa}. Biochar showed more significant effects at lower tensions which is indicated by the increased moisture content at FC_{-6kPa} for 4% RSD, 4% WS, and 7% WS. The 7% RSD showed a reduction in retention at FC_{-6kPa}. The 7% RSD, 4% WS, and 7% WS were all statistically significant. In general, biochar amendment reduced the PWP of the soil. However, the 7% RSD amendment was the only amendment that significantly changed the $PWP_{-1500kPa}$; all other samples were not significant. Similarly, samples (minus the 7% RSD) showed a reduction in θ_r. However, biochar did not significantly affect the θ_r. All samples showed an increase in θ_s; only 4% RSD, 4% WS, and 7% WS samples were significant. In general, biochar amendment showed a greater effect on the soil in wet field conditions, indicating that biochar amendment impacts water retention at lower matric potentials.

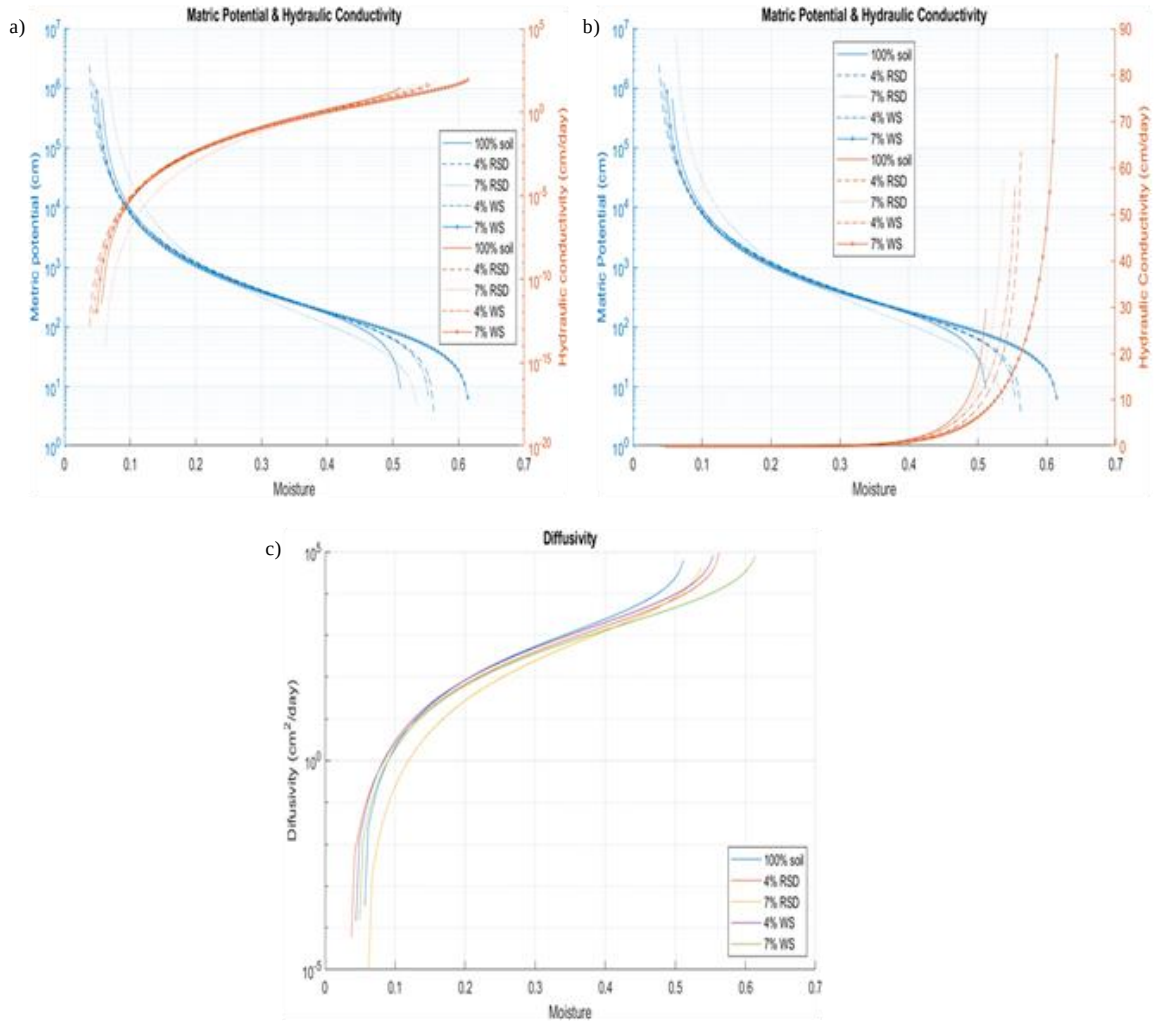

Figure 6: Matric potential, hydraulic conductivity, and diffusivity curves for all samples. The matric potentials (blue axes) are displayed in positive values but are inherently negative values. a) denotes the matric potential and hydraulic conductivity (in log scale) vs. moisture content. b) displays the matric potential and hydraulic conductivity (in normal scale) vs. moisture content. c) shows the diffusivity vs. moisture content. a) and b) are included to highlight hydraulic conductivity changes in both dry and wet conditions. The generated curves are the averages of the four sample replicates.

From these parameters in Table 4, Table 2, and equations 12 through 16, the matric potential curve (water retention curve, WRC), the hydraulic conductivity curve, and the diffusivity curve for each of the samples are generated in Figure 6. Figure 6 was generated using the averaged VG parameters from each of the four sample replicates. Figure 6 shows that with biochar amendment, there is minimal change to water retention through matric potentials ranging from -10^2 to -10^5 cm. Despite more deviation from the Control at tensions around -10^5, the changes to PWP and θ_r were not significant. Therefore, it is probable that the changes to water retention around tensions of -10^5 were not significant. However, in saturated conditions, biochar showed more significant effects. The observed deviation in water retention from the Control in Figure 10 would further indicate that biochar shows greater impact in changing the soil hydraulic properties in wet conditions. At tensions around -

10^2 hPa, the 4% RSD,4% WS, and 7% WS showed increased water retention at the same matric potential. The 7% RSD deviated from the other samples and showed a reduction in water retention at the same matric potentials. In general, the RSD amendment showed inconsistent effects on water retention. The inconsistency creates difficulties in making definitive statements regarding the effects of the RSD amendment on the silt loam soil. The greater effect of biochar and an apparent increase in water retention indicates that the change in soil porosity induced by biochar allows more water to be retained in the soil. This is consistent with Devereux et al. (2013) and Gaskin et al. (2007), who showed increases in the water holding capacity at tensions of -20 kPa to -100 kPa (Devereux et al., 2013; Gaskin et al., 2007). The increase in consistency observed with the WS samples could indicate that the particle size and surface interactions affected the pore characteristics in the soil differently (Z. L. Liu et al., 2017) but more consistently. However, the alterations in soil hydraulic properties induced by biochar amendments are general trends and may or may not be significant.

The increase in effect from biochar amendment observed in wetter conditions translated to more significant changes to the unsaturated hydraulic conductivity (K) as the soil approached saturated conditions. The saturated hydraulic conductivity (K_{sat}) values, estimated from the PTF's, showed significant ($\alpha = 0.05$) increases in K_{sat} when amended with biochar (both concentration and type). Generally, biochar amendment showed an apparent reduction in unsaturated hydraulic conductivity as the soil approached saturated conditions (moisture contents > 0.35 or 35%). This is consistent with research performed by Barnes et al. (2014). They found that despite an increase in porosity and a reduction in BD, the hydraulic conductivity of the soil decreased. Further, they pointed to two mechanisms that could be driving these effects: the internal structure of biochar and the high field capacity of biochar. They described that the high internal porosity of the biochar creates two theoretical flow pathways for water to move, one in the interstitial space between the soil and biochar particles and the second within the biochar itself. The second of which increases the tortuosity of the soil, which would decrease K. Lastly, their research pointed to the idea that biochar has a high field capacity, and therefore water may have continued to be absorbed by the biochar; leading to an observation of an apparent decrease in K despite more water being in the soil (Barnes et al., 2014). These two mechanisms could be driving the reduction in unsaturated K observed in this work. In sandy loam soils, the addition of biochar enhanced the transport of water under unsaturated conditions by reducing the formation of larger pores (draining pores) and promoting finer inter-particle pore formation (Villagra-Mendoza & Horn, 2018). The apparent reduction in unsaturated K could indicate greater air space in the soil matrix, increasing water movement as a vapor in the soil, although this was not measured. The shape of the diffusivity curve mimics the conductivity curves for each of the soil samples. The effects of biochar (both concentration, 4% and 7%, and type, RSD, and WS) were consistent between the conductivity curves and the diffusivity curves.

Model output

Both RSD and WS amendments were simulated in the developed model, consistent with the initial conditions and theory described in the methods section. Both biochar types were amended at 4% and 7% concentrations by dry mass. The model simulated the drying of the soil for 60 days (beginning on April 30th of 2010) and tracked

the changes in soil moisture on an hourly basis. Figure 7 displays the moisture difference plots from each of the four biochar samples tested. Figure 7 displays the changes in moisture content at the end of simulated period.

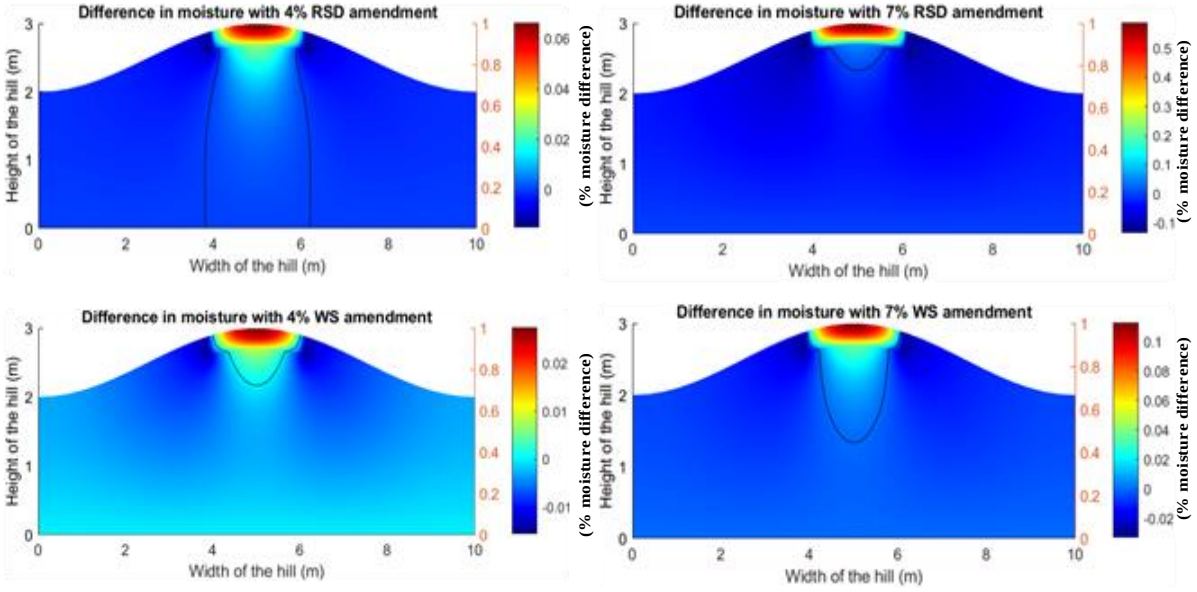

Figure 7: Simulated moisture difference plots at the end of the simulated growing season. All amendment samples are shown, which display areas of increased and decreased moisture. The black contour line indicates the zero-contour line, which displays no change in moisture between the Control and the biochar amendment

The above plots denote the difference in moisture at the end of the simulation between the biochar amendment and the Control. The black contour line denotes a zero-contour line, which indicates the area in the plot in which no observed change in moisture is present. More specifically, areas outside of the zero-contour line indicate a reduction in moisture content, whereas the area inside of the contour line will denote an increase in moisture content. All biochar samples showed an increase in moisture content in and around the amendment area. The magnitude in which the retention increased varied between each of the samples, with the 7% RSD having the largest increase in moisture content, upwards of a 0.5% increase in moisture in some areas compared to the Control. The 4% WS sample showed a smaller maximum increase in retention with just over 0.02% increase in retention from the Control. This is minimal. The 4% RSD and 7% WS samples were similar in capacity to increase retention leading to a maximum increase in retention of 0.06% and 0.1% increase from the Control for the 4% RDS and 7% WS, respectively. All samples showed a decrease in moisture content on either side adjacent to the amendment area. There was no additional water input into the system throughout the simulation, which indicates that less moisture was distributed laterally from the top of the hillslope, which led to less moisture in these areas. This is consistent with expectations. The differences in moisture generated from biochar amendment were, in general, minimal. However, it is important to note that biochar will change how moisture is retained and redistributed in the soil.

It is unclear what precisely caused the differences between the RSD and WS samples. Research by Barnes et al. (2014) makes a compelling case for the reasons how biochar particle size and porosity affect the soil matrix and, more specifically, the hydraulic conductivity (Barnes et al., 2014). This research points to the porosity and particle size of biochar having the primary influence on the conductivity. They attributed the biochar's internal porosity and particle size to changing the flow pathways that water can take in the soil matrix. The research also denoted adding biochar to the soil increases the field capacity (Barnes et al., 2014). These things in tandem act to have an effect on the hydraulic conductivity and the water retention in the soil.

The zero-contour lines indicate differences in vertical redistribution of water deeper into the soil profile. The 4% RSD sample showed the most vertical redistribution of water into the soil profile. The 4% RSD sample showed the largest increase in unsaturated hydraulic conductivity, which would account for more vertical moisture redistribution into deeper portions of the soil profile. Despite the 4% WS amendment having a larger increase in the unsaturated hydraulic conductivity compared to the 7% WS sample, the 7% WS sample showed more vertical redistribution. The 7% RSD amendment showed minimal vertical redistribution of water.

It is important to note that this discussion involves the change in moisture observed at the end of the simulation. While the results at the end of the simulation highlight the potential effects of biochar deep into the growing season, it does not provide a full picture of biochar's effects on soil water throughout the entire simulation. The change in moisture from biochar would be cumulative, and any difference in moisture observed at any point in the simulation would influence theoretical hydrologic and crop processes. The developed model allows for the animation of the model over time, which can be found here: youtube.com/watch?v=IP5YZSIXFiM.

Additionally, plotting the difference in soil moisture between the biochar amendment and the Control over time for a specific location provides an indication of the cumulative effects of biochar amendment. Figure 8 displays the moisture difference between a respective biochar amendment and the control sample for a specific node in the soil profile over time. The node is located at position (5, 2.89) which is near the soil surface in the amendment area.

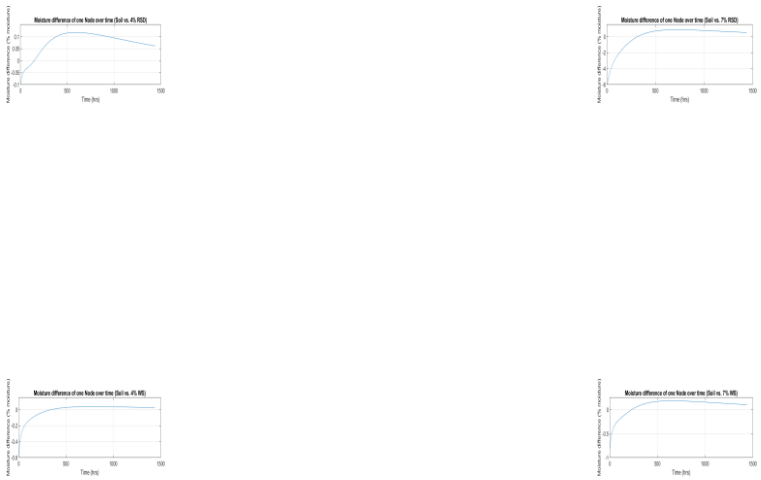

Figure 8: Moisture difference plot (BC amendment vs. Control) for one node throughout the duration of the simulation

Figure 8 provides a clearer understanding of how biochar amendment changes over time. Initially, all samples showed a reduction in moisture content when amended with biochar. This is attributed to the differences in the FC_{-33kPa} with biochar amendment. These graphs would change with the initial conditions set for the model (exp. If the field was initially saturated moisture content). Despite the initial decrease in moisture content, over time, all samples showed eventual increases in moisture content as the soil dried. The magnitude of the changes in moisture content varied depending on the amendment type and concentration.

One primary hydrologic factor that makes this model more realistic to the Palouse region is lacking in the current iteration of the model. Argillic and fragipan horizons are found in the Palouse, restrict water flow vertically. These layers generate higher runoff and lateral flow, courtesy of the formation of perched water tables (Brooks et al., 2004, 2012). This model neglects this complexity, and therefore, displays more vertical redistribution of water than likely possible with a shallow restrictive layer. Implementing this into the soil profile would change the output of this model and would require further exploration. Despite this limitation, the 7% RSD amendment shows indications that it would be effective in shallow restricted soils. Water was predominately held in and around the amendment area for the 7% RSD sample, suggesting that even when applied to shallow restricted soils, it may be effective at increasing the soil moisture content where applied.

This research culminates in one primary finding; biochar amendment will change moisture redistribution in an undulating topography. The magnitude of the change in soil moisture may vary; however, in general, biochar

retained more moisture in the tops of the hillslopes. The effectiveness of amendment will vary depending on the soil type, biochar properties, and initial moisture content that the model sets. This is consistent with findings throughout research which found varied effectiveness of biochar amendment depending on the physiochemical properties of the biochar and soil (Agegnehu et al., 2017; Razzaghi et al., 2020; Verheijen et al., 2010). Therefore, despite the promising output from the simulations in this work, more research is required to definitively assert that biochar amendment influences soil water redistribution in these ways. The model provides information that may inform stakeholders and decision-makers around integrating biochar into precision agriculture.

Conclusion

Biochar amendment to a Palouse silt loam soil changed the redistribution of water in a soil profile. Increasing the biochar amendment concentration correlated with more positive effects on the soil water holding capacities. Biochar amendment showed little effect on the matric potential across normal unsaturated conditions. However, in saturated or near-saturated conditions, the soil was able to retain more water when amended with biochar. There was an apparent reduction in unsaturated K for both amendment concentrations despite an increase in K_{sat} for both amendments. Ultimately, biochar appeared to have greater influence in the soil under saturated or near-saturated conditions, exhibiting more promising results with amendment. The developed vadose zone model showed promise as a tool for predicting changes in soil moisture over time. Over the simulated period of 60 days, the amended soil showed increased soil moisture at the tops of the hillslopes. This was consistent with all amendment types and concentrations. Additionally, the cumulative effects of biochar indicated the biochar amendment retains more water than the Control as the soil dries. While the magnitude of the increase in retention varied amongst samples, the results are promising. These results indicate that while biochar type affects the soil matrix differently, both the WS and RSD samples could be effective in manipulating water redistribution in uniform Palouse soils.

Literature Cited

Adamchuk, V. I., Hummel, J. W., Morgan, M. T., & Upadhyaya, S. K. (2004). *On-the-go soil sensors for precision agriculture*. *44*, 71–91. https://doi.org/10.1016/j.compag.2004.03.002

Agegnehu, G., Srivastava, A. K., & Bird, M. I. (2017). The role of biochar and biochar-compost in improving soil quality and crop performance: A review. *Applied Soil Ecology*, *119*, 156–170. https://doi.org/10.1016/j.apsoil.2017.06.008

Aller, D., Rathke, S., Laird, D., Cruse, R., & Hatfield, J. (2017). Impacts of fresh and aged biochars on plant available water and water use efficiency. *Geoderma*. https://doi.org/10.1016/j.geoderma.2017.08.007

Barnes, R. T., Gallagher, M. E., Masiello, C. A., Liu, Z. L., & Dugan, B. (2014). Biochar-Induced Changes in Soil Hydraulic Conductivity and Dissolved Nutrient Fluxes Constrained by Laboratory Experiments. *PLoS One*, *9*(9). https://doi.org/ARTN e10834010.1371/journal.pone.0108340

Beven, K. J., & Kirkby, M. J. (1979). A physically based, variable contributing area model of basin hydrology. *Hydrological Sciences Bulletin*, *24*(1), 43–69. https://doi.org/10.1080/02626667909491834

Bezerra-Coelho, C. R., Zhuang, L., Barbosa, M. C., Soto, M. A., & Van Genuchten, M. T. (2018). Further tests of the HYPROP evaporation method for estimating the unsaturated soil hydraulic properties. *Journal of Hydrology and Hydromechanics*, *66*(2), 161–169. https://doi.org/10.1515/johh-2017-0046

Bhogal, A., Nicholson, F. A., & Chambers, B. J. (2009). Organic carbon additions: Effects on soil bio-physical and physico-chemical properties. *European Journal of Soil Science*, *60*(2), 276–286. https://doi.org/10.1111/j.1365-2389.2008.01105.x

Biederman, L. A., & Stanley Harpole, W. (2013). Biochar and its effects on plant productivity and nutrient cycling: A meta-analysis. *GCB Bioenergy*, *5*(2), 202–214. https://doi.org/10.1111/gcbb.12037

Brooks, E., Boll, J., & McDaniel, P. A. (2004). A hillslope-scale experiment to measure lateral saturated hydraulic conductivity. *Water Resources Research*, *40*(4), 1–10. https://doi.org/10.1029/2003WR002858

Brooks, E., Boll, J., & McDaniel, P. A. (2012). Hydropedology in Seasonally Dry Landscapes: The Palouse Region of the Pacific Northwest USA. *Hydropedology*, 329–350. https://doi.org/10.1016/B978-0-12-386941-8.00010-1

Brown, M., Heinse, R., Johnson-Maynard, J., & Huggins, D. (2021). Time-lapse mapping of crop and tillage interactions with soil water using electromagnetic induction. *Vadose Zone Journal*, *November 2020*, 1–16. https://doi.org/10.1002/vzj2.20097

Burt, T. ., & Butcher, D. P. (1985). Topographic controls of soil moisture distributions. *Journal of Soil Science*, *36*(3), 469–486. https://doi.org/10.1111/j.1365-2389.1985.tb00351.x

Campbell, G., Campbell, C., Cobos, D., Crawford, L. B., Rivera, L., & Chambers, C. (2015). *Operation Manual for HYPROP*. http://library.metergroup.com/Manuals/UMS/Hyprop_Manual.pdf

Campbell, G., Campbell, C., Cobos, D., Crawford, L. B., Rivera, L., & Chambers, C. (2021). *How to measure soil hydraulic conductivity— Which method is right for you?* https://www.metergroup.com/environment/articles/how-to-measure-soil-hydraulic-conductivity-which-method-is-right-for-you/

Campbell, G. S., & Shiozawa, S. (1992). Prediction of hydraulic properties of soils using particle-size distribution and bulk density data. In *International Workshop on Indirect Methods for Estimating the Hydraulic Properties of Unsaturated Soils*.

Caroline A. Masiello, Brandon Dugan, Catherine E. Brewer, Kurt A. Spokas, Jeffrey M. Novak, Z. L. and G. S. (2019). Biochar effects on soil hydrology. In J. Lehmann & S. Joseph (Eds.), *Biochar for Environmental Management* (Second, pp. 543–562). https://doi.org/10.4324/9780203762264-26

Castellini, M., Giglio, L., Niedda, M., Palumbo, A. D., & Ventrella, D. (2015). Soil & Tillage Research Impact of biochar addition on the physical and hydraulic properties of a clay soil. *Soil & Tillage Research*, *154*, 1–13. https://doi.org/10.1016/j.still.2015.06.016

Chowdhury, Z. Z., Karim, M. Z., Ashraf, M. A., & Khalid, K. (2016). Influence of Carbonization Temperature on Physicochemical Properties of Biochar derived from Slow Pyrolysis of Durian Wood (Durio zibethinus) Sawdust. *Bioresources*, *11*(2), 3356–3372.

Chung, C.-K., Kim, J.-H., Kim, J., & Kim, T. (2018). Hydraulic Conductivity Variation of Coarse-Fine Soil Mixture upon Mixing Ratio. *Advances in Civil Engineering*, *2018*, 1–11. https://doi.org/10.1155/2018/6846584

Devereux, R. C., Sturrock, C. J., & Mooney, S. J. (2013). The effects of biochar on soil physical properties and winter wheat growth. *Earth and Environmental Science Transactions of the Royal Society of Edinburgh*, *103*(1), 13–18. https://doi.org/10.1017/S1755691012000011

Dokoohaki, H., Miguez, F. E., Laird, D., Horton, R., & Basso, A. S. (2017). Assessing the Biochar Effects on Selected Physical Properties of a Sandy Soil: An Analytical Approach. *Communications in Soil Science and Plant Analysis*, *48*(12), 1387–1398. https://doi.org/10.1080/00103624.2017.1358742

Eagleson, P. (1978). Introduction to Water Balance Dynamics. *Water Resources Research*, *14*(5), 705–712.

Edeh, I. G., & Buss, W. (2020). *Science of the Total Environment A meta-analysis on biochar ' s effects on soil water properties – New insights and future research challenges*. *714*. https://doi.org/10.1016/j.scitotenv.2020.136857

El-naggar, A., Soo, S., Rinklebe, J., Farooq, M., & Song, H. (2019). Geoderma Biochar application to low

fertility soils : A review of current status , and future prospects. *Geoderma*, *337*(May 2018), 536–554. https://doi.org/10.1016/j.geoderma.2018.09.034

Frazier, B. E., & Cheng, Y. (1989). Remote sensing of soils in the Eastern Palouse region with landsat thematic mapper. *Remote Sensing of Environment*, *28*(C), 317–325. https://doi.org/10.1016/0034-4257(89)90123-5

Fuentes, J. P., Flury, M., Huggins, D. R., & Bezdicek, D. F. (2003). Soil water and nitrogen dynamics in dryland cropping systems of Washington State, USA. *Soil and Tillage Research*, *71*(1), 33–47. https://doi.org/10.1016/S0167-1987(02)00161-7

Gaskin, J. W., Speir, A., Morris, L. M., Ogden, L., Harris, K., Lee, D., & Das, K. C. (2007). *Potential for Pyrolysis Char to Affect Soil Moisture and Nutrient Status of a Loamy Sand Soil*.

Hall, M., Young, D. L., & Walker, D. J. (1999). Agriculture in the Palouse, a Portrait of Diversity. *Statistics, Idaho Agricultural County, Latah*.

Hardie, M., Clothier, B., Bound, S., Oliver, G., & Close, D. (2014). Does biochar influence soil physical properties and soil water availability? *Plant and Soil*, *376*(1–2), 347–361. https://doi.org/10.1007/s11104-013-1980-x

Hartmans, M. A., & Michalson, E. L. (2000). *Evaluating the Economic & Environmental Impacts of Farming Practices on the Palouse Using PLANETOR*.

Hubbert, M. K. (1957). Darcy's law and the field equations of the flow of underground fluids. In *International Association of Scientific Hydrology. Bulletin* (Vol. 2, Issue 1). https://doi.org/10.1080/02626665709493062

Hudson, B. (1994). Soil organic matter and available water capacity. *Soil and Water Conservation*, *April*, 189–194.

Jeffery, S., Verheijen, F. G. A., van der Velde, M., & Bastos, A. C. (2011). A quantitative review of the effects of biochar application to soils on crop productivity using meta-analysis. *Agriculture, Ecosystems and Environment*, *144*(1), 175–187. https://doi.org/10.1016/j.agee.2011.08.015

Jeffery, Simon, Abalos, D., Spokas, K. A., & Verheijen, F. G. A. (2019). Biochar effects on crop yield. In J. Lehmann & S. Joseph (Eds.), *Biochar for Environmental Management* (Second, pp. 1–2). https://doi.org/10.4324/9780203762264-19

Jin, K., Cornelis, W. M., Schiettecatte, W., Lu, J., Yao, Y., Wu, H., Gabriels, D., De Neve, S., Cai, D., Jin, J., & Hartmann, R. (2007). Effects of different management practices on the soil-water balance and crop yield for improved dryland farming in the Chinese Loess Plateau. *Soil and Tillage Research*, *96*(1–2), 131–144. https://doi.org/10.1016/j.still.2007.05.002

Kaiser, V. (1967). Soil Erosion and Wheat Yields in Whitman County, Washington. *Northwest Science*, *41*(2),

85–91.

Kirkham, M. B. (2005). *Principles of Soil and Plant water relations* (K. Sonnack (ed.)). Dana Dreibelbis. http://www.esalq.usp.br/lepse/imgs/conteudo_thumb/Principles-of-Soil-and-Plant-Water-Relations-by-M-B--Kirkham--2005-.pdf

Kühling, I., Redozubov, D., Broll, G., & Trautz, D. (2017). Impact of tillage, seeding rate and seeding depth on soil moisture and dryland spring wheat yield in Western Siberia. *Soil and Tillage Research*, *170*, 43–52. https://doi.org/10.1016/j.still.2017.02.009

Lehmann, J., & Joseph, S. (2009). *Biochar for Environmental Management* (First, p. 449). Earthscan.

Lehmann, J., & Kleber, M. (2015). The contentious nature of soil organic matter. *Nature*, *528*(7580), 60–68. https://doi.org/10.1038/nature16069

Lier, Q. de J. van. (2017). Field capacity, a valid upper limit of crop available water? *Agricultural Water Management*.

Lim, T. J., Spokas, K. A., Feyereisen, G., & Novak, J. M. (2016). Predicting the impact of biochar additions on soil hydraulic properties. *Chemosphere*, *142*, 136–144. https://doi.org/10.1016/j.chemosphere.2015.06.069

Liu, Z. (2016). *Interactions between Biochar, Soil, and Water*. https://search.proquest.com/pqdtglobal/docview/1999348435/83940BAE4E3E42FEPQ/1?accountid=15115

Liu, Z. L., Dugan, B., Masiello, C. A., & Gonnermann, H. M. (2017). Biochar particle size, shape, and porosity act together to influence soil water properties. *PLoS One*, *12*(6). https://doi.org/ARTN e017907910.1371/journal.pone.0179079

Logsdon, S. (2019). Should Upper Limit of Available Water be Based on Field Capacity? *Agrosystems, Geosciences & Environment*, *2*(1), 1–6. https://doi.org/10.2134/age2019.08.0066

MathWorks. (2006). *Partial differential equation toolbox: for use with MATLAB : COMSOL AB*. http://books.google.com/books?id=A7jpQgAACAAJ

McDaniel, P. A., Gabehart, R. W., Falen, A. L., Hammel, J. E., & Reuter, R. J. (2001). Perched Water Tables on Argixeroll and Fragixeralf Hillslopes. *Soil Science Society of America Journal*, *65*(3), 805–810. https://doi.org/10.2136/sssaj2001.653805x

McDaniel, P. A., Regan, M. P., Brooks, E., Boll, J., Barndt, S., Falen, A., Young, S. K., & Hammel, J. E. (2008). Linking fragipans, perched water tables, and catchment-scale hydrological processes. *Catena*, *73*(2), 166–173. https://doi.org/10.1016/j.catena.2007.05.011

National Cooperative Soil Survey. (2021). *Estimated Soil Water Retention Curve for Palouse Silt Loam Soil*. https://ncsslabdatamart.sc.egov.usda.gov/rptExecute.aspx?p=31724&r=6&submit1=Get+Report

NOAA. (2021). *Climate Data Online*. www.ncdc.noaa.gov/cdo-web

Palansooriya, K. N., Ok, Y. S., Awad, Y. M., Lee, S. S., Sung, J. K., Koutsospyros, A., & Moon, D. H. (2019). Impacts of biochar application on upland agriculture: A review. *Journal of Environmental Management*, *234*, 52–64. https://doi.org/10.1016/j.jenvman.2018.12.085

Rawls, W. J., Pachepsky, Y. A., Ritchie, J. C., Sobecki, T. M., & Bloodworth, H. (2003). Effect of soil organic carbon on soil water retention. *Geoderma*, *116*(1–2), 61–76. https://doi.org/10.1016/S0016-7061(03)00094-6

Razzaghi, F., Bilson, P., & Arthur, E. (2020). Geoderma Does biochar improve soil water retention ? A systematic review and meta- analysis. *Geoderma*, *361*(October 2019), 114055. https://doi.org/10.1016/j.geoderma.2019.114055

Schindler, U., Durner, W., von Unold, G., & Muller, L. (2010). *Evaporation Method for Measuring Unsaturated Hydraulic Properties of Soils : Extending the Measurement Range*. *74*(4), 1071–1083. https://doi.org/10.2136/sssaj2008.0358

Schlegel, A. J., Assefa, Y., Haag, L. A., Thompson, C. R., Holman, J. D., & Stone, L. R. (2017). Yield and soil water in three dryland wheat and grain sorghum rotations. *Agronomy Journal*, *109*(1), 227–238. https://doi.org/10.2134/agronj2016.07.0387

Schneider, M., & Goss, K.-U. (2012). Prediction of the water sorption isotherm in air dry soils. *Geoderma*, *170*, 64–69. https://doi.org/10.1016/j.geoderma.2011.10.008

Sheets, K. R., & Hendrickx, J. M. H. (1995). Noninvasive Soil Water Content Measurement Using Electromagnetic Induction. *Water Resources Research*, *31*(10), 2401–2409. https://doi.org/10.1029/95WR01949

Šimůnek, J., M. Šejna, A., Saito, H., Sakai, M., & Genuchten, M. T. Van. (2013). The HYDRUS-1D software package for simulating the movement of water, heat, and multiple solutes in variably saturated media, version 4.17. In *HYDRUS Software Series 3D* (Issue June). https://www.pc-progress.com//Downloads/Pgm_Hydrus1D/HYDRUS1D-4.17.pdf

Staff, S. S. (2021). *Palouse Series*. https://soilseries.sc.egov.usda.gov/OSD_Docs/P/PALOUSE.html

USDA. (1978). *Palouse cooperative river basin study.* //catalog.hathitrust.org/Record/000302437

USDA. (2003). Soil Survey Standard Test Method Organic Carbon. *Soil Survey Standart Test Method*, 1–5. http://citeseerx.ist.psu.edu/viewdoc/download?doi=10.1.1.165.1882&rep=rep1&type=pdf

Van Genuchten, M. T. (1980). A Closed-form Equation for Predicting the Hydraulic Conductivity of Unsaturated Soils. *Soil Science Society of America Journal*, *May*. https://doi.org/10.2136/sssaj1980.03615995004400050002x

Verheijen, F., Jeffery, S., Bastos, A. C., Van Der Velde, M., & Diafas, I. (2010). Biochar Application to Soils: A Critical Scientific Review of Effects on Soil Properties, Processes and Functions. In *Environment* (Vol. 8, Issue 4). https://doi.org/10.2788/472

Wang, Y., Merlin, O., Zhu, G., & Zhang, K. (2019). A Physically Based Method for Soil Evaporation Estimation by Revisiting the Soil Drying Process. *Water Resources Research*, *55*(11), 9092–9110. https://doi.org/10.1029/2019WR025003

Western, A. W., Grayson, R. B., & Blöschl, G. (2002). Scaling of soil moisture: A hydrologic perspective. *Annual Review of Earth and Planetary Sciences*, *30*, 149–180. https://doi.org/10.1146/annurev.earth.30.091201.140434

Whalley, W. R., Ober, E. S., & Jenkins, M. (2013). *Measurement of the matric potential of soil water in the rhizosphere*. *64*(13), 3951–3963. https://doi.org/10.1093/jxb/ert044

Wilson, D. J., Western, A. W., & Grayson, R. B. (2005). A terrain and data-based method for generating the spatial distribution of soil moisture. *Advances in Water Resources*, *28*(1), 43–54. https://doi.org/10.1016/j.advwatres.2004.09.007

Yourek, M. A. (2016). *An Investigation of Crop Senescence Patterns Observed in Palouse Region Fields Using Satellite Remote Sensing and Hydrologic Modeling A Thesis Presented in Partial Fulfillment of the Requirements for the Degree of Master of Science with a Major in Environ* (Issue January). University of Idaho.

Zhu, Q., Lin, H., & Doolittle, J. (2010). Repeated Electromagnetic Induction Surveys for Determining Subsurface Hydrologic Dynamics in an Agricultural Landscape. *Soil Science Society of America Journal*, *74*(5), 1750–1762. https://doi.org/10.2136/sssaj2010.0055

Chapter 3: Validation of MATLAB soil moisture redistribution model with laboratory experimentation

Abstract

The developed vadose zone transport model was calibrated/validated with laboratory experimentation. An experiment was developed to measure soil moisture (SM) change over time in a confined soil sample. With a confined soil sample, changes in SM would only be driven by the evaporation from the soil surface; other hydrologic fluxes would be negligible. This theory is interchangeable with the methodology of the MATLAB model, which will allow for direct comparison between the simulated and measured data. By measuring the indoor air temperature and relative humidity throughout the validation experiment, the model was executed with those parameters and similar geometry making it consistent with the indoor laboratory conditions. Then be run utilizing those direct measurements. The simulated SM and measured SM were then analyzed and compared statistically for validity/effectiveness. In general, the MATLAB model showed that it struggled to capture the change in evaporation rate over time (specifically when the soil was approach drier conditions). As soil dries, the evaporation rate decreases due to decreases in matric potential. The evaporation equation, which was tested for validation, was unable to capture the non-linear nature of evaporation. This prompts the need for further exploration and refinement of the evaporation equation driving the MATLAB model. However, in the current form, the MATLAB model is validated to the best of its ability and can be used to describe general trends for the effects of biochar amendment. Care should be taken to refrain from absolute statements regarding the predictive nature of the model and the magnitude of change simulated from the model until further refinement of the evaporation equation.

Introduction

The primary work presented in this thesis involved water redistribution modeling using MATLAB's partial differential equation toolbox. Paring this model with direct laboratory measurements of soil and soil + biochar mixtures allowed for the numerical model to be rooted in physical characteristics. Theoretically and intuitively, this approach is reasonable. However, assessing the effectiveness of a model relies upon validating said model against observed or measured data. Further, simply getting right or wrong answers when comparing the model output to observed data is not adequate; there should be a pursuit of getting the right answers for the right reasons (Kirchner, 2006). Kirchner asserts that the key to advancing hydrologic modeling and hydrology is developing theories that get the right answers and testing that they are getting the right answers for the right reasons. He also notes that scientific progress will primarily be achieved through the collision of data and theory and not by creating models with significant numbers of parameters that "dance to match the calibration data even if the underlying premises are unrealistic" (Kirchner, 2006). Most physically-based model development for hydrology to date is based on an implicit upscaling premise which assumes that the microphysics in a heterogeneous subsurface will scale to larger system and be governed by the same equations (Kirchner, 2006), which fits into the premise that models can use parameters to match the calibration data. These assertions made by Kirchner are important to consider when developing any hydrologic or mathematical model and evaluating

its output. Models are tools and are valuable in assisting the interpretations of data and testing various hypotheses (Grayson et al., 1992). Pertaining to prediction, models must be used with caution, if at all, and all uncertainties surrounding the predictions and model output should be clearly and fully discussed (James & Burges, 1982; Klemes, 1982). Great care is required for developing adequate tools (models) for testing/evaluating hydrologic, soil systems, and environmental hypotheses. All the cautions and reservations with model use point to one common notion, models are tools, and these tools should be used to assist decision-making and not definitively predict the future. Additionally, attempting to use these tools outside of the intended scope and capabilities of the model leads to a reduction in validity of the model and poor use. Despite these warnings, models should continue to be developed, calibrated, and used; and calibration of the model developed throughout this research is required.

The model that was developed throughout this research is novel. Throughout preliminary research, no other model was found had the specific focus that was pursued throughout the research. Furthermore, other models that were evaluated for applying the hypotheses in this work did not have the adequate resolution that was required for complete understanding. This led to the development of the novel redistribution model that is detailed in chapters 2 and 3. With novel model development and the uniqueness of the hypotheses, measured data used for calibration is lacking, especially pertaining to long-term soil moisture (SM) measurements of biochar amendment soils. Additionally, the fast pace of biochar development, diversity of feedstocks, biochar production methods, and responses by agricultural, horticultural, silvicultural and rangeland systems, coupled with short funding cycles and the lack of a comprehensive, coordinated approach, have left significant gaps in this knowledge base (Amonette et al., 2021) and required data for biochar model calibration. These knowledge gaps have generated a need for coordinated, large-scale, regionally focused, long-term studies of biochar production and application to answer questions about the technology's cost and potential impact and to guide future development (Amonette et al., 2021). The lack of knowledge and measurements regarding long-term biochar SM data led to an effort to calibrate the redistribution model through other means. The model operates under the same driving forces regardless of if biochar amendment has occurred or not, driven by evaporation. Theoretically, calibrating one scenario of the model would then lead to sufficient model calibration of all scenarios. Regardless of if the results are inadequate or acceptable, the confidence in all model outputs will be increased. SM data is relatively available for natural soil and could have been used. However, the current state of the model operates with no precipitation input into the system after the model is initiated. Instead of attempting to remove precipitation and the effects of precipitation on SM measurements from field measurements, laboratory experimentation would provide a simpler approach to acquiring the necessary data.

Methods

Calibration Theory

The MATLAB model is an evaporation-driven model that tracks the moisture change over time. The evaporation equation, which drives the MATLAB model, relies upon relative humidity and temperature to determine the evaporation rate off of a soil surface. Wang et al. (2019) documented research that described a

physically based approach to estimating evaporation. In this work, Wang et al., (2019) applied a Kelvin equation under dry conditions to calculate the equilibrium matric potential of the soil surface with atmospheric air (Wang et al., 2019). This equation is given by:

$$\varphi_a = \frac{RT}{Mg} ln(RH) \quad [17]$$

Where ϕ_a is the matric potential of the soil surface water, R is the universal gas constant (8.314 J·mol−1·K−1), T (Kelvin) is the absolute temperature, M is the molecular weight of water (0.018015 kg mol−1), g is the gravitational acceleration (9.81 m s−2), and RH is the in-equilibrium relative humidity at the soil surface (Wang et al., 2019). By applying Newton's law of cooling via convection, the evaporation rate is assumed to be proportional to the difference between the soil potential at the soil surface and the air potential calculated from equation 17. Equating the evaporation rate to the rate of change of moisture content at the surface, the following is true:

$$\frac{d\theta}{dt} = \varepsilon(\varphi - \varphi_a) \quad [18]$$

Where ε is the evaporation constant, and ϕ is the matric potential of the soil at the surface, and ϕ_a is the air potential. The evaporation constant [$L^{-1}T^{-1}$] is similar to the convective heat transfer coefficient in a thermal system. The values of ε will vary depending on the soil temperature, air temperature, wind speed, and other energy sources driving evaporation. The evaporation rate is defined as the depth of water evaporated per unit of time per unit gradient of matric potential. This has a unit of T^{-1}. Equation 18 is the fundamental equation that acts as the surface boundary for the MATLAB model, which drives the drying process in the hillslope profile.

The MATLAB model reads relative humidity and air temperature data to determine ϕ_a from equation 17. Pairing this data with the matric potential, the evaporation rate at any moisture content and ambient air temperatures could be known. This is applicable for outside conditions, without precipitation being input into the system.

The developed experiment to measure SM as a soil sample dries took place in an indoor laboratory. To make the MATLAB model consistent with indoor laboratory conditions, the indoor RH and air temperature needs to be measured. The geometry in the MATLAB model would need to be changed to the geometry of the soil sample used in the experiment. Inputting the RH and air temperature into equation 17, and sequentially, ϕ_a into equation 18, the evaporation equation would be consistent with indoor conditions. By iteratively executing the model and comparing the simulated vs. measured SM data, the evaporation constant, ε, that accurately captures the change in SM over time could be determined. This iterative methodology was used to determine which constant to use for equation 18.

Experimental Setup

Theoretically, this experiment is akin to Schindler's evaporation experiment, which measures the tension of the soil as a confined soil sample dries (Schindler et al., 2010). However, the primary difference is the measurement of SM over time. Tracking SM is the primary goal since SM is an easily accessible parameter from the

MATLAB model. The developed experiment utilizes a large soil column that was constructed from clear PVC and PVC fittings. A schematic of the soil column is found in Figure 9.

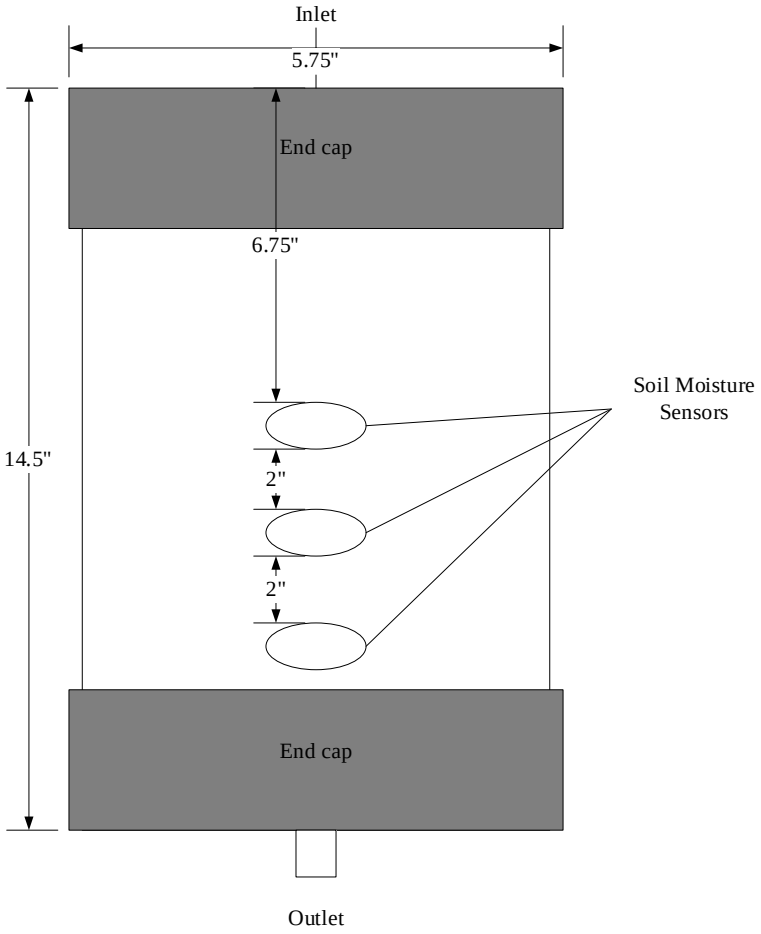

Figure 9: Soil column schematic

Additional pictures and descriptions of manufacturing can be found in Appendix 1. The soil sample was intentionally packed into the soil column to a target bulk density of 1.22 g/cm^3, which is a typical bulk density for Palouse silt loam soil (Survey & USDA, 2021). The soil sample was then saturated using DI water to at or near field capacity. The soil sample was deemed to be saturated adequately when the water dripped the bottom outlet consistently. Once this occurred, saturation of the sample stopped, and the weight of the system was taken. The sample was then left to equilibrate overnight. The next day, the mass of the system was taken after the dripping ceased. This was deemed to be consistent with soil conditions at or near field capacity. The sample was then left to dry throughout the experiment. Weights of the system were taken periodically to track the amount of water leaving the system. The soil sample is confined on all sides but the soil surface, which only allows water to leave the system out of the soil surface. The soil column was then left to dry over time. SM was tracked at three locations throughout the soil column. These positions correspond to the positions shown in Figure 9. 5TM soil moisture (SM) sensor from METER Group (formerly Decagon Devices) in Pullman, Washington, logged the changes in SM over time. Calibration curves were generated for each of the 5TM

moisture sensors. Calibration of the sensors was determined by creating soil samples with known volumetric water content and then taking readings from the SM sensors for each of the different soil samples. The known values were then plotted against the measured values, and curves + equations were generated, allowing for adequate adjustment of the measured values. The 5TM sensors recorded the SM in 10-minute intervals, providing sufficient resolution to observe any fluctuations in the data. The driving forces from the confined soil sample are the temperature, RH, and wind speed. However, the air in the building is primarily stagnant (the room does not have a central HVAC system to control temperature). The effects of wind on this system are therefore deemed negligible. The RH and internal air temperature were tracked using HOBO relative humidity/temperature data logger from ONSET (Onset Computer Corporation, 2021). The HOBO logger sampled the internal laboratory conditions every hour. This sample rate provides adequate resolution to capture changes in RH and air temperature throughout the day and night. SM, RH, and internal air temperature data were collected and exported into excel for data manipulation.

Statistical Testing

Pearson coefficient of determination (R^2), the root mean square error (RSME), mean absolute error (MAE), and percent bias (PBIAS) were used for model validation. The R^2 analysis denotes how well the model output is representative of the observed model. While the RSME is an indicator for the differences between the predicted and observed values that is standardized over the number of samples. The MAE estimates the average magnitude of the error in the predicted values. PBIAS describes the average tendency of simulated data to be larger or smaller than the observed values (Gupta et al., 1999). Pairing these statistical tests together indicates how well the model is performing against observed values. The equations for each of the statistical testing is as follows:

$$R^2 = 1 - \frac{\sum_{i=1}^{n}\left(Y_i^{obs} - Y_i^{sim}\right)^2}{\sum_{i=1}^{n}(y_i^{obs} - y^{mean})^2} \quad [19]$$

$$RSME = \frac{\left[\sqrt{\sum_{i=1}^{n}\left(Y_i^{obs} - Y_i^{sim}\right)^2}\right]}{\sqrt{n}} \quad [20]$$

$$MAE = \frac{\sum_{i=1}^{n}\left|Y_i^{obs} - Y_i^{sim}\right|}{n} \quad [21]$$

$$PBIAS = \left[\frac{\sum_{i=1}^{n}\left(Y_i^{obs} - Y_i^{sim}\right) * 100}{\sum_{i=1}^{n}(Y_i^{obs})}\right] \quad [22]$$

These statistical tests provide information on how well the evaporation equation models the observed data. R^2 values above 0.5 are deemed acceptable values. RSME and MAE values that are smaller than half the standard deviation of the observed values are acceptable. PBIAS values within ± 25% are acceptable (Moriasi et al.,

2007). Statistical testing for the simulated moisture content from the MATLAB model was run against each of the three measured soil moisture curves from the lab experiment. While the MATLAB model outputs three SM curves corresponding to each of the locations measured in the lab experimentation. These simulated curves did not significantly differ from each other, and therefore to ease statistical analysis, the SM corresponding to the middle location was chosen for analysis. This was consistent for all evaporation constants tested.

Results and Discussion

The soil sample had a bulk density of 1.13 g/cm^3, which was deemed adequate. The model validation experiment was constructed and left to run for 27 days. The measured SM was extracted from the data logger along with the temperature and RH for data manipulation. The SM data was then converted into hourly time steps (consistent with the MATLAB model output and the measured temperature and RH data). The measured soil moisture data, temperature, and RH data are displayed below in Figure 10.

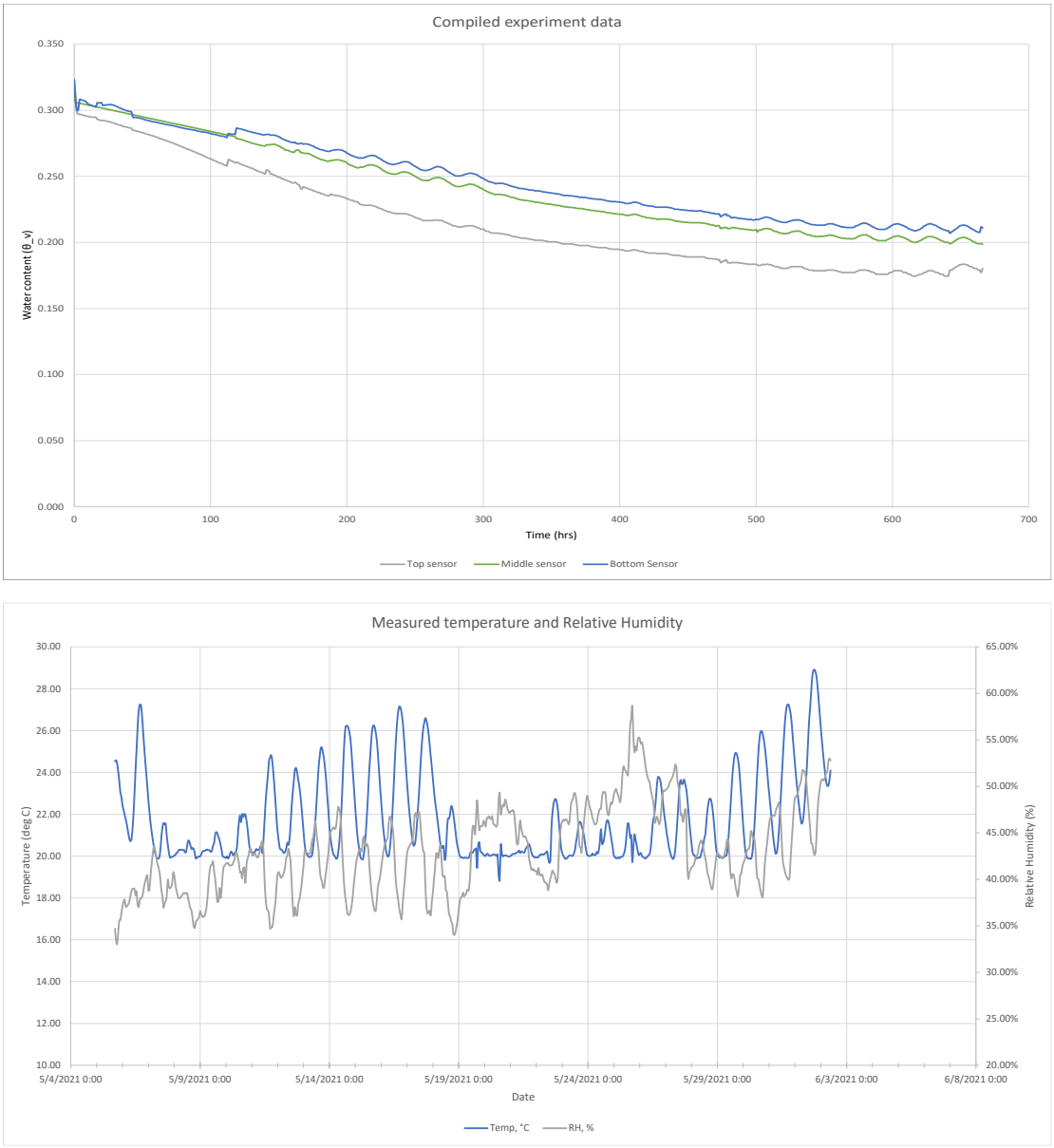

Figure 10: Measured SM, temperature, and RH obtained from the laboratory experiment

The temperature and RH obtained from the indoor laboratory experimentation were used to calculate the ϕ_a from equation 17. The MATLAB model then simulated the SM change from the indoor conditions and the laboratory experiment's geometry Figure 9. In equation 18, both ϕa and ϕ are fixed as they are dependent on the ambient air conditions and the soil conditions, respectively. There is some flexibility with this calibration approach will allows for changing the evaporation equation to better fit the measured data. The evaporative constant, ε, can be scaled to better represent the measured values. To determine an evaporative constant that best fit the data, the simulation was ran iteratively with different ε values. The calibration of the evaporation constant yielded the following:

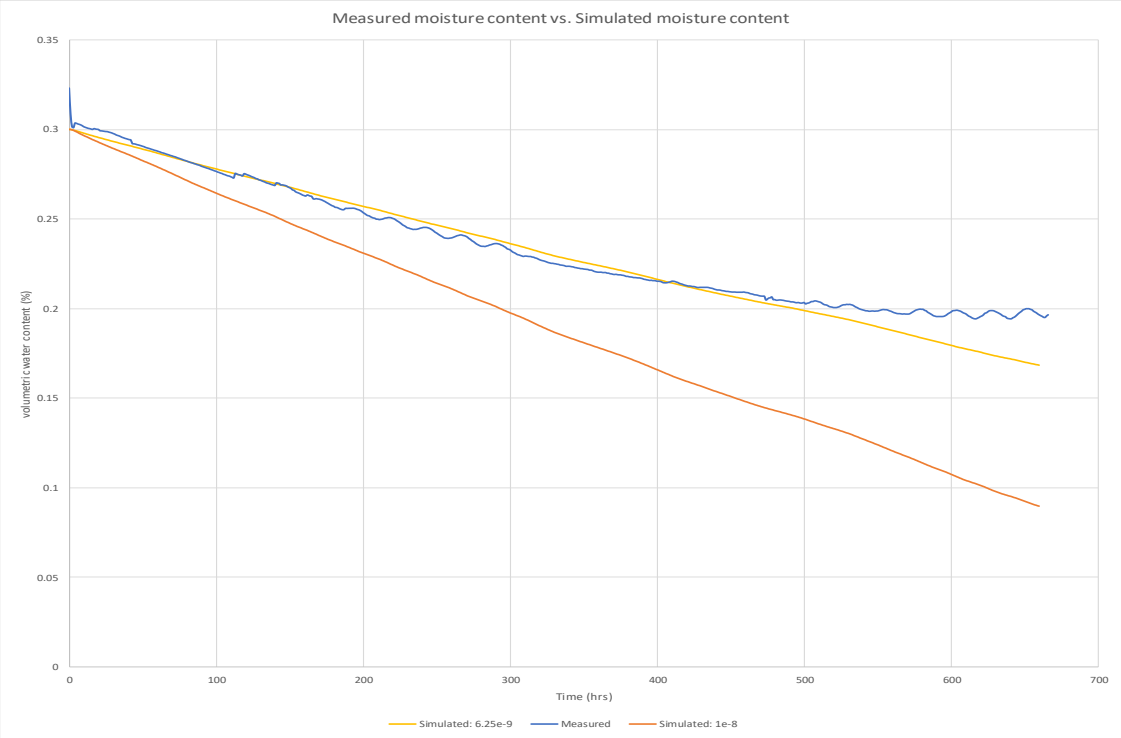

Figure 11: Measured moisture content (averaged between the three sensors) vs. Simulated moisture content

Figure 11 displays the simulated SM achieved with varied evaporation constants similar in value to the measured SM values. Ideally, the evaporation equation used in the MATLAB model would simulate SM that would closely align with the measured values. Graphically, the two potential evaporation constants that align with the measured SM values are the 1e-8 and 6.25e-9 evaporation constants. It is important to note that the simulated SM ideally would lose SM to evaporation at relatively the same rate as the measured data. Comparing the slope of each of the simulated lines graphically, the 6.25e-8 evaporative constant loses SM at a similar rate to the middle and bottom SM sensors. While it differs from the SM measured from the top sensor, using the 6.25e-8 evaporative constant would prevent some degree of overshoot during simulation. This indicates that the evaporation constant of 6.25e-9 would yield appropriate results regarding the MATLAB model operating for the larger scope of the project.

Statistical analysis

The statistical analysis was performed for two evaporation constants, 6.25e-9 and 1e-8. These constants were tested against the measured SM sensor data from each of the sensors. This provides an indication of how each of the evaporation constants are performing against each of the measured SM sensor data. The compiled statistical analysis with each of the outcomes for the respective test is found in
Table 5 for analysis with sensor 7 (top sensor), Table 6 for analysis with sensor 6 (middle sensor), and Table 7 for analysis with sensor 5 (bottom sensor).

Table 5: Statistical analysis from the simulated SM data with the measured SM data from sensor 7 (top sensor)

Statistical testing against Sensor 7	6.25e -9		1e -8	
	Value	Outcome	Value	Outcome
Coefficient of determination (R^2)	96.3%	Good	96.6%	Good
RSME	0.085	Poor	0.085	Poor
MAE	0.077	Poor	0.077	Poor
PBIAS	-34.1%	Poor	-34.1%	Poor

Table 6: Statistical analysis from the simulated SM data with the measured SM data from sensor 6 (middle sensor)

Statistical testing against Sensor 6	6.25e -9		1e -8	
	Value	Outcome	Value	Outcome
Coefficient of determination (R^2)	99.1%	Good	99.3%	Good
RSME	0.061	Poor	0.061	Poor
MAE	0.053	Poor	0.053	Poor
PBIAS	-21.2%	Acceptable	-21.2%	Acceptable

Table 7: Statistical analysis from the simulated SM data with the measured SM data from sensor 5 (bottom sensor)

Statistical testing against Sensor 5	6.25e -9		1e -8	
	Value	Outcome	Value	Outcome
Coefficient of determination (R^2)	99.0%	Good	99.2%	Good
RSME	0.054	Poor	0.054	Poor
MAE	0.047	Poor	0.047	Poor
PBIAS	-18.2%	Acceptable	-18.2%	Acceptable

The results from the statistical analysis were consistent for both evaporation constants used. Both evaporation constants yielded roughly the same values when evaluated for performance against the measured data. In general, the comparison with sensor 7 was poor. The R^2 was good (96.3% and 96.6% for the 6.25e-9 and 1e-8 constants respectively). However, for all other statistical testing, the simulated SM performed poorly with sensor 7. Consistently, the simulated SM performed better against sensors 5 and 6, which indicates the evaporation rates chosen were better at modeling soil moisture change deeper in a soil profile. However, these results were still unsatisfactory. Both evaporation constants performed poorly in RSME and MAE when analyzed with measured data from any SM sensor. Testing for PBIAS showed acceptable performance when compared with sensors 5 and 6. All values were within a 25% margin of error, with the most acceptable value being achieved when analyzing the evaporation constants against sensor 5.

The high R^2 score is misleading. Intuitively, the higher R^2 would indicate little difference between the predicted and simulated results, which points to good model performance. However, when visually inspecting Figure 3 as the soil dries, the deviation between the simulated SM and the measured SM increases. This creates more error between the predicted and observed values, manifesting in poor model performance for RSME and MAE. The error is reduced when simulated SM for both 1e-8 and 6.25e-9 are is compared to sensors 5 and 6. Since these outputs align more closely with the measured values, the PBIAS reduces to an acceptable range.

Model Limitations and concerns

The primary concern regarding this evaporation equation is that the output appears linear, despite being a non-linear equation, in its current form. As soil dries, the matric potential of the soil decreases, which requires more energy for water to leave the soil profile. Simply there is less water in the soil to evaporate, and the water that is in the profile is held more tightly by the soil, so the evaporation rate slows. This is observed by examining the measured SM over time in Figure 11. The matric potential is included in equation 18, and therefore the effect of decreasing matric potential should be captured. However, due to the linear nature of the simulated SM curve in Figure 11, this is not the case. It appears that the magnitude of ϕ_a is overshadowing any effects that the matric potential would have on evaporation rate, leading to matric potential not being a factor. In drier conditions, where matric potential is larger in magnitude (decreased), the effect of matric potential on evaporation is currently lost. This indicates that the evaporation constant would need to be a function of other evaporation driving forces (exp. Wind speed, temperature, or radiative energy) to appropriately catch the changing influence of the matric potential as the soil dries. These findings prompted further exploration of equation 18 and further refinement to better apply heat transfer to evaporation off the soil surface. Discussion regarding refinement of the current evaporation equation and possibilities of using a more standard evaporation method (Penman-Monteith) can be found in Chapter 6: Future work.

Conclusion

Despite the limitations in the model's current form, the evaporation constants tested in this analysis are the most representative constants that can be used in the MATLAB model. It is recommended that these evaporation constants be used in the model. As for the conclusion regarding model validation, this model is as validated as it can be without long-term soil moisture data. The model in its current form should perform reasonably well to predict general trends in biochar amendment. The mechanics that the model relies upon, finite element analysis, and how water moves in the soil profile are valid. These are fundamental soil physics mechanics that have been proven by many researchers. Therefore, the model should respond reasonably and intuitively. However, care should be taken to refrain from absolute statements regarding the model's effectiveness and biochar.
Furthermore, this analysis points to the need to refine the evaporation equation to include more comprehensive evaporation and evapotranspiration equation. The model would benefit from a more refined and appropriate evaporation equation that does not lose the effect of matric potential as the soil dries.

Literature Cited

Amonette, J. E., Blanco-Canqui, H., Hassebrook, C., Laird, D. A., Lal, R., Lehmann, J., & Page-Dumroese, D. (2021). Integrated biochar research: A roadmap. *Journal of Soil and Water Conservation*, *76*(1), 24A-29A. https://doi.org/10.2489/jswc.2021.1115A

Grayson, R. B., Moore, I. D., & McMahon, T. A. (1992). Physically-based hydrologic modeling: 2. Is the concept realistic? *Water Resources Research*, *28*(10), 2659–2666. https://doi.org/10.1029/92WR01259

Gupta, H. V., Sorooshian, S., & Yapo, P. O. (1999). Status of Automatic Calibration for Hydrologic Models: Comparison with Multilevel Expert Calibration. *Journal of Hydrologic Engineering*, *4*(2), 135–143. https://doi.org/10.1061/(asce)1084-0699(1999)4:2(135)

James, L., & Burges, S. (1982). Selection, calibration, and testing of hydrologic models. In *Hydrologic modeling of small watersheds* (pp. 437–472). http://scholar.google.com/scholar?hl=en&btnG=Search&q=intitle:Selection,+calibration,+and+testing+of+hydrologic+models#0

Kirchner, J. W. (2006). Getting the right answers for the right reasons: Linking measurements, analyses, and models to advance the science of hydrology. *Water Resources Research*, *42*(3), 1–5. https://doi.org/10.1029/2005WR004362

Klemes, V. (1982). Empirical and Causal Models in Hydrology. *Scientific Basis of Water-Resource Management, Studies in Geophysics*, 95–104.

Onset Computer Corporation. (2021). *HOBO MX1104 Data Logger Specifications*. www.onsetcomp.com/support/contact

Schindler, U., Durner, W., von Unold, G., & Muller, L. (2010). *Evaporation Method for Measuring Unsaturated Hydraulic Properties of Soils : Extending the Measurement Range*. *74*(4), 1071–1083. https://doi.org/10.2136/sssaj2008.0358

Survey, N. C. S., & USDA. (2021). *Estimated Soil Water Retention Curve Report*. https://ncsslabdatamart.sc.egov.usda.gov/rptExecute.aspx?p=31724&r=6&submit1=Get+Report

Wang, Y., Merlin, O., Zhu, G., & Zhang, K. (2019). A Physically Based Method for Soil Evaporation Estimation by Revisiting the Soil Drying Process. *Water Resources Research*, *55*(11), 9092–9110. https://doi.org/10.1029/2019WR025003

Chapter 4: Soil Moisture Routing (SMR) Modeling of Targeted Biochar Amendment in Undulating Topographies: An Analysis of Biochar's Effects on Streamflow

Abstract

In this work, a five-cell soil moisture routing (SMR) model was developed to explore integrating biochar into precision agriculture technologies/techniques. Targeted amendment of two types of biochar, Redwood Sawdust (RSD) and Wheat straw (WS), were applied to the topmost grid-cell. A single hillslope version of a gridded SMR model was utilized to simulate the changes to the hydrologic fluxes in a small gridded catchment. The model performed adequately when simulated hydrographs for two scenarios (restrictive and non-restrictive soil profiles) were manually calibrated with Palouse river measured streamflow data. A Nash-Sutcliffe efficiency (NSE), root mean squared error ratio with the observations standard deviation ratio (RSR) and mean absolute error (MAE) showed adequate performance with 0.32, 0.07, and 0.34 respectively for the restricted soil profile and 0.37, 0.13, and 0.33 for non-restricted. With a percent bias (PBIAS) outside of the ± 25% acceptable range (33% and 34% for restricted and non-restricted, respectively), the model cannot accurately predict the magnitude of change for the fluxes. The uncertainty is primarily due to this model being a single hillslope SMR model, which will not capture the hydrological changes of an entire watershed. With an increased storage capacity range (Field capacity (FC) = -6 kPa), biochar was effective at increasing the evapotranspiration (ET) and reducing the lateral flow. In specific cases, percolation increased, and saturation excess runoff was reduced. These are positive results for integrating biochar into precision agriculture technologies/practices. Biochar was a minimally effective management strategy with FC set to -33 kPa. These findings indicate further exploration is needed to accurately define the correct range for a soil profile's storage capacity and biochar's effects on overall soil storage capacity. Additionally, these findings promote further investigation of integrating biochar into precision agriculture technologies.

Introduction

Hydrologic modeling is an important tool that researchers can utilize to inform shareholders, stakeholders, and decision-makers regarding hydrologic systems and the environment allowing for informed decisions regarding policy and the environment. Further, numerical modeling of hydrologic systems is a balancing act between accurately simulating natural observations without the model expanding beyond the models' scope. Modeling can be effective for a broad range of systems. Using modeling to examine a precision agricultural technique's effect on the greater hydrologic system is well within the scope of computer modeling. Soil and Water Assessment Tool (SWAT) (Neitsch et al., 2011), Environmental Policy Integrated Climate Model (EPIC) (Gerik et al., 2015), Water Erosion Prediction Project (WEPP) (Flanagan & Livingston, 1995), and soil moisture routing models (SMR) are commonly utilized for modeling different systems, and each has its benefits. Hydrologists use models to solve practical problems of managing and predicting floods or droughts, managing water resources, and designing water supply infrastructure (Kirchner, 2006). Wagener et al. 2004

documented three different types of models; either metric, parametric, or mechanistic models (Wagener et al., 2004). These models are colloquially known as black-box (data-based/empirical models), grey box (conceptual models) (Dawson & Wilby, 2001), and white box (physically-based models) (Davie, 2008). The primary difference between each type of model is in their development (setting up) and operating procedure and not in their concept (Jajarmizadeh et al., 2012). Hydrologic systems are complex systems that have many inputs and outputs. Many aspects of hydrologic responses depend on topographic characteristics, and accurately representing a catchment's hydrologic responses due to topography is fundamental to accurate representations of surface and subsurface runoff processes (Grayson et al., 1992a).

Choosing which model to use is an important consideration when modeling a system. In this paper, an SMR model was selected due to the simplicity in design and input parameters. An SMR model is a simple distributed water balance model that operates on a daily time step to predict daily hydrologic responses at any point in a watershed (Frankenberger et al., 1999). This model utilizes a grid cell approach to monitor soil moisture (SM) storage changes in daily time steps. Five grid cells are aligned linearly, and soil moisture is routed from one to another in a stepwise nature. The physical representation and distributed nature of SMR models permit the assessment of watershed response to precipitation on both integrated and distributed levels (Johnson et al., 2003). The simplicity of SMR modeling and the small number of inputs benefits the exploration of biochar amendment as a precision agriculture technique. The simplicity helps prevent over-parameterization. Furthermore, SMR has shown to be useful for analyzing spatially distributed processes (Johnson et al., 2003), which is desirable in this analysis. It is important to note that this work relies upon research by Frankenburger et al. (1999) and Brooks et al. (2007), who utilized a gridded watershed SMR approach; it differs in that this work uses a single hillslope SMR approach.

Objectives of the study

This study explores how using biochar as a precision agriculture technique would impact the greater hydrological processes in the Palouse. Operating under the primary hypothesis of this work, biochar amendment would be applied selectively to the top of a generic hillslope. The SMR model would simulate how biochar affects the hydrologic processes in a small catchment. Operating under the premise that biochar amendment would be applied to the top of a generic hillslope, exploring how biochar amendment would influence the hydrologic processes in a small catchment is pursued throughout this work. Research has shown that biochar potentially influences the soil hydrologic properties of the soil, water retention, and soil fertility (Aller et al., 2017; Dokoohaki et al., 2017; Jeffery et al., 2019; Verheijen et al., 2010). Understanding the role biochar plays in the greater hydrologic system when used as a precision agriculture technique, is important and lacking. The soil was amended with biochar at rates, procedures, and measurements consistent with chapter 2 of this thesis (refer to the methods section for a comprehensive presentation of sample preparation and measurements, a brief discussion will occur in this chapter). The processes under consideration are lateral flow, evapotranspiration (ET), baseflow, percolation, and runoff. Additionally, the impact on crop yield will be evaluated by analyzing the available water present in the profile throughout the growing season. This was done using a soil moisture

routing (SMR) model similar to work done by Frankenburger et al. 1999 and Yourek et al. 2019 (Frankenberger et al., 1999; Yourek et al., 2019). These developed models were relied upon throughout this analysis, and referring to their works would provide a deeper understanding of SMR model development theory.

Site Description

While a specific site for the model is not defined, the model will analyze a catchment outside of Moscow, Idaho, United States, and in the Palouse region. Therefore, the hydrological, topographical, and climate aspects of the model will be representative of Moscow, Idaho, and the surrounding region. The Palouse follows precipitation patterns similar to the Mediterranean climates with cold, wet winters and warm, dry summers (McCool et al., 2001), which is further characterized by a xeric moisture regime (Soil Survey Staff, 2006). Roughly 60% of the annual precipitation accumulates in November through March, while roughly 5% occurs between July and August (Kaiser, 1967). An additional 10% of moisture occurs between March and May (Brooks et al., 2012). The soil throughout the region is dominated by Palouse Silt Loam that is classified as fine-silty, mixed, superactive, mesic Pachic Ultic Haploxerolls (Soil Survey Staff, 2021).

The Palouse has an undulating topography that creates complex hydrologic systems. Since the cultivation of the region began, all of the original topsoil has been lost from 10% of the region, and one-fourth to three-fourths of the original topsoil has been lost from another 60 percent of the cropland (USDA, 1978). From 1939 to 1977, the average annual rate of erosion was 9.2 tons/acre of available cropland (USDA, 1978). A study in Whitman county found an average annual erosion rate over 26 years of 0.7 tons of soil for each bushel of wheat raised, and in some places, the figure was as high as 2.3 tons of topsoil lost per bushel of wheat (Kaiser, 1967). Research results lead to mitigating erosion in the region, and presently, erosion has been reduced. However, this does not negate the effects erosion plays on the hydrologic processes throughout the region. At the tops of the hills, argillic and fragipan horizons are common, leading to perched water in the winter months (Brooks et al., 2012). These perched water tables accelerate the eluviation of clays in albic Esoil horizons (McDaniel et al., 2001). The fragipan layers can form in as little as 0.65 m depth, reducing the soil depth in these areas and influencing the surface and subsurface hydrology (Brooks et al., 2004). In the hills, the hydrologically restrictive layers enhance the downslope lateral movement of water, leading to a greater potential for delivery of fertilizers and other containments to streams through saturation-excess runoff and by-pass flow mechanisms (McDaniel et al., 2008), contributing the hydrologic complexities in the Palouse. The formation of the restrictive layers in the soil drives the subsurface hydrology in the region (Brooks et al., 2012), which is important for generating a representative model.

Model development

The developed 5-cell SMR model simulates soil water storage over time within a “typical” catchment found in the Palouse. This model is based upon work by Frankenburger et al. (1999) and Brooks et al. (2007), who developed a simple distributed water balance model for the entire gridded watershed. Brooks et al. (2007) built upon the model and modified it to meet their research goals. Yourek et al. (2019) further adapted this initial

gridded watershed SMR model and applied a budyko framework to identify subfield-scale hydrologic classes (Yourek et al., 2019). The SMR model that was developed in this work relies upon the previous work (primarily Frankenburger et al. (1999) and Brooks et al. (2007) to model targeted amendment of biochar to the top of a hillslope. This work utilizes a single grid cell hillslope SMR approach as opposed to an entire gridded watershed approach. Each grid cell (10 m by 10 m) in the model is aligned linearly together and follows the typical topography of a hillslope in the Palouse region found in (and therefore will have a different slope for each grid cell). The grid cells have a depth of 1.5 m.

This work's goal was to simulate targeted amendment of biochar to the top of a hillslope and simulate the effects on the greater hydrologic processes regarding the Palouse and the complex hydrology found in the region. The soil profile characteristics should, therefore, be representative of profiles that are found in the Palouse. Hydrologically restrictive layers (fragipan and argillic horizons) can form during the winter months, which enhance the downslope lateral movement of water (McDaniel et al., 2008). When coupled with relatively high winter precipitation, a primary hydrologic consequence of argillic and fragipan horizons is an extensive network of seasonal perched water tables (PWTs) (Brooks et al., 2012). The SMR model allowed for hydrologically restrictive layers to form at the bottom of each grid cell. The water that percolates out of the bottom of the grid cell is based on the subsurface hydraulic conductivity (Ksub). Changing K_{sub} to allow less water to percolate downward simulates a restricted soil profile. It was desired to account for biochar amendment in both restricted and non-restricted soil profiles, which is accounted for by manipulating the K_{sub} values. In the simulated restricted soil profile, PWTs can form at the base of each grid cell and accumulate upwards towards the surface. Based upon the work by Yourek et al. (2019), a two-layer grid cell approach was implemented to allow for the depth of biochar amendment to vary depending upon research interests. The two-layer grid cell is isolated to the topmost grid cell (the primary area of interest for biochar amendment). A two-layer grid cell allows for the pairing of lab-measured soil hydraulic and physical properties to simulate soil changes in response to biochar amendment. The soil properties measured in the previous chapters of this work was used in the SMR model to simulate different concentrations and types of biochar amendment in the topmost (first) grid cell. Biochar amendment can be varied in depth and surface area by changing the size of the grid cells. The two-layer grid cell allows for the transmission of water across the boundary layer (biochar layer to soil layer), which is accounted for by Darcy's law.

$$Q = -K\left(\frac{\Delta\phi}{l}\right) \quad [23]$$

Where, Q is the flux between the two layers in the soil profile (cm/day), K is the hydraulic conductivity of the soil layers (cm/day), $\Delta\varphi$ is the difference in matric potential between two soil layers, layer 1 minus layer 2 (hPa), and l is the length between the two layers, the distance between the midpoints of each of the layers across the boundary (cm) (Hubbert, 1957). K, in the above equation, will either be K_{sat} if the soil layer is saturated or unsaturated K if the soil is in unsaturated conditions. Soil hydraulic properties are linked to the current water content in a grid cell, which will change daily. Subsequently, there will be variation between the matric potentials and hydraulic conductivities between the two soil layers. A harmonic mean of the hydraulic

conductivities of each layer is used to generate the average hydraulic conductivity and matric potential across the boundary. The harmonic mean is equivalent to "serial flow" in stacked soil layers or cells and may be more adapted to the one-dimensional setting, favoring small conductivity values (associated with bottlenecks in the water flow) (Liu et al., 2016).

$$K_s = \frac{D_t}{\frac{D_j}{K_{sj}} + \frac{D_{j+1}}{K_{sj+1}}} \quad [24]$$

Where K_s is the harmonic mean of the hydraulic conductivities between the two layers, D_t is the total depth of the soil profile (cm), D_j and D_{j+1} are the depths of each respective soil layer (top and bottom respectively in cm), K_{sj} is the conductivity of the top layer (cm/day), and K_{sj+1} is the conductivity of the lower layer (cm/day). Darcy's law therefore becomes:

$$Q = -\left(\frac{D_t}{\frac{D_j}{K_{sj}} + \frac{D_{j+1}}{K_{sj+1}}}\right) * \left(\frac{\Psi_{top} - \Psi_{bottom}}{l}\right) \quad [25]$$

Each layer's matric potential and hydraulic conductivity at any water content are known from the HYPROP and WP4C measurements for each of the soil and biochar samples (refer to chapter 2). The moisture redistribution between the layers will occur whenever there is a difference in storage between the layers. Water will move from higher storage to lower storage in both directions vertically. The redistribution will occur at the end of each day. This approach assumes that water is uniformly distributed throughout each grid cell at the end of each day.

The model operates under the premise that the fluxes out of the topmost grid cell will flow into each adjacent grid cell. Consistent with Frankenburger et al. 1999, the inputs into the SMR model are elevation, daily weather parameters (precipitation, potential evapotranspiration, and average temperature), and soil parameters (depth to restrictive layer, saturated hydraulic conductivity, saturated moisture content, field capacity (FC), and permanent wilting point (PWP)) (Frankenberger et al., 1999). Vertical water fluxes and lateral water fluxes are included in each grid cell to simulate the change in soil moisture in and out of the system. Vertical fluxes in and out of each grid cell include rainfall, snowmelt, evapotranspiration (ET), percolation below the root zone depth.

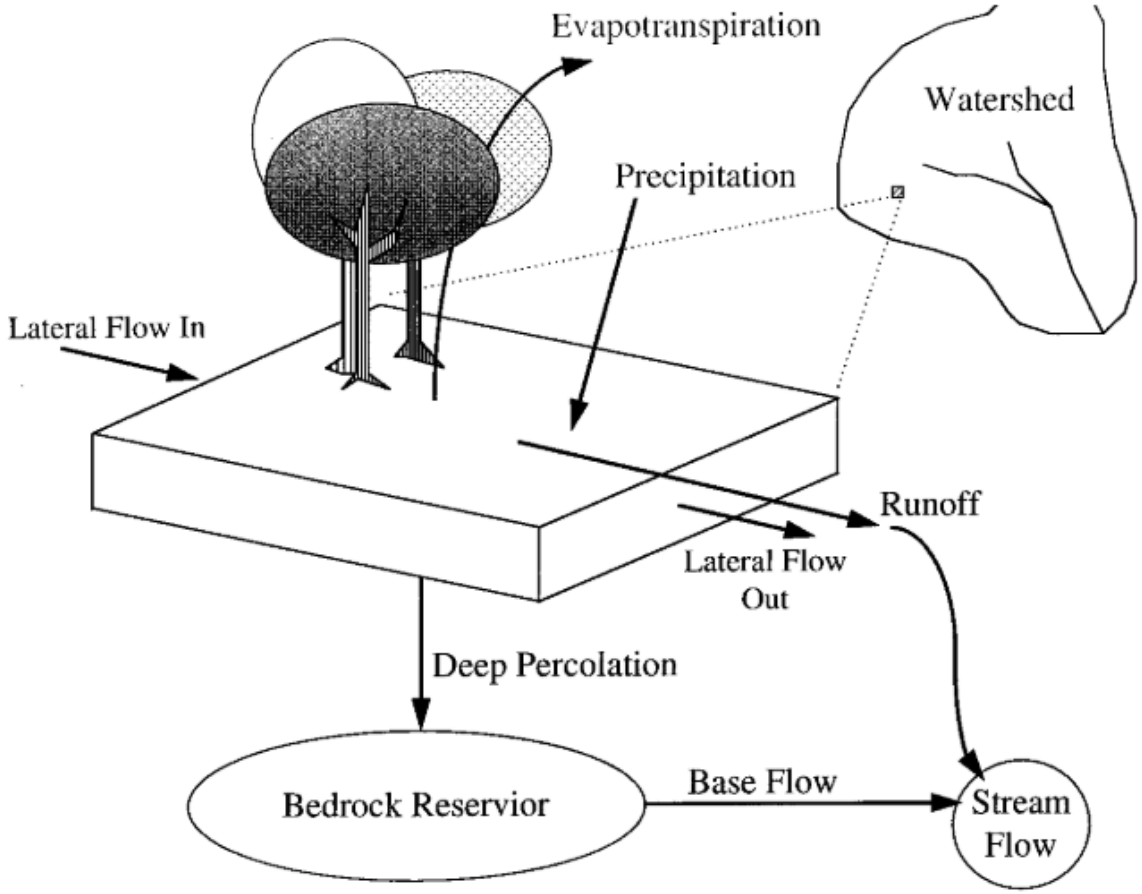

Figure 12: Conceptual model depicting the hydrologic fluxes, taken from (Frankenberger et al., 1999)

Lateral water fluxes for the system include lateral flow, saturation excess runoff at the surface, baseflow, and streamflow. These fluxes are discussed in greater detail in the original SMR work (Frankenberger et al., 1999). The precipitation/snowmelt, lateral flow, runoff, percolation, baseflow, streamflow, and aquifer storage are all accounted for similarly to work presented in Frankenburger et al. (1999) and Brooks et al. (2007). The Hargreaves 1985 model was used to calculate the reference ET hillslope (Allen, 2013). Actual ET was modeled consistent with the work by Brooks et al. (2007). A dynamic root zone depth approach was employed compatible with Yourek et al. (2019). A single crop coefficient was implemented based upon the Food and Agriculture Organization's irrigation and drainage paper 56 and "Reference Evapotranspiration calculation software documentation for FAO and ASCE standardized equations" by Richard Allen (Allen, 2013; Allen et al., 1998). Winter wheat was used to determine the crop coefficient at any point throughout the year. The dynamic root zone drives ET flux out of the system, as more mature crops will pull more water out of the soil. Root growth occurs depending upon three considerations: the current day is a growing degree day, the current day is during the growing season for winter wheat (October to August), and the current day is not in the dormancy period for winter wheat. The typical growing season for Winter Wheat throughout the Palouse is October 15th to August 1st- 15th. Winter Wheat has a dormancy period throughout winter (assumed when

temperatures dip below a base temperature of 4.4 ˚C (~39 ˚F)) (Allen et al., 1998; North Dakota State University, 2021). During this time, the roots are assumed to not grow in length and will be stagnant. Similarly, the root development will begin again when the temperature is consistently above the base temperature of 4.4 ˚C the following spring. Naturally, this will vary from year to year. For simplicity, winter is assumed to begin on November 1st and end at the beginning of March. A growing degree day is determined consistent with guidelines by North Dakota State University (North Dakota State University, 2021). Biochar's effects on crop yield are estimated from increases in the flux water out of the system from ET. It is assumed that this water is crop use water and translates to increases in crop yield. Baseflow is modeled using an unconfined non-linear reservoir. Streamflow is the summation of the baseflow, lateral flow, and runoff.

Materials and Methods

The methodology of this model is explored in three parts: sample measurements, initial conditions for the model, and calibration, statistical testing, and sensitivity analysis for the model.

Sample Measurement

The sample measurement methodology is consistent with chapter 2 in this work. Biochar was added to the soil at a rate of 4% and 7% concentrations per mass. Two types of biochar, redwood sawdust biochar (RSD) and wheat straw (WS), were mixed and tested, both obtained from Carbon Logic. The biochar was manually mixed until the soil and biochar were homogenous. The soil and soil + biochar samples were measured using the HYPROP and WP4C from METER Group in Pullman, Washington. Refer to chapter 2, which describes, in detail, the procedure and setup for measuring the samples from the HYPROP and WP4C. The Van Genuchten (m = 1-1/n) was used to fit the measured values. This is consistent throughout this work. Furthermore, the K_{sat} values were estimated by pedotransfer functions (PTF's) in HYDRUS 1-D, consistent with chapter 2. Table 8 displays the sample characteristics of interest that were obtained from the sample measurement methodology.

Table 8: Physical properties of each of the samples measured by the HYPROP and WP4C devices. Values reported in this table are averaged between the four replicates and displayed with the standard deviation. It is important to note that the field capacity (FC) is displayed at two different tensions, and similarly, the Plant available water (PAW) is also shown. PAW_{low} is the PAW over the FC_{-33kPa} to PWP while the PAW_{high} is for the range of FC_{-6kPa} to PWP. While PAW_{low} is more traditionally used PAW_{high} is important. Van Genuchten parameters are displayed in the bottom portion of the table. Lateral K_{sat} is scaled as the % change that was observed in the vertical K_{sat}.

Soil sample and desired properties					
	100% soil	**4% RSD BC**	**7% RSD BC**	**4% WS BC**	**7% WS BC**
Bulk Density (g/cm^3)	1.22 ± 0.07	1.06 ± 0.01	0.94 ± 0.02	1.07 ± 0.01	0.96 ± 0.03
Porosity	54% ± 3%	60% ± 1%	65% ± 1%	60% ± 1%	64% ± 1%
Field capacity (-33 kPa)	33.2% ± 2.3%	33.1% ± 2.2%	27.2% ± 0.9%	32.6% ± 0.7%	32.4% ± 1.8%
Field capacity (-6 kPa)	48% ± 1.3%	50.7% ± 2.1%	44% ± 0.8%	50.3% ± 0.9%	53.7% ± 4.2%
PWP (1500 kPa)	9.1% ± 0.5%	8.7% ± 0.5%	7.1% ± 0.5%	8.5% ± 0.1%	8.5% ± 0.8%

Plant Available Water (PAW_{low})	24.1% ± 2%	24.4% ± 1.9%	20.1% ± 0.7%	24.1% ± 0.8%	23.9% ± 2.2%
Plant Available Water (PAW_{high})	39% ± 1.4%	42% ± 2%	37% ± 0.9%	41.8% ± 1%	45.2% ± 4.8%
K_{sat} (cm/day)	49.4	102.3	148.0	101.2	157.3
Lateral K_{sat} (cm/day)	247.0	264.1	492.0	258.5	538.0
V.G. Parameters					
Alpha	0.007 ± 0.002	0.010 ± 0.002	0.017 ± 0.003	0.009 ± 0.002	0.012 ± 0.003
n	1.54 ± 0.140	1.46 ± 0.086	1.39 ± 0.048	1.50 ± 0.059	1.51 ± 0.074
θ_r	5.2% ± 1.5%	3.3% ± 1.7%	5.7% ± 7%	4.0% ± 1.0%	4.4% ± 0.3%
θ_s	51.5% ± 1%	56.4% ± 1.6%	54.2% ± 1.5%	55.7% ± 0.4%	61.8% ± 3.8%

The sample properties displayed in Table 8 are based upon which amendment of biochar is applied during the simulation. Biochar amendment occurs on the topmost grid cell and at a specified depth. This grid cell is layered to account for the changes to soil properties introduced by the biochar amendment. All remaining grid cells will remain with 100% soil characteristics.

Initial Conditions

The model is fed data from a SNOTEL site in the Palouse region. The Moscow Mountain SNOTEL site is found just outside of Moscow, Idaho. The weather data from this site is deemed representative of certain portions throughout the Palouse region. While this data may not represent the entire region, it is adequate in understanding the greater hydrologic processes. Daily values for snow water equivalent (SWE), precipitation, observed temperature, max temperature, and minimum temperature were taken from the SNOTEL site for the 2013 to 2019 water years. The Moscow Mountain SNOTEL site is located at roughly 4,700 feet, while Moscow is at 2,579 feet. The temperature and precipitation throughout the entire data set were scaled to adjust for the differences in elevation. These scaled parameters were then used to model various hydrologic processes. Five 10 m by 10 m grid cells are aligned linearly. Each grid cell is set to 1.5 m soil depth. The grid cells vary in slope, simulating an undulating topography. The slope of each grid cell is as follows: cell 1 = 5%, cell 2 = 30%, cell 3 = 40%, cell 4 = 10 %, and cell 5 = 3%, which leads to an average slope of 18%.

Biochar amendment will occur in the topmost grid cell, resembling a targeted application of biochar. The biochar amendment is applied to the entire depth of the grid cell and is assumed to be distributed uniformly in the soil profile. This reduces the need for water redistribution between the biochar and soil layers (if biochar was only applied to half of the grid cell). Biochar amendment to the entire 1.5 m depth is not representative of current biochar application technology, but this analysis would represent the high-end potential of biochar impact in the soil. Biochar will affect the FC, PWP, θ_{sat}, θ_r, soil depth, and K_{sat} (both vertical and lateral) in the amended grid cell. The degree in which these properties are affected correlates with the measured values from the HYPROP and WP4C and the estimated values from the PTF's (displayed in Table 8). It is necessary to note that the PTF's only determined the vertical K_{sat} values. Actual hillslope lateral K_{sat} can be 5 to 10 times larger

than laboratory K_{sat} values (Brooks et al., 2004). The lateral K_{sat} for the control sample was multiplied by 5 to get the lateral K_{sat}.

The effects of biochar on the lateral K_{sat} values are relatively unknown, and multiplying the vertical K_{sat} values for biochar led to high values for lateral discharge. Therefore, the lateral K_{sat} values for biochar were scaled based on the observed % increase in vertical K_{sat} from the baseline. These values are displayed in Table 8. Biochar amendment adds soil depth. We assume that a 4% biochar amendment contributes to a 2 cm increase in soil depth and a 7% amendment increases the soil depth by 4 cm. The initial storage of each grid cell is set to PWP and changed according to the amendment type and concentration. The simulation begins at the 2013-2014 water year, and soil at PWP would indicate soil storage around October 1st. Fluxes of water into and out of each grid cell occurs in a stepwise pattern in the following order: lateral flow, root zone storage/root zone depth/plant available water, crop coefficient and actual ET, percolation, moisture redistribution between the layers, runoff, aquifer storage, baseflow, and finally streamflow. Each of these hydrologic processes is tracked individually and across all grid cells. Additionally, it is assumed that rainfall and melt on any given day will infiltrate entirely into the soil profile. This model does not simulate infiltration from melt, rain, or excess saturation surface runoff.

Model Calibration: Statistical testing and sensitivity analysis

Statistical testing for hydrologic models is an important factor in determining the validity, applicability, scope, and limitations of a model. Simulated hydrographs were generated and then calibrated against measured streamflow data from the Palouse River outside of Potlatch, Idaho, USA. Predicting hydrographs is not the primary purpose of SMR modeling. Streamflow integrates hydrologic response from across the watershed, which can then be used to assess the validity of model predictions (Frankenberger et al., 1999). Moriasi et al. recommends a combination of graphical and statistical techniques should be used for calibration; Nash-Sutcliffe efficiency (NSE), percent bias (PBIAS), and the ratio of the root mean square error to the standard deviation of measured data (RSR) (Moriasi et al., 2007). These statistical methods calibrate this SMR model along with R^2 correlation and mean absolute error (MAE). NSE evaluates how well a model describes the observed variability relative to the mean observed value for the selected period (Brooks et al., 2007), RSME resembles the standard deviation of the error between the model observations and predictions (Brooks et al., 2007), and RSR standardizes based on the observation standard deviation (Moriasi et al., 2007), PBIAS describes the average tendency of simulated data to be larger or smaller than the observed values (Gupta et al., 1999), and R^2 describes how closely the simulated values are correlated to the observed/measured values. Lastly, MAE determines the average magnitude of the errors in the prediction. The equations used to determine each of the statistical tests for model assessment are as follows:

$$NSE = \left[\frac{\sum_{i=1}^{n}\left(Y_i^{obs} - Y_i^{sim}\right)^2}{\sum_{i=1}^{n}(Y_i^{obs} - Y^{mean})^2}\right] \quad [26]$$

$$PBIAS = \left[\frac{\sum_{i=1}^{n}\left(Y_i^{obs} - Y_i^{sim}\right) * 100}{\sum_{i=1}^{n}(Y_i^{obs})}\right] \quad [27]$$

$$RSR = \frac{RSME}{STDEV_{obs}} = \frac{\sqrt{\sum_{i=1}^{n}\left(Y_i^{obs} - Y_i^{sim}\right)^2}}{\sqrt{\sum_{i=1}^{n}(Y_i^{obs} - Y^{mean})^2}} \quad [28]$$

$$R^2 = 1 - \frac{SS_{res}}{SS_{tot}} = \frac{\sum_{i=1}^{n}(y_i - f(x_i))^2}{\sum_{i=1}^{n}(y_i - y_{bar})^2} \quad [29]$$

$$MAE = \frac{\sum_{i=1}^{n}|y_{obs} - y_{sim}|}{n} \quad [30]$$

NSE values between 0 and 0.5 were acceptable, with values exceeding 0.5 showing good model performance. PBIAS is deemed acceptable with bias being within ± 25%. RSR values below 0.70, R^2 values above 0.5, and MAE values less than ½ the standard deviation are all deemed acceptable.

Sensitivity analysis was performed on the individual variables of the model. Sensitivity analysis helps identify parameters that impact model output and, therefore, influence model response (Devak & Dhanya, 2017). The effects of FC, PWP, lateral K_{sat}, θ_{sat}, and soil depth were all tested with sensitivity analysis. With sensitivity analysis, the magnitude of impact from biochar amendment on hydrologic responses could then be determined. Combining model calibration and sensitivity analysis, the effect of biochar on the hydrologic processes in a hillslope could be estimated.

Results

Model Calibration and Sensitivity analysis

The model simulated hydrologic water fluxes from the years 2013 to 2019. Two soil profiles were simulated: a soil profile with an argillic/fragipan horizon and a non-restrictive Palouse silt loam soil. A restrictive layer is denoted by restricting percolation to a max of 0.5 cm/day (can be less depending upon the conditions in a cell), whereas in a non-restricted soil profile, percolation is capped at no more than 20 cm/day. Hydrographs were generated for 100% soil profile for all five grid cells. The measured and simulated hydrographs are displayed in Figure 13. While the simulated hydrographs undershoot the more significant streamflow events and overshoot some areas of the measured data, the hydrographs track the yearly streamflow events well. Streamflow increases and decreases at similar times throughout the year, which indicates the model is performing adequately. The model appears to track the timing of the observed increase in rain and snow that hits the region in the late fall and winter months and captures the timing of melt and wet spring months. The model does not capture significant streamflow fluctuations observed in the measured streamflow data during peak discharge events. The simulated streamflow is consistently later at discharging water that occurs during the summers, indicating that the simulated soil storage may be initially higher in the summer.

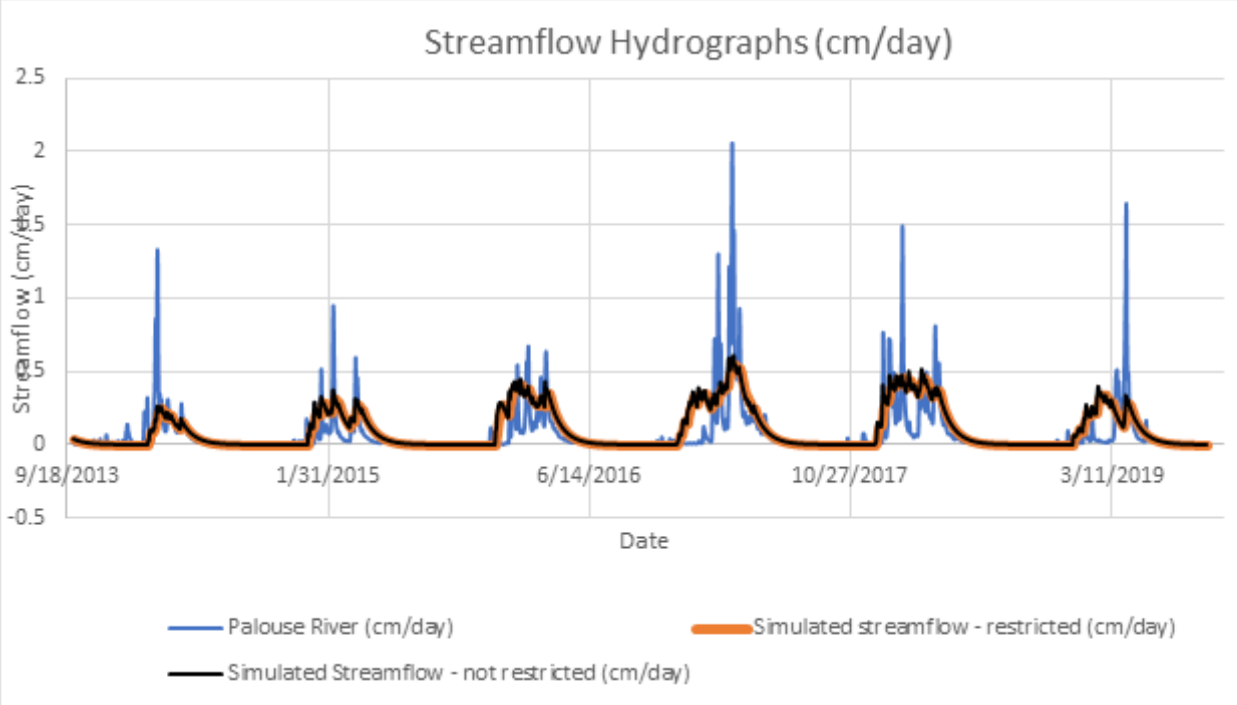

Figure 13: Streamflow hydrographs for the years 2013 to 2019 (cm/day)

Based upon the guidelines set by Moriasi et al. (2007), the simulated scenarios showed acceptable levels of performance. Both simulated scenarios performed acceptably in NSE, MAE, and RSR. However, both scenarios performed inadequately when tested with PBAIS, R^2, and RSME. These results are summarized in Table 9.

Table 9: Summary of streamflow statistics for the water years of 2013 to 2019. Simulated Restricted and non-restrictive soil profiles vs. measured streamflow from Palouse River.

Statistical test	Restricted	Non-restricted
NSE	0.32	0.37
RSME	0.14	0.13
MAE	0.07	0.07
PBIAS	-0.33	-0.34
RSR	0.34	0.33
R^2	0.39	0.42

Between the graphical inspection and the statistical testing, the model was deemed to be performing adequately for predicting outcomes from biochar amendment in both restricted and non-restricted profiles. It is important to note that the model's performance is hindered due to the differences in setup between the single SMR theory and the hydrological responses of an entire watershed. A single hillslope SMR approach will not capture the

complexities of an entire watershed. Still, the statistical analysis showed that the model performs well for being a single hillslope SMR model. Adopting a full-gridded watershed SMR model would likely increase the model's performance.

The sensitivity analysis yields how changing a model input affects the model output. Sensitivity analysis was performed with a restricted and non-restricted soil profile by changing the baseline input value by 3% in both positive and negative directions incrementing by 1%.

Table 10: Sensitivity equations for each influential model parameter. Displayed are the linear equations for each parameter

	Restricted soil profile		Non- Restricted soil profile	
Input	Streamflow Sensitivity	ET Sensitivity	Streamflow Sensitivity	ET Sensitivity
PWP	6.5x + b	-4.9x + b	6x + b	-4.9x + b
FC	-23.2x + b	17.4x + b	-23.5x + b	17.7x + b
Soil depth	-12.2x + b	9.1x + b	-12.3x + b	9.3x + b
θ_sat	-0.04x + b	0.04x + b	0.002x + b	0.002x + b
Lateral K_sat	0.02 x + b	-0.01x + b	0.001x + b	-0.001x + b
Initial Storage amount (cm)	1.4 x + b	0.9x + b	1.4x + b	0.9x + b

Table 10 displays the sensitivity analysis performed on each input parameter regarding only ET and streamflow. Streamflow and ET have an inverse relationship, but the input parameters' influence on the streamflow and ET will vary based on the input. Additionally, the two fluxes vary in magnitude, indicating that the parameter sensitivity regarding streamflow can affect either lateral flow, percolation, or runoff, which contributes to influencing streamflow. This analysis shows that the PWP, FC, and soil depth are the most sensitive parameters and will affect the model output more substantially than changes in the other inputs.

Targeted Biochar amendment

Biochar amendment occurred in the topmost grid cell. The topmost grid cell was amended with both RSD and WS biochar samples at both 4% and 7% concentrations. It is important to note that in Table 8, FC is reported at two static tensions, -33 kPa and- 6 kPa. Commonly FC is reported at -33 kPa, -10 kPa or -6 kPa. These values are used in soil balance models (like this one) to define the maximum water storage in a grid cell (Lier, 2017). Crop water uptake may occur at water contents higher than FC, and this water may represent a significant share of total uptake leading to the defined FC not being a true upper limit of available water (Lier, 2017). Given this notion, the model was simulated for biochar's effects on FC at both -33 kPa and -6 kPa, in both restricted and non-restricted soil profiles. In a non-restricted soil profile and at FC bounds of -33 kPa, biochar amendment had variable effects. The % change in each of the simulated fluxes from biochar amendment are displayed in Figure 14.

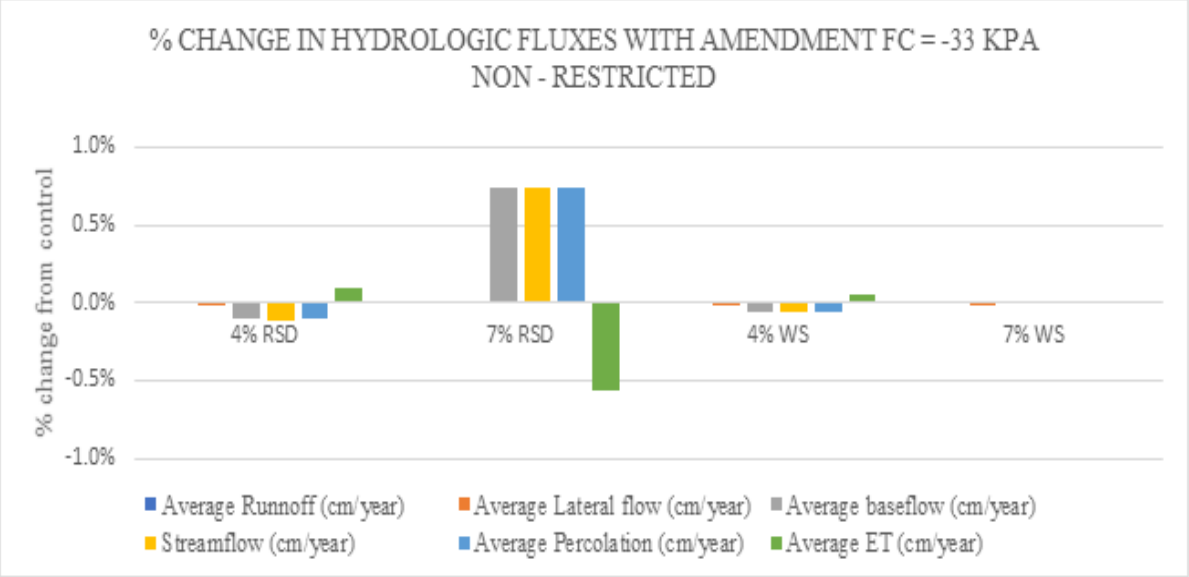

Figure 14: % change from control with biochar amendment, non-restricted soil profile and FC set to 33 kPa.

It is important to note that there is minimal lateral flow or runoff in a non-restricted soil profile and FC of -33 kPa. Most of the streamflow is generated from the percolation of water out of the grid cell, which occurs whenever the grid cell is above field capacity. The 4% RSD and 4% WS samples showed minor reductions in the baseflow, percolation, and streamflow. This reduction in streamflow water manifested in minor increases in ET for both samples. The 7% WS sample showed very minimal effects on hydrologic processes. The 7% RSD showed more significant increases in percolation and therefore baseflow and streamflow. ET is inversely related to percolation, and an increase in percolation leads to a reduction in ET. The variation between the samples is likely attributed to varied effects on FC -33 kPa combined with a consistent decrease in PWP across all amendments. The results for a non-restricted soil at FC of -6 kPa are more significant due to biochar's increased effect on field capacity at -6 kPa. The % change in hydrologic fluxes in a non-restricted soil profile and at a FC of -6 kPa is displayed in Figure 15. Increasing the grid cell storage capacity to -6 kPa values reduces the difference in soil moisture between FC and $\theta_{sat,}$ making the grid cells more susceptible to lateral flow and runoff. The results from biochar amendment at -6 kPa water storage limits are more consistent. Across all samples, biochar amendment reduced the lateral flow and percolation exiting the grid cells. In this scenario, ET increased. The degree in which the fluxes were affected varied between samples. The 4% RSD amendment was more effective than the 7% amendment. While increasing the WS amendment from 4% to 7% showed increased effects on percolation and ET and decreased lateral flow.

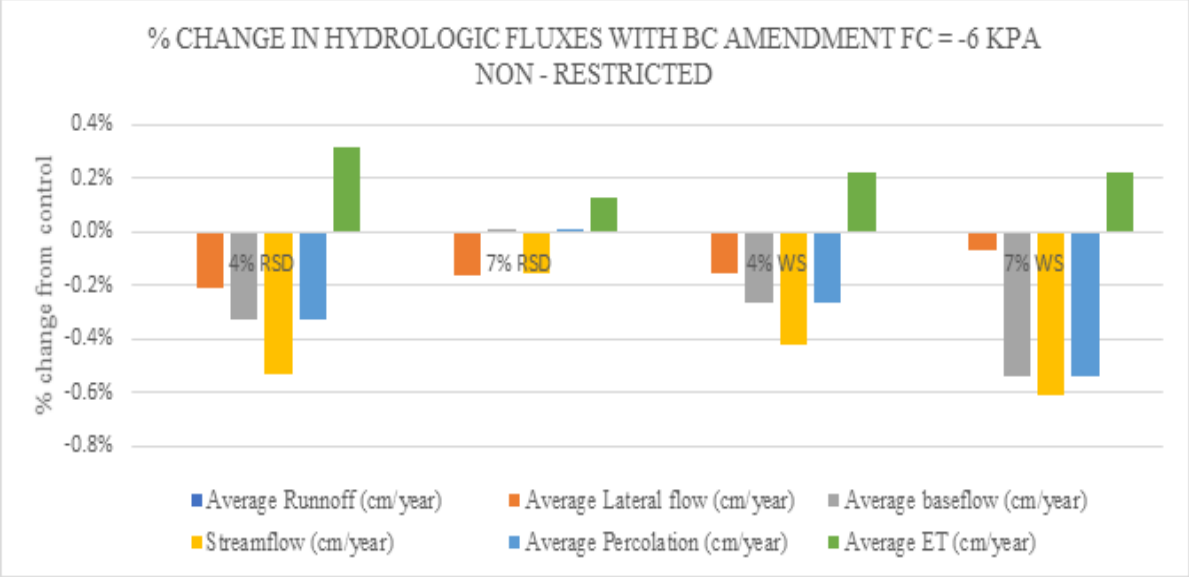

Figure 15: % change from control with biochar amendment, non-restricted soil profile, and FC set to 6 kPa.

In restricted soils, biochar amendment similarly showed varied results at FC of -33 kPa. 4% RSD and 4% WS samples showed a minor reduction in streamflow fluxes and slight increases in ET. These changes were minimal and insignificant. The 7% WS samples showed minor increases in lateral flow and a reduction in percolation, leading to no net change on yearly streamflow. The ET was not affected. In the 7% RSD amendment, lateral flow and percolation increased, causing a combined increase in yearly streamflow, leading to a decrease in yearly ET.

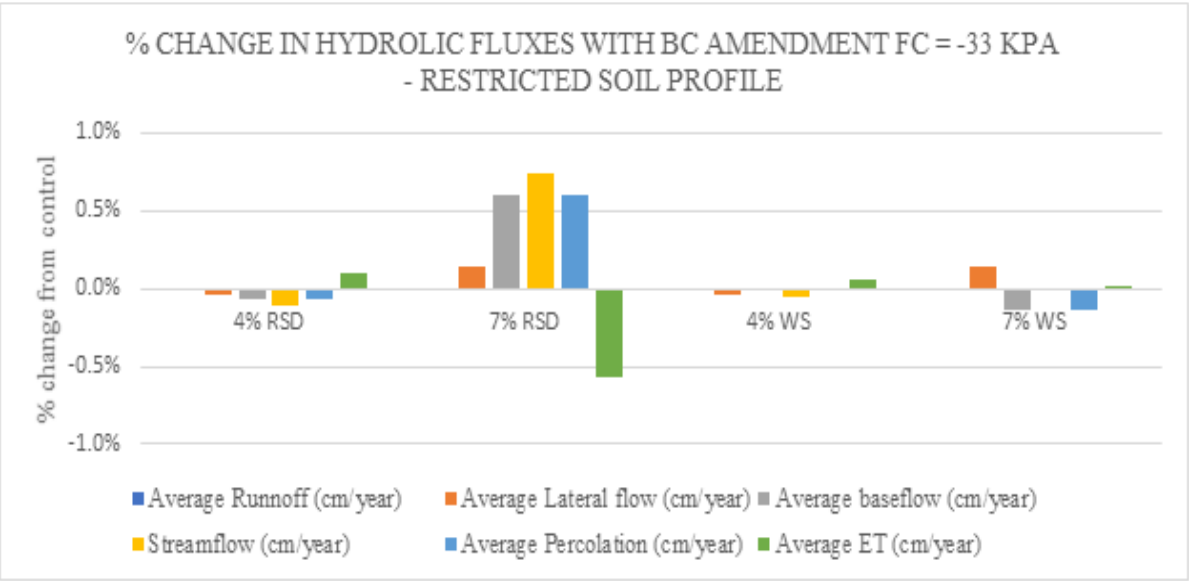

Figure 16: % change from control with biochar amendment, restricted soil profile, and FC set to 33 kPa.

At upper limits of storage capacity (FC values of -6 kPa) and in restricted soils, biochar showed more consistent effects. Runoff is more prevalent with increase storage capacity in restricted soils. In general, the biochar amendment showed a decrease in yearly runoff and an increase in yearly ET. The 7% WS amendment was the only amendment that showed a reduction in percolation. There was an observed reduction in yearly streamflow from all amendments.

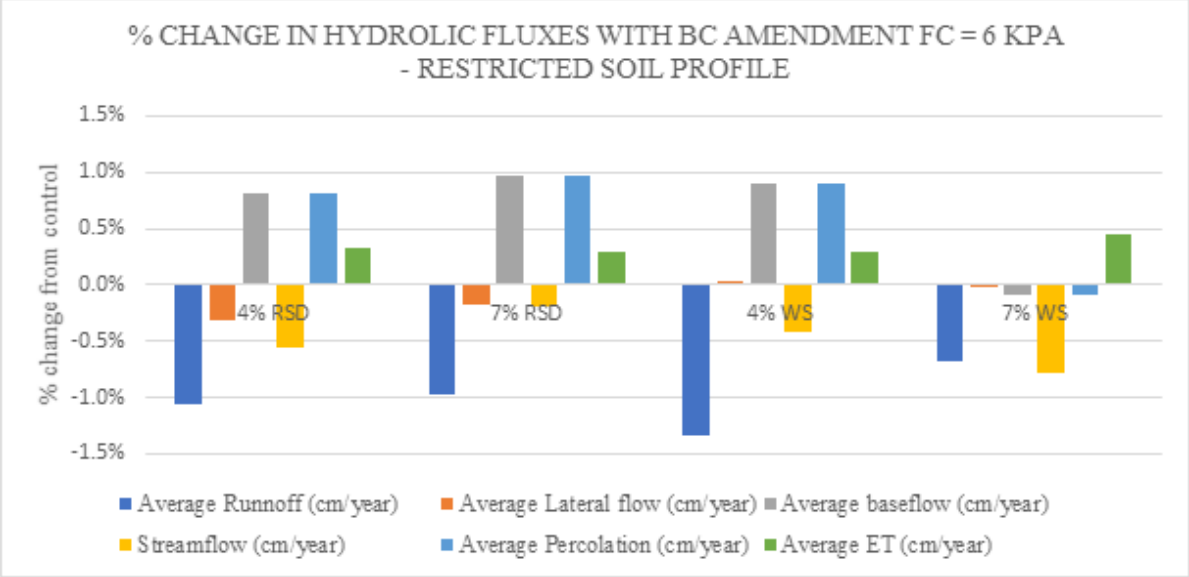

Figure 17: % change from control with biochar amendment, restricted soil profile, and FC set to 6 kPa

Discussion

Testing both restricted and non-restricted soils provides valuable information regarding biochar use as a precision agriculture technique. The effects from amendment for both restricted and non-restricted soil profiles were more significant when the grid cell's storage capacity (FC) was increased from -33 kPa to -6 kPa. Biochar consistently increased the -6 kPa storage capacity of the soil after amendment. Biochar amendment also consistently reduced the PWP of the soil, which, when combined with increases in -6 kPa FC, lead to an overall extension in the stored water range. This increase was consistent across all amended soils, which reasons to be why the observed changes in fluxes were more consistent when simulated with -6 kPa as the FC value.

Ultimately, biochar amendment was minimally and variably effective when amended into soils with storage capacity set to -33 kPa. From the HYPROP, the biochar amendment minimally affected the FC at -33 kPa, and in some cases, decreased the value. A reduction in FC at -33 kPa, measured in the 7% RSD amendment, leads to a reduction in the overall storage capacity of the soil. While the PWP of the 7% RSD amendment also decreased, the magnitude in which the -33 kPa FC decreased was more significant. Therefore the 7% RSD amendment reduced the overall storage capacity of the soil. This created more substantial changes to the hydrologic fluxes than the other biochar samples for restricted and non-restricted soils. A reduction in the stored water capacity led to increases in lateral flow, percolation, and streamflow and decreases in ET for both the restricted and non-restricted soil profiles. This is not ideal. However, this trend was not consistent with other biochar samples. The 7% RSD amendment has more significant effects on both restricted and non-restricted soils; these findings are inconsistent from other samples. Therefore, no definitive statement can be made regarding the effectiveness of biochar at impacting stored water at this range.

At FC set to -6 kPa and in non-restricted soils, this increase manifested in reductions to yearly percolation and lateral flow combining to reduce the yearly streamflow. Additionally, the yearly ET increased. These findings are promising. Pairing reduced streamflow with increased ET indicates more water is stored in the profile and is available for crop use. Since winter wheat is growing throughout this simulation (roughly nine months out of the year), increasing ET points to more water available for crop growth. Increased ET indicates that biochar amendment increases the water available for crops, which is desired. Increased lateral flow and saturation excess runoff due to restrictive layers can be detrimental to soil systems. These fluxes, especially saturation excess runoff, make system more susceptible to erosion, reducing soil depth and crop growth.

Additionally, increasing the FC from -33 kPa to -6 kPa showed a significant increase in the system's susceptibility to runoff due to shrinking the difference between FC at -6 kPa and θ_{sat}. Ideally, biochar amendment to the restricted soils would reduce the runoff and lateral flow in the system and increase ET. This was observed for all the simulations. This indicates that the yearly water used by crops increases, pointing to potential increases in overall crop yield. The reduction of runoff and lateral flow indicates that less water leaves the system yearly as fluxes that may increase the erosion, indicating that biochar may be an effective runoff

mitigation tactic. The observed increase in percolation would suggest that the increased storage throughout the year would increase potential aquifer storage/capacity. However, aquifer storage is a complex system that was not specifically tracked in this work. Theoretically, increasing the storage capacity of restricted soil layers would increase the susceptibility of peak discharge events (high runoff scenarios), which is not ideal. Significant rainfall events would facilitate potential peak discharge events.

Ultimately, the effectiveness of targeted biochar amendment and its' effects on the hydrologic processes relies upon potential increases in ET without increasing lateral flow or runoff. This notion hinges upon the definition of FC and what water is deemed plant available. Biochar showed increased water retention in the saturated soil moisture tensions (refer to chapter 2), specifically at FC of -6kPa. This indicates that biochar amendment increases the overall storage capacity of the soil. If a -6 kPa FC is more accurate for Palouse soils, then biochar amendment effectively increases the ET for both restricted and non-restricted soils.

Additionally, the percolation generally increased in restrictive soils, indicating a potential tool for promoting aquifer recharge from these soil profiles. Increasing the ET in the soil would indicate an increase in crop growth potential throughout the growing season. Washington State University's extension office suggests that for every 2.54 cm (1 inch) increase in available moisture contributes to a six bu/acre increase in crop yield (Koenig, 2005). Using this as a recommendation, the following was determined:

Table 11: Potential bu/acre increase from amendment area from restricted and non-restricted soils at 6 kPa FC

Sample	Non-restricted (bu/acre)	Restricted (bu/acre)
4% RSD	1.1	1.1
7% RSD	0.4	1.0
4% WS	0.8	1.0
7% WS	0.8	1.6

While this displays a small potential increase in bu/acre from biochar amendment, the amendment area is small, and any bu/acre increase is desirable for farmers. However, if the more commonly reported -33 kPa FC value is the bounds for water capacity, biochar amendment is minimally effective and does not promote desired changes to hydrologic properties.

The output from this SMR model displays one type of biochar application (deep application and top of hillslope amendment). Different combinations of amendments would yield different results. The biochar amendment discussed in this chapter is different than the amendment described in chapter 2, in which a smaller amendment area was used. To briefly touch on what that specific amendment shows in this model, the model was changed to the effects of biochar in a shallower amendment. When changing the model to be consistent with the overall research hypotheses used in previous chapters, the biochar amendment showed similar trends to the results

presented in this chapter. In general, the average yearly ET increased with shallow biochar amendment. Hydrologic fluxes of lateral flow and percolation both reduced, contributing to a reduction in baseflow and overall streamflow. Due to a smaller amendment, the effectiveness of the biochar amendment was reduced. All fluxes either increased or decreased within 0.03% change in either direction. The changes to these fluxes may not be significant, but they can be a good indicator of the trends that biochar can induce in the soil. This reinforces that biochar could be used to increase stored water and potentially plant available water, even in small applications. Additionally, biochar shows promise as a way to increase the infiltration of soils and reduce erosion.

Limitations to the model

The developed SMR model is an effective tool that can be used to determine biochar's effects on the greater hydrologic processes in a hillslope. This model can provide valuable information to stakeholders when making hydrologic decisions. The strength of a model relies not only upon consistent calibration and statistical testing (Moriasi et al., 2007), but clear and distinct presentation regarding the limitations of the model (Grayson et al., 1992b). In an effort for clarity, the limitations of the model are presented here. This model performed poorly for PBIAS, R^2, and RSME statistical tests for the initial baseline hydrographs. This indicates that the describes that the model tends to over or under predict the streamflow compared to the observed values. Furthermore, this leads to uncertainty in the magnitude in which the hydrologic fluxes may change, although this should not affect general trends from biochar amendment. The uncertainty is largely a function of comparing a single hillslope output to an entire watershed. It is unrealistic to expect a single hillslope model to capture the complexities of an entire watershed. The model can be manipulated to bring the PBIAS to acceptable levels at no cost of other statistical tests; however, these conditions were not indicative of the baseline conditions and therefore not presented. This model does not account for frozen soils in the wintertime, which would affect the hydrologic fluxes of water, which is a limitation that may lead to poor simulation for some years in the winter months.

This model lacks some parameters that may affect the model output, mainly infiltration from rainfall and from saturation excess runoff. Incorporating these fluxes would provide a more complete model. Implementing the more standard reference ET model, Penman-Montieth's reference ET model (Allen et al., 1998), would increase the accuracy of the daily actual ET flux out of the system. The reference ET is the same for biochar amendment soils and non-biochar amended soils. However, amending the soils with biochar will affect the rate of ET and, therefore the reference ET. It is unclear exactly how it will affect ET, and further research is required.

Conclusion

This model has shown to be an effective tool in determining the effectiveness of biochar as a precision agriculture technique. Biochar amendment showed minimal effect on hydrologic fluxes when FC was held at -33 kPa. However, increasing the FC to -6 kPa lead to more significant changes to the hydrologic fluxes in the system. For non-restricted soil profiles, biochar amendment showed an increase in ET and a reduction in lateral flow and percolation, leading to an overall reduction in yearly streamflow out of the hillslope. In restricted soil

profiles, biochar amendment reduces the saturation excess runoff and lateral flow while increasing the percolation and ET. This leads to an overall reduction in yearly streamflow out of this simulated catchment. However, increasing the storage capacity of the soil may lead to increased susceptibility to peak rainfall events generating more saturation excess runoff. Ultimately, these results are promising if the upper limit of available water (FC) is, in fact, -6 kPa or less. This analysis shows promise for integrating biochar into precision agriculture and warrants further research and exploration in the field.

Literature Cited

Allen, R. G. (2013). REF-ET: Reference Evapotranspiration Calculation Software. *University of Idaho Research and Extension Center*, 82.

Allen, R. G., Pereira, L. S., Raes, D., & Smith, M. (1998). Crop evapotraspiration guidelines for computing crop water requirements. In *FAO Irrigation & drainage Paper 56*. Food and Agriculture Organization of the United Nations. https://www.scscourt.org/complexcivil/105CV049053/volume3/172618e_5xAGWAx8.pdf

Aller, D., Rathke, S., Laird, D., Cruse, R., & Hatfield, J. (2017). Impacts of fresh and aged biochars on plant available water and water use efficiency. *Geoderma*. https://doi.org/10.1016/j.geoderma.2017.08.007

Brooks, E., Boll, J., & Mcdaniel, P. A. (2007). *Distributed and integrated response of a geographic information system-based hydrologic model in the eastern Palouse region , Idaho*. *122*(July 2006), 110–122. https://doi.org/10.1002/hyp

Brooks, E., Boll, J., & McDaniel, P. A. (2004). A hillslope-scale experiment to measure lateral saturated hydraulic conductivity. *Water Resources Research*, *40*(4), 1–10. https://doi.org/10.1029/2003WR002858

Brooks, E., Boll, J., & McDaniel, P. A. (2012). Hydropedology in Seasonally Dry Landscapes: The Palouse Region of the Pacific Northwest USA. *Hydropedology*, 329–350. https://doi.org/10.1016/B978-0-12-386941-8.00010-1

Davie, T. (2008). Fundamentals of Hydrology. In J. Gerrard (Ed.), *Ecological Engineering* (Second Edi, Vol. 22, Issue 3). Routledge. https://doi.org/10.1016/j.ecoleng.2004.06.001

Dawson, C. W., & Wilby, R. L. (2001). Hydrological modelling using artificial neural networks. *Progress in Physical Geography*, *25*(1), 80–108. https://doi.org/10.1177/030913330102500104

Devak, M., & Dhanya, C. T. (2017). Sensitivity analysis of hydrological models: Review and way forward. *Journal of Water and Climate Change*, *8*(4), 557–575. https://doi.org/10.2166/wcc.2017.149

Dokoohaki, H., Miguez, F. E., Laird, D., Horton, R., & Basso, A. S. (2017). Assessing the Biochar Effects on Selected Physical Properties of a Sandy Soil: An Analytical Approach. *Communications in Soil Science and Plant Analysis*, *48*(12), 1387–1398. https://doi.org/10.1080/00103624.2017.1358742

Flanagan, D. C., & Livingston, S. J. (1995). *WEPP user summary*. *11*, 141.

Frankenberger, J. R., Brooks, E. S., Walter, M. T., Walter, M. F., & Steenhuis, T. S. (1999). A GIS-based variable source area hydrology model. *Hydrological Processes*, *13*(6), 805–822. https://doi.org/10.1002/(SICI)1099-1085(19990430)13:6<805::AID-HYP754>3.0.CO;2-M

Gerik, T., Williams, J., Dagitz, S., Magre, M., Meinardus, A., Steglich, E., & Taylor, R. (2015). *Environmental Policy Integrated Climate*. *810*(September), 102. https://blackland.tamu.edu/models/epic/

Grayson, R. B., Moore, I. D., & McMahon, T. A. (1992a). Physically based hydrologic modeling: 1. A terrain-based model for investigative purposes. *Water Resources Research*, *28*(10), 2639–2658. https://doi.org/10.1029/92WR01258

Grayson, R. B., Moore, I. D., & McMahon, T. A. (1992b). Physically based hydrologic modeling: 2. Is the concept realistic? *Water Resources Research*, *28*(10), 2659–2666. https://doi.org/10.1029/92WR01259

Gupta, H. V., Sorooshian, S., & Yapo, P. O. (1999). Status of Automatic Calibration for Hydrologic Models: Comparison with Multilevel Expert Calibration. *Journal of Hydrologic Engineering*, *4*(2), 135–143. https://doi.org/10.1061/(asce)1084-0699(1999)4:2(135)

Hubbert, M. K. (1957). Darcy's law and the field equations of the flow of underground fluids. *Hydrological Sciences Journal*, *2*(1), 23–59. https://doi.org/10.1080/02626665709493062

Jajarmizadeh, M., Harun, S., & Salarpour, M. (2012). A review on theoretical consideration and types of models in hydrology. *Journal of Environmental Science and Technology*, *5*(5), 249–261. https://doi.org/10.3923/jest.2012.249.261

Jeffery, S., Abalos, D., Spokas, K. A., & Verheijen, F. G. A. (2019). Biochar effects on crop yield. In J. Lehmann & S. Joseph (Eds.), *Biochar for Environmental Management* (Second, pp. 1–2). https://doi.org/10.4324/9780203762264-19

Johnson, M. S., Coon, W. F., Mehta, V. K., Steenhuis, T. S., Brooks, E. S., & Boll, J. (2003). Application of two hydrologic models with different runoff mechanisms to a hillslope dominated watershed in the northeastern US: A comparison of HSPF and SMR. *Journal of Hydrology*, *284*(1–4), 57–76. https://doi.org/10.1016/j.jhydrol.2003.07.005

Kaiser, V. (1967). Soil Erosion and Wheat Yields in Whitman County, Washington. *Northwest Science*, *41*(2), 85–91.

Kirchner, J. W. (2006). Getting the right answers for the right reasons: Linking measurements, analyses, and models to advance the science of hydrology. *Water Resources Research*, *42*(3), 1–5. https://doi.org/10.1029/2005WR004362

Koenig, R. T. (2005). *Dryland Winter Wheat : Eastern Washington Nutrient Management Guide*. http://pubs.cahnrs.wsu.edu/publications/wp-content/uploads/sites/2/publications/eb1987e.pdf

Lier, Q. de J. van. (2017). Field capacity, a valid upper limit of crop available water? *Agricultural Water Management*.

Liu, R., Welfert, B., & Houston, S. (2016). Comparison of conductivity averaging methods for one-dimensional unsaturated flow in layered soils. In *8th International Symposium on Stratified Flows*. https://doi.org/10.1016/j.advwatres.2011.05.011

McCool, D. K., Huggins, D. R., Saxton, K. E., & Kennedy, A. C. (2001). Factors affecting agricultural sustainability in the Pacific Northwest , USA: An overview. *Sustaining the Global Farm. Selected Papers from the 10th International Soil Conservation Organization Meeting Held May 24-29, 1999 at Purdue University and the USDA-ARS National Soil Erosion Research Laboratory*, 255–260.

McDaniel, P. A., Gabehart, R. W., Falen, A. L., Hammel, J. E., & Reuter, R. J. (2001). Perched Water Tables on Argixeroll and Fragixeralf Hillslopes. *Soil Science Society of America Journal*, *65*(3), 805–810. https://doi.org/10.2136/sssaj2001.653805x

McDaniel, P. A., Regan, M. P., Brooks, E., Boll, J., Barndt, S., Falen, A., Young, S. K., & Hammel, J. E. (2008). Linking fragipans, perched water tables, and catchment-scale hydrological processes. *Catena*, *73*(2), 166–173. https://doi.org/10.1016/j.catena.2007.05.011

Moriasi, D. N., Arnold, J. G., Van Liew, M. W., Bingner, R. L., Harmel, R. D., & Veith, T. L. (2007). Model Evaluation Guidelines for Systematic Quantification of Accuracy in Watershed Simulations. *Soil & Water Division of ASABE*, *50*(3), 885–900. https://doi.org/10.13031/2013.23153

Neitsch, S. ., Arnold, J. ., Kiniry, J. ., & Williams, J. . (2011). Soil & Water Assessment Tool Theoretical Documentation Version 2009. *Texas Water Resources Institute*, 1–647. https://doi.org/10.1016/j.scitotenv.2015.11.063

North Dakota State University. (2021). *Wheat Growth Stage Prediction using growing degree days (GDD)*. https://ndawn.ndsu.nodak.edu/help-wheat-growing-degree-days.html

Soil Survey Staff. (2006). Keys to Soil Taxonomy, tenth edition. In *Change*. https://www.nrcs.usda.gov/Internet/FSE_DOCUMENTS/nrcs142p2_052172.pdf

Staff, S. S. (2021). *Palouse Series*. https://soilseries.sc.egov.usda.gov/OSD_Docs/P/PALOUSE.html

USDA. (1978). *Palouse cooperative river basin study.* //catalog.hathitrust.org/Record/000302437

Verheijen, F., Jeffery, S., Bastos, A. C., Van Der Velde, M., & Diafas, I. (2010). Biochar Application to Soils: A Critical Scientific Review of Effects on Soil Properties, Processes and Functions. In *Environment* (Vol. 8, Issue 4). https://doi.org/10.2788/472

Wagener, T., Wheater, H. S., & Gupta, H. V. (2004). Rainfall-Runoff Modelling in Gauged and Ungauged Catchments. In *Rainfall-Runoff Modelling in Gauged and Ungauged Catchments*. Imperial College Press. https://doi.org/10.1142/p335

Yourek, M., Brooks, E. S., Brown, D. J., Poggio, M., & Gasch, C. (2019). Development and application of the soil moisture routing (SMR) model to identify subfield-scale hydrologic classes in dryland cropping systems using the Budyko framework. *Journal of Hydrology*, *573*(April 2018), 153–167. https://doi.org/10.1016/j.jhydrol.2019.03.030

Chapter 5: Conclusion

Site-Specific water management

The Palouse is a dryland agricultural system that relies on stored water deep into the dry summer months to supply crops with the necessary water for growth. In portions of the Palouse, there is minimal irrigation, leading to dependency upon precipitation and melt to feed the stored water, making precipitation a critical but uncertain input into dryland agriculture (Yourek, 2016). Patterns of stored water will vary based upon the to the topography (Beven & Kirkby, 1979; Wilson, Western, & Grayson, 2005), cropping sequences (Schlegel et al., 2017), tillage practices (Fuentes, Flury, Huggins, & Bezdicek, 2003; Jin et al., 2007; Kühling, Redozubov, Broll, & Trautz, 2017), and climatic changes (Brown, Heinse, Johnson-Maynard, & Huggins, 2021). In eroded soils, the ability to store water is hindered, creating poorer yielding farmland and low fertility soil. Prolonged drought causes instability in agricultural systems, and ensuring the soil is storing and using water efficiently is important for dealing with persistent drought. The need for site-specific restoration of degraded soils to improve water holding capacity will be key to dryland agriculture in a changing climate. Management practices to plan for changes to seasonal water, especially in the drier sections of the Palouse, will likely need to consider management practices that conserve soil water, especially minimal or no-till management practices to increase the soil infiltration capacity and reduce evaporative losses (Brooks et al., 2010). Additional management practices to restore soil health, increase organic matter, and increase water retention should be considered in the future.

Degraded soils generally have less topsoil. Areas with less topsoil, ridgetops, and south-facing slopes (Yourek, 2016), have low organic matter, poor water retention, and poor nutrient use/cycling, which has been linked to the shallow topsoil depth (Kaiser, 1967). Topsoil and soil organic matter loss impairs the soil's water-storage capacity, reduces the soil's natural fertility, and requires increased use of fertilizers to maintain yields (Hartmans & Michalson, 2000). Pairing the knowledge regarding complications of eroded soils with hydrologic modeling provides information to farmers and stakeholders about locations that would benefit from soil restoration. Accurate hydrologic modeling can capture the spatial distribution of moisture in a field and predict areas that are likely to develop water stress conditions (Yourek, 2016). In the same vain, using hydrologic modeling to isolate areas that would benefit from targeted soil restoration would be of value to the Palouse region.

The case for biochar

This work explores the notion of integrating biochar into precision agriculture techniques in the Palouse region. The primary hypothesis for this work explored targeted amendment of biochar as a soil restoration precision agriculture technique. Through hydrologic modeling, the effects of biochar on soil water movement and retention in undulating topographies. Two types of biochar, Redwood Sawdust (RSD) and Wheat Straw (WS) were amended to a Palouse silt loam soil at 4% and 7% concentrations by mass. Biochar amendment showed the ability to change the water movement and redistribution when applied in a targeted manner. Biochar

amendment increased the organic matter of the soil, increased the porosity of the soil and, reduced the bulk density ($\alpha = 0.05$). The HYPROP and WP4C devices from METER group were used to measure and derive soil hydraulic properties and evaluate the impact of biochar amendment on soil. Biochar amendment showed minimal effect on changing the permanent wilting point (PWP) of the control sample. However, it showed to be more effective in changing soil hydraulic properties in more saturated conditions. Biochar amendment did not significantly change field capacity of -33 kPa (FC_{-33kPa}); this was consistent with both type and concentration. However, biochar amendment did change the FC at -6 kPa. For three samples (4% RSD, 4% WS, and 7% WS) the amendment increased FC_{-6kPa} while the 7% RSD amendment reduced FC at -6 kPa. Furthermore, the amendment of biochar, in general, increased water retention in wetter or saturated conditions. It is unclear if the increase is significant. Biochar amendment reduced the unsaturated hydraulic conductivity in as the soil approached saturation while simultaneously significantly increasing the saturated hydraulic conductivity of all soil samples (estimated by pedotransfer functions). These findings were consistent for the 4% RSD, 4% WS and 7% WS samples; the 7% RSD amendment was inconsistent. The influence of biochar on soil physical and hydraulic properties is promising for soil restoration.

Two hydrologic models were developed and employed to simulate the change in moisture over time and biochar's impacts on the greater hydrologic processes in undulating topographies. A novel vadose zone redistribution model was developed in MATLAB using partial differential equation toolbox and soil physics theorems to simulate the change in moisture in a growing season under evaporative forces. This model demonstrated that targeted amendment of biochar to the tops of the hillslopes would change moisture redistribution in a soil profile. When applied in small amounts (4% concentration by mass), biochar showed increased water retention at and around the amendment area. Additionally, biochar amendment affected the water redistribution in the soil profile, manifesting in more vertical infiltration of water deeper into the soil profile. These were primarily general trends simulated from biochar amendment, and the magnitudes of the changes observed were inconsistent between samples.

The output from the MATLAB model was paired with a single hillslope gridded SMR model that utilized a linear grid cell approach and to simulate change in storage of a soil profile under common hydrologic processes. Biochar was amended to the topmost grid cell, and changes in hydrologic fluxes and soil water was simulated from 2013 to 2019 water years. The model simulated both restricted and non-restricted soil profiles, consistent with two soil profiles found in the Palouse. Biochar and soil samples were consistent between both models. The output from this SMR showed that biochar amendment, even in small amounts, could be used to increase stored and plant available water in shallow soil profiles. In some cases, biochar showed increases in percolation. Biochar amendment showed reduced lateral flow and saturation excess runoff, primarily in restricted soil profiles. These are two hydrologic processes that can cause erosion in soil profiles. The model simulated greater influence on hydrologic fluxes when the field capacity was set at -6 kPa, indicating the importance of understanding the water holding capacity of soils.

The results from both models, when analyzed simultaneously, demonstrate support for the primary hypothesis of this work. While the magnitude of the effect and the degree in which biochar amendment enhances soil fertility is unclear, the general trends from this work are promising. Biochar will change the soils physical and hydrologic properties and impact water redistribution, hydrologic fluxes, and water holding capacity in soils. This work demonstrates that field studies of biochar should be performed to provide further insight into biochar amendment in the region and answer research questions that are left unanswered. While not perfect, the developed models show promise to be used as tools to inform stakeholders regarding biochar amendment in the region.

Literature Cited

Beven, K. J., & Kirkby, M. J. (1979). A physically based, variable contributing area model of basin hydrology. *Hydrological Sciences Bulletin*, *24*(1), 43–69. https://doi.org/10.1080/02626667909491834

Brooks, E., Boll, J., Snyder, A. J., Ostrowski, K. M., Kane, S. L., Wulfhorst, J. D., … Mahler, R. (2010). Long-term sediment loading trends in the Paradise Creek watershed. *Journal of Soil and Water Conservation*, *65*(6), 331–341. https://doi.org/10.2489/jswc.65.6.331

Brown, M., Heinse, R., Johnson-Maynard, J., & Huggins, D. (2021). Time-lapse mapping of crop and tillage interactions with soil water using electromagnetic induction. *Vadose Zone Journal*, (November 2020), 1–16. https://doi.org/10.1002/vzj2.20097

Fuentes, J. P., Flury, M., Huggins, D. R., & Bezdicek, D. F. (2003). Soil water and nitrogen dynamics in dryland cropping systems of Washington State, USA. *Soil and Tillage Research*, *71*(1), 33–47. https://doi.org/10.1016/S0167-1987(02)00161-7

Hartmans, M. A., & Michalson, E. L. (2000). Evaluating the Economic & Environmental Impacts of Farming Practices on the Palouse Using PLANETOR.

Jin, K., Cornelis, W. M., Schiettecatte, W., Lu, J., Yao, Y., Wu, H., … Hartmann, R. (2007). Effects of different management practices on the soil-water balance and crop yield for improved dryland farming in the Chinese Loess Plateau. *Soil and Tillage Research*, *96*(1–2), 131–144. https://doi.org/10.1016/j.still.2007.05.002

Kaiser, V. (1967). Soil Erosion and Wheat Yields in Whitman County, Washington. *Northwest Science*, *41*(2), 85–91.

Kühling, I., Redozubov, D., Broll, G., & Trautz, D. (2017). Impact of tillage, seeding rate and seeding depth on soil moisture and dryland spring wheat yield in Western Siberia. *Soil and Tillage Research*, *170*, 43–52. https://doi.org/10.1016/j.still.2017.02.009

Schlegel, A. J., Assefa, Y., Haag, L. A., Thompson, C. R., Holman, J. D., & Stone, L. R. (2017). Yield and soil water in three dryland wheat and grain sorghum rotations. *Agronomy Journal*, *109*(1), 227–238. https://doi.org/10.2134/agronj2016.07.0387

Wilson, D. J., Western, A. W., & Grayson, R. B. (2005). A terrain and data-based method for generating the spatial distribution of soil moisture. *Advances in Water Resources*, *28*(1), 43–54. https://doi.org/10.1016/j.advwatres.2004.09.007

Yourek, M. A. (2016). *An Investigation of Crop Senescence Patterns Observed in Palouse Region Fields Using Satellite Remote Sensing and Hydrologic Modeling A Thesis Presented in Partial Fulfillment of the Requirements for the Degree of Master of Science with a Major in Environ*. University of Idaho.

Chapter 6: Future Work

This work has many different components and, while related, they each have parts or sections that need work or refinement. The final chapter of this work will serve as a statement of the work that is still required to move the overall project forward. This chapter will go into a major step that would aid every chapter in this work and then address the chapters that require future work individually. The future work for some of the chapters may be minimal; however, denoting what work is still needed provides direction for future analysis.

Next step for the overall research

The larger goal of this project is to provide the basis for the use of biochar as a precision agriculture technique. The combination of model development and laboratory testing provides valuable information that serves as a base understanding for the next step in the process. This information is presented throughout this work. However, laboratory testing and model presentation can often present a picture of the ideal case for research, especially in hydrology/biological engineering. In the field, what is observed may deviate from laboratory testing and model simulation. Field testing is required to provide a clearer picture of how biochar can be integrated into precision agriculture techniques. Field testing would involve four parts: 1) Targeted amendment of biochar in the field 2) Obtaining field data that would align with model validation 3) Obtaining data for how biochar affects crop growth/nutrient retention, and 4) Long term field studies.

The first part of field testing would be to obtain data that would evaluate the overall hypothesis of this work; can biochar be used in a targeted manner to increase soil fertility in eroded soils? This would involve field application of biochar to a plot of land that mimics the primary hypothesis of this work. Soil moisture, evaporation rate, soil matric potential, and other key parameters would be measured to analyze how the targeted application of biochar affects field conditions. Monitoring biochar's effects on nutrients and nutrient retention should be part of this fieldwork as well. The second component of field testing would obtain data specific to the model validation. This closely aligns with the first part of field testing, but special care should be used to obtain the required data to support model validation or the setup of the developed models. Another component of initial field testing would be crop growth studies. The ultimate feasibility of biochar use as a precision agriculture technique lies in increasing crop yields for farmers directly from biochar amendment. Increasing the crop yield or reducing input costs in the long term are two channels farmers would see a reasonable return on investment (ROI) with biochar amendment. Ultimately, if the ROI for farmers is too long, then the feasibility of using biochar in the region is small. This is where crop growth studies would fit. Examining how the targeted amendment of biochar affects crop growth would lead to a better understanding of the potential ROI for farmers. Growth studies can begin with greenhouse growth studies, if necessary, and then can be translated into larger field studies. An auxiliary component of this should evaluate the effect of biochar amendment on pesticide, herbicide, and fertilizer use. These are significant inputs into farming, and evaluating how biochar affects these components would be valuable. Lastly, there is a lack of long-term field data for biochar (Amonette et al., 2021). The initial signs for how biochar ages in the soils is promising (Hernandez-Soriano et al., 2016; Kalu et al., 2021); more research is required. How biochar ages in the soil is key regarding the

feasibility of biochar's use. Once amended to the soil, biochar remains and does not rapidly degrade, so understanding the long-term effects of biochar would answer key questions or fill knowledge gaps in this research.

Chapter 2: Model future work

The developed model presented throughout this work is acceptable. Furthermore, it is adequate for predicting trends regarding the impact of biochar use in the region. However, this does not infer that the model is 100% complete or does not need improvement. This model is the first step in creating a tool that farmers could use for targeted amendment of biochar. The current soil profile is a small hillslope that does not represent a specific location or is not indicative of many hillslopes in the region. This hillslope was used to ensure the model was functioning appropriately prior to upscaling the model to more complex topographies and soil profiles. Nevertheless, this provides an idealistic output that is not entirely representative of specific areas and lacks complexities that are incorporated with farming in the Palouse. Argillic and fragipan layers form restrictive layers that drive subsurface hydrology (Brooks et al., 2004, 2012). This creates a more complex soil profile and subsequently subsurface hydrology which would significantly affect model output. Upscaling the model to a larger area and actual topography would be advantageous. These effects are lost in the current iteration of the model. Implementing these properties into the model geometry, or at least the opportunity when applicable, would make the model more representative of the Palouse and more accurate for multiple complex profiles. This model is only under the forces of evaporation and lacks the effect of crop growth on evaporation, transpiration. Spending some time to integrate evapotranspiration (ET) into the model would be beneficial. Additionally, the model's driving equation for evaporation does not capture some portions of the soil's drying curve. This creates some doubt in the model output. Refining the evaporation equation or utilizing a commonly used method (Penman-Monteith, PM) would benefit the model and reduce doubt. In the long-term, if the goal of this model is to be used as a tool for farmers to understand the greater role of biochar amendment as a precision agriculture technique, switching software programs or development of user interfaces that would be more intuitive for use by farmers would be beneficial. MATLAB works for this iteration of the model, but the model can already be computationally intensive and has some limitations. Pivoting to other software programs, like ANSYS, may provide better results for similar computational energy (however, this is unclear without more exploration). The effectiveness of any tool lies in its usability by consumers, or in this case, farmers. Looking into the future, but with a potential end goal in sight, developing a usable tool would require a user interface, data analytics, and other user-friendly aspects that would make this tool appealing to use and beneficial for farmers. While this is getting ahead of the current progress of this research, it is important to keep the long-term end goal in sight.

Chapter 3: Refining the current evaporation equation

Chapter 3 evaluated the validation of the model. While adequate for the current progress, the model validation highlighted components of the model that require work, primarily with the evaporation equation. The current model utilizes the following equation to drive evaporation off the soil surface:

$$\frac{d\theta}{dt} = \varepsilon(\varphi_a - \varphi_{soil}) \quad [31]$$

Where, dθ/dt is the change in moisture content over time, ε is the evaporation constant (m), φ is the air potential, and φsoil is the soil potential. Refer to Chapter 2 for the derivation, theory, and discussion regarding this equation. The discussion in Chapter 3 highlighted and discussed limitations for this equation in its current form. The future work for this section will primarily support future work that refines and addresses the limitations of the evaporation equation and consequent MATLAB model. The future work would consist of three parts: refine the current equation and implement the PM evaporation equation. Refining the current evaporation equation could take two different approaches: regression analysis and manipulating the current equation. Regression analysis consists of taking the current equation and expanding it to represent the parameters that drive evaporation. It is well known that the wind speed and the air temperature will affect the evaporation rate on any given day (Allen, 2013; Allen et al., 1998). Additionally, to reduce the effect of the air potential on the evaporation rate, the equation can be separated to have each driving force of evaporation have a specific constant associated with each force. Including these changes into equation 31, the new evaporation equation becomes the following:

$$\frac{d\theta}{dt} = C1(\varphi_a) + C2(\varphi_{soil}) + C3(wind) + C4(Temp) + C5 + error \quad [32]$$

Where, dθ/dt is the change in moisture over time, ϕa and ϕsoil are the potentials for the air and soil, respectively (both in log scale), temp is the air temperature (°C), wind is the wind speed measured at 2 m above the surface (cm/s), and C1 through C8 are constant coefficients. This equation is a first-order regression model, which lacks interaction. Applying interaction terms would yield a second-order regression equation, which is as follows:

$$\frac{d\theta}{dt} = C1(\varphi_a) + C2(\varphi_{soil}) + C3(wind) + C4(Temp) + C5(\varphi_a * wind) + C6(\varphi_a * temp) + C7(wind * temp) + C8 + error \quad [33]$$

Both the first-order and second-order regression equations may be used as the new evaporation equation. It is important to note that, for both equations, when being applied to a simulated field or profile, the matric potential of the soil is initially unknown. The matric potential is dependent upon the current soil moisture content. Attempting to simulate the change in soil moisture over time with a parameter-dependent upon the soil moisture requires iterative regression analysis. Multiple iterations of the same model would converge on a constant term for the matric potential. Applying iterative regression, initially without the matric potential of the soil yields the following equation:

First iteration:

$$\frac{d\theta}{dt} = C1(\varphi_a) + C3(wind) + C4(temp) + C5(\varphi_a * wind) + C6(\varphi_a * temp) + C7(wind * temp) + C8 \quad [34]$$

This would predict the change in moisture content. The matric potential would then be able to be calculated based on the evaporation and subsequent soil moisture.

Second and all subsequent iterations:

$$\frac{d\theta}{dt} = C1(\varphi_a) + C2(\varphi_{soil}) + C3(wind) + C4(temp) + C5(\varphi_a * wind) + C6(\varphi_a * temp) + C7(ind * temp) + C8 \quad [35]$$

When performing the iterative regression, there was adequate convergence after two iterations. The constants for both the regression (first-order) and regression with interaction (second-order) are tabulated in Table 12.

Table 12: Regression coefficients obtained from two iterations of regression analysis

First-Order			Second Order		
Variable	**Coefficient**	**Value**	**Variable**	**Coefficient**	**Value**
ϕ_a	C1	0.1238	ϕ_a	C1	1.4083
Φ_{soil}	C2	-0.1348	Φ_{soil}	C2	-0.1452
μ	C3	0.0018	μ	C3	-0.1782
T_{avg}	C4	0.0159	T_{avg}	C4	0.3808
Intercept	C5	-0.4035	$\phi_a * \mu$	C5	0.0460
			$\phi_a * T_{avg}$	C6	-0.0925
			$\mu * T_{avg}$	C7	0.000
			Intercept	C8	-5.4743

This equation can then be regressed against the more standard PM ET model. This regression analysis aims to determine an improved reference ET equation that can be used to estimate ET from soil. The input requirements for this model are few: temperature, relative humidity, wind speed, and matric potential. Most of this data is openly available in meteorological databases. In the US, the USDA and the national cooperative soil survey provide an extensive database for Van Genuchten parameters for different soil samples. This can then be used to calculate the matric potential of various soils at any moisture content, making access to this information easily accessible in the US. If similar records are kept in other areas of the world, it would be theoretically possible to apply this equation elsewhere as well. The first and second-order equations were regressed against the PM FAO-56, (PM) reference ET equation with a scaling factor for the moisture content ((θ_i-θ_pwp)/(θ_fc-θ_pwp)). Using the coefficients in Table 12, Figure 18 was generated, which depicts the model performance against the PM-FAO method for both the first and second-order regression models.

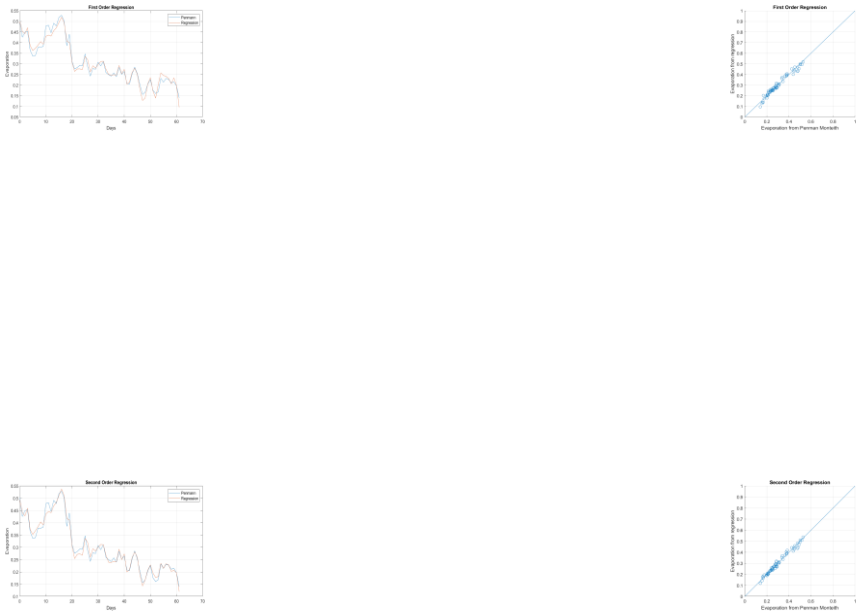

Figure 18: Regression analysis for both the higher and lower order regression equations. One-to-one plots for each respective equation are plotted against the Penman-Monteith model

Both models performed adequately against the PM ET; 96.37% R2 and 97.84% R2 and 0 p-values for both first-order and second-order regression models (α of 0.05). The statistical analysis shows good correlation between both models and the PM-FAO model. With the R2 values for both the higher and lower order models very similar in performance, the lower order model is sufficient.

Despite this analysis showing positive correlation, it leaves two primary questions unanswered: 1) Should the model simply utilize the standard PM equation? 2) Why were the results presented in this work not simulated with the new regression equation if it demonstrates sufficient correlation? The answers to both these questions are related. Both the regression equation and the PM equation utilize evaporation rate in cm/day. These are valuable for SMR modeling or other hydrologic models that utilize cm depth of water as the simulated soil storage. However, the developed MATLAB model simulates the change in water over time on a volumetric water content θv basis (% water). Each node in the model is associated with a specific area (model is two dimensions) in the soil profile and subsequent θv for that area. These areas are not consistent in size, and therefore, the “average” θv for the profile would need to include a variation of a weighted average based upon

the node's area and θv. Additionally, the ET rate from both the regression model and PM models simulate the total moisture that could evaporate + transpire from the soil profile on any given day. The model would require further manipulation to generate the cumulative ET rate for the soil profile. Currently, the ET rate is assigned to nodes at the surface (boundary) of the profile, and the evaporation rate is generated as a consistent hourly rate from the soil surface (on a θv basis). This is akin to heat transfer principles and theoretical heat leaving the surface of a material. There is minimal volume to the nodes at the soil surface, which hinders the application of either the regression or PM equations. These considerations require addressing, which would take substantial rework. The time required for this rework was unavailable and can be addressed in the future. Finally, the PM method is not adequate for indoor conditions. Model validation data was limited for the scope for the model, which promoted inside validation, and thus, the PM could not be used for validation of the model mechanics.

A related but unique approach would be to re-evaluate the current equation to account for evaporative forces without significant changes to the original equation or the mechanics of the model.

$$\frac{d\theta}{dt} = \varepsilon(\varphi_a - \varphi_{soil}) \quad [36]$$

In this equation, ε was assumed to be a constant value. This was primarily for ease, despite acknowledgment that ε would be a function of wind speed, air temperature, or radiation. Implementing ε as a function of evaporative forces would lead to a better representation of the evaporation. Additionally, the effect of φa could be scaled to reduce the effect of φa, which was the primary cause of this equation to appear linear despite the equation being non-linear and simulating a non-linear process.

Chapter 4: 5 cell SMR model Future Work

The 5-cell SMR model is functioning adequately for its current state. However, certain portions of the model can be upgraded to better represent the greater hydrologic system in the Palouse. First, this model lacks infiltration rate, both from the precipitation/snowmelt and infiltration from saturation excess runoff. Implementing these factors would increase the representativeness of the model to the Palouse; however, it is not required. The model performs adequately; however, some time and effort could be spent improving the accuracy of the model, particularly pertaining to the Nash-Sutcliffe efficiency (NSE) and other statistical tests. Applying the model to larger catchments and watersheds would likely increase the efficiency of the model. Larger topographies and catchments would provide valuable information for biochar's impact on a larger area, which is desired in the long term. Lastly, the model could be upgraded to other software, which would make it more intuitive and usable for many people than its current form.

Literature Cited

Allen, R. G. (2013). REF-ET: Reference Evapotranspiration Calculation Software. *University of Idaho Research and Extension Center*, 82.

Allen, R. G., Pereira, L. S., Raes, D., & Smith, M. (1998). Crop evapotraspiration guidelines for computing crop water requirements. In *FAO Irrigation & drainage Paper 56*. Food and Agriculture Organization of the United Nations. https://www.scscourt.org/complexcivil/105CV049053/volume3/172618e_5xAGWAx8.pdf

Amonette, J. E., Blanco-Canqui, H., Hassebrook, C., Laird, D. A., Lal, R., Lehmann, J., & Page-Dumroese, D. (2021). Integrated biochar research: A roadmap. *Journal of Soil and Water Conservation*, *76*(1), 24A-29A. https://doi.org/10.2489/jswc.2021.1115A

Brooks, E., Boll, J., & McDaniel, P. A. (2004). A hillslope-scale experiment to measure lateral saturated hydraulic conductivity. *Water Resources Research*, *40*(4), 1–10. https://doi.org/10.1029/2003WR002858

Brooks, E., Boll, J., & McDaniel, P. A. (2012). Hydropedology in Seasonally Dry Landscapes: The Palouse Region of the Pacific Northwest USA. *Hydropedology*, 329–350. https://doi.org/10.1016/B978-0-12-386941-8.00010-1

Hernandez-Soriano, M., Kerre, B., Goos, P., Hardy, B., Dufey, J., & Smolders, E. (2016). Long-term effect of biochar on the stabilization of recent carbon : soils with historical inputs of charcoal. *GCB Bioenergy*, 371–381. https://doi.org/10.1111/gcbb.12250

Kalu, S., Simojoki, A., Karhu, K., & Tammeorg, P. (2021). Agriculture , Ecosystems and Environment Long-term effects of softwood biochar on soil physical properties , greenhouse gas emissions and crop nutrient uptake in two contrasting boreal soils. *Agriculture, Ecosystems and Environment*, *316*, 107454. https://doi.org/10.1016/j.agee.2021.107454

Appendix A - Research Pathway

Research can be a long process with many different twists and turns. Initially, research is filled with self-study and familiarizing oneself with a specific topic, and gathering as much understanding about said topic as possible from this knowledge base, testing, and exploration of that topic in greater detail. However, if the project and direction of the project is not detailed initially and there is not a clear direction, then the self-study portion may differ from the project that is completed at the end of the degree (whether masters' or Ph.D.). At the beginning of this thesis work, the project was not ironed out for the first year or so of the masters' program. The research was primarily going to deal with biochar, but it lacked specificity of what the end goal of the thesis and overall reserach should be . This led to exploration of topics throughout biochar production, pretreatment for production, and a biochar cookbook of different feedstocks and process parameters. The knowledge gathered was pointing to the exploration of different biochar production systems that would culminate in manufacturing a biochar production system. Courses were taken that set up the potential for this to be a viable thesis option. However, roughly a year into the program, my major professor, Dr. Dev Shrestha, spearheaded modeling how biochar affects soil water and water redistribution in an undulating topography. This was the first concrete step towards a specific direction regarding the research, primarily exploring how biochar affects soil properties, crop yield, and more specifically, how biochar affects water redistribution and retention when used as a precision agriculture technique (targeted application of biochar). From this initial step, the thesis work began to resemble more of the work presented in this thesis.

Primary research questions that required further exploration and propelled the current status of the work:

- How does biochar, both type, and concentration, affect soil hydraulic properties?
- How does biochar, both type, and concentration, affect water redistribution in an undulating topography?
- Is biochar an effective precision agriculture technique for increase soil fertility, water retention, and ultimately crop yield?

Brief overview of the theory of water movement, retention, and key soil hydraulic properties

Water movement and retention of a soil is variable depending on many factors. The structure of a soil profile, soil texture, amount and structure of organic matter, soil porosity, particle size, particle shapes, and surface adsorption can all affect soil water retention and movement through a soil profile (Mcmillan, 2012; Or et al., 2009). While the characteristics mentioned previously are not a fully comprehensive list of all the factors that affect soil's ability to retain water and water's ability to move through a soil profile, it provides an idea of the complexity of the relationship between soil and water. Ultimately, these factors come together and are described by three primary properties that soil holds: the matric potential (ψ), hydraulic conductivity (K), and diffusivity (D) of a soil. The matric potential is the force at which the water is held in the soil, which is directly related to the amount of water that can be held in a soil profile, the soil water content (Or et al., 2009), and how easily water will move through a soil profile. The hydraulic conductivity is the ability of a soil profile to transmit

water (Or et al., 2009). The hydraulic conductivity is either under saturated/near-saturated conditions or unsaturated conditions, known simply as the saturated hydraulic conductivity and unsaturated hydraulic conductivity, respectively. The diffusivity of a soil is directly related to the hydraulic conductivity and is the ratio of the unsaturated hydraulic conductivity to the specific water capacity (which is the slope of the soil-water characteristic curve) (Or et al., 2009). For more information regarding the soil hydraulic properties, their relation to the soil-water relationship, and in-depth exploration of soil physics fundamentals, please refer to the following works: Environmental Soil Physics by Daniel Hillel (Hillel, 1998) or Agriculture and Environmental Soil Physics by Dani Or et al. (2009) or related works.

These soil hydraulic properties are key to the greater research questions regarding this thesis work. They are interconnected and affect the soil water retention and water movement through profile. Furthermore, previous chapters of this work detailed the effects of biochar on soil hydraulic properties, which it has been shown to impact. This made it necessary to further understand soil hydraulic properties and the components that influence them, when attempting to model biochar's effects on the soil. The matric potential of a soil is commonly measured by using tensiometers, which directly measure the suction pressure of the soil in relation to water. The saturated hydraulic conductivity of a soil can be measured and then used to estimate the unsaturated hydraulic conductivity of the soil across the entire soil saturation range. These experiments can easily be researched and performed, but they are briefly discussed later in this section. While the soil hydraulic properties are important, key equations relate these properties to water flow through soil and other porous media. Martinus Th. Van Genuchten developed key equations that allow for determination of the soil hydraulic properties given the water retention curve (WRC) or soil-water characteristic curve (SWCC). In his fundamental 1980 paper "A Closed-form Equation for Predicting the Hydraulic Conductivity of Unsaturated Soils," built upon work by Mualem (Mualem, 1976), he describes the relationship between matric potential or head pressure and soil water content and how they can be used to predict the hydraulic conductivity and diffusivity of soils (Van Genuchten, 1980). These equations are now known as the Van Genucthen-Mualem model equations. Exploration of Van Genuchten's 1980 paper would provide greater insight into the theory and development of these key equations; however, the equations that were fundamental to this work are briefly described below. The matric potential of the soil is commonly measured by experimentation in a lab and is not presented in the work. However, to determine the unsaturated hydraulic conductivity at any given moisture content the following relationship can be used:

$$K_r(\theta) = \theta^{(1/2)} * \left(1 - \left(1 - \theta^{(1/m)}\right)^m\right)^2 \quad [37]$$

Where $K_r(\theta)$ is the relative hydraulic conductivity of the soil in terms of the water content of the soil, θ (also seen as S_e) is the relative moisture content of the soil given by the following relation ($\theta = (\theta - \theta_r)/(\theta_s - \theta_r)$), and m is a Van Genuchten parameter denoted by the relationship ($m = 1 - 1/n$) (Van Genuchten, 1980). The relative hydraulic conductivity can then be converted to the actual hydraulic conductivity of a soil by the following equation:

$$K(\theta) = K_r * K_{sat} \quad [38]$$

Where $K(\theta)$ is the hydraulic conductivity of the soil at a given water content, K_r is the relative hydraulic conductivity calculated from equation 37, and K_{sat} is the saturated hydraulic conductivity of the soil (Van Genuchten, 1980). The saturated hydraulic conductivity is measured directly or estimated by other methods for each desired soil sample. The diffusivity of a soil was also presented in the Van Genuchten work which is as follows:

$$D(\theta) = K(\theta)\left|\frac{d\psi}{d\theta}\right| \quad [39]$$

Where $D(\theta)$ is the diffusivity of the soil at any given water content, $K(\theta)$ is the hydraulic conductivity at any given water content calculated from equation 38, $d\Psi$ is the difference in matric potential between water contents, and $d\theta$ is the difference in water contents (Van Genuchten, 1980). Therefore, by measuring the WRC and the K_{sat} of a soil sample, the unsaturated hydraulic conductivity across the entire saturation range and the diffusivity of the soil can be determined. These properties can then be used in Darcy's Law to model how water will move through a soil profile.

A fundamental soil physics equation regarding water movement through a soil, or flux of water through a soil, was developed by Henry Darcy and Darcy's Law. Darcy's Law states the following:

$$Q = -KA * \left(\frac{d\phi}{dl}\right) \quad [40]$$

Where K is hydraulic conductivity, A is the area, ϕ is hydraulic potential (or often the hydraulic head) and l is the distance in the direction of flow of the soil column or profile. Darcy's law is based on the flow of water through a soil column and can be translated to broader applications through Richard's equation. Regardless, Darcy's Law is valid only for laminar flow, which occurs for Reynold's number less than 1. Reynold's number (Re) for flow through a porous medium is defined as: $Re = \rho VL/\mu$, where ρ and μ are the density and viscosity of the liquid, V is the flow velocity (Q/A), and L is a characteristic length, typically taken as the mean grain diameter of the medium. Most practical applications of groundwater flow have $Re < 1$, and thus can be modeled with Darcy's Law.

Model development: Theory and parameter requirements

To effectively model how moisture redistributes in a soil profile, the properties used in the Van Genuchten-Mualem equations and Darcy's law are required. Darcy's law is key to modeling water movement and redistribution of water within a soil profile. Using Darcy's law and the assumptions regarding Reynold's number presented previously, Darcy's law can be refined to be more appropriate for t modeling water flow in undulating topographies. For the purposes of the model, the hydraulic potential is the primary driving force for the movement of moisture throughout the soil profile and therefore is the primary driving force in Darcy's law, equation 40. Imagining the soil (or any porous media) as a unit cube the flow of water in and out of the cube (change in amount of water over time) will be based on the forces driving the water across the boundary layers of the cube. This notion is presented mathematically by the rate of change of moisture θ in a unit soil cube. This

rate of change, θ over time in a unit cube, is determined by the divergence of the flow into the soil matrix, which is given by:

$$\frac{d\theta}{dt} = \text{Divergence of } Q = \nabla \cdot K \nabla \phi \quad [41]$$

Where, dθ/dt is the change in water content, θ, over time in a unit cube of soil, K is the hydraulic conductivity of the soil, and ϕ is the hydraulic potential. Divergence measures the gradient of soil properties in the x, y, and z directions and determines the amount of moisture that will enter and leave a soil particle. For saturated soil conditions, ϕ, is the sum of pressure head (h) and elevation heads (z) given by the following:

$$\phi = h + z \quad [42]$$

Equation 41 neglects velocity head, which is a common practice to do. For a saturated soil column with no flow, the sum of elevation and pressure head is constant. At soil-air boundary interface, the pressure head can be assumed to be zero-gauge pressure since the boundary is the ambient environment. For a saturated soil, at boundary, the potential gradient is just the gradient of the elevation head.

In unsaturated soil conditions, water and air are contained in the pore space. The air is connected to the atmospheric pressure and hence the pressure head is assumed to be zero. Generally, for unsaturated soil, flow is caused by the gradient of matric potential and gravitational potential. The osmotic potential of the soil is deemed negligible. A matric potential gradient is caused by the spatial distribution of water and the differences in tension (suction) between the soil particles and water. The tension of a soil is the attractive force that the soil particles have toward water. The water movement in unsaturated soil due to matric potential can be modeled as a diffusion process. The diffusivity is proportional to the moisture gradient and is dependent on soil type and structure. For unsaturated soil, the hydraulic potential is given by:

$$\phi = \psi + z \quad [43]$$

Where ψ is the matric potential of the soil, z is the elevation head, and ϕ is the hydraulic gradient. The matric potential is the portion of the water potential that can be attributed to the attraction of the soil matrix for water. The matric potential used to be called the capillary potential because, over a large part of its range, the matric potential is due to capillary action. However, as the water content decreases in a porous material, water that is held in pores due to capillarity becomes negligibly small, when compared to the water held directly on particle surfaces. Therefore, the term matric potential covers phenomena beyond those for which a capillary analogy is appropriate [8]. Combining equations 42 and 43, we can write the total potential as:

$$\phi = h + \psi + z \begin{cases} h = 0 \text{ for unsaturated soil or at the upper boundary} \\ \psi = 0 \text{ for saturated soil} \\ z = \text{elevation} \end{cases} \quad [44]$$

The matric potential (ψ) is zero for saturated soil and has a negative value for unsaturated soil. The matric potential will vary whenever there is gradient in moisture content (θ).

For saturated soil, the spatial gradient of ϕ can be used to further refine the diffusivity gradient of soils. The spatial gradient of ϕ can therefore be expressed as

$$\nabla\phi = \frac{d\phi}{dl} = \frac{d(h+\psi+z)}{dl} = \frac{d\psi}{d\theta}\frac{d\theta}{dl} + \frac{dz}{dl} = DK\nabla\theta + \nabla z \quad [45]$$

Then by combining equations 41 and 44,

$$\frac{d\theta}{dt} = \nabla \cdot (D\,\nabla\theta + K\nabla z) \quad [46]$$

By separating variables with θ, equation 46 can be expressed as

$$\frac{d\theta}{dt} - \nabla \cdot D\,\nabla\theta = K\nabla z \quad [47]$$

With ∇z=1 in vertical direction and 0 in any other direction. Equation 47 displays the final equation for modeling moisture redistribution and flow through a desired profile. This equation displays the necessary soil properties to determine the flow and change in moisture over time, K and D. Recalling that Van Genuchten demonstrated that by obtaining the WRC, the K and D of a soil sample can be determined using equations 37, 38, and 39. Therefore, measuring the matric potential is necessary. Furthermore, utilizing equation 38, K_{sat} is required for the determination of the unsaturated hydraulic conductivity and therefore requires measuring or estimating.

Despite the theory presented above, the direct measurement of diffusivity and hydraulic conductivity was first attempted prior to the determination of the WRC and estimation of K_{sat} values for the soil. Different experimental setups were tried to adequately measure D and K throughout the duration of the research. These various experiments are presented sequentially by time in the following sections to provide justification and documentation for the reasoning why certain methods were chosen in this body of work. The final section provides the methods of choice that was used for data collection throughout this work, determination of K_{sat} values, and measurement of the WRC (matric potential vs. water content).

Diffusivity Experiment 1: The box setup

The methods for measuring the hydraulic conductivity of the soil appear more readily available and more well known, and therefore, are discussed in subsequent sections. Measuring the diffusivity (D) of the soil therefore became the primary focus of the research. The experimental setup began with evaluating equation 47 and understanding how to measure the different elements of that equation. The diffusivity will vary for unsaturated soil conditions. Furthermore, based on the degree of saturation throughout the soil profile, the diffusion rate of water through the soil matrix will be different. Therefore, the diffusion rate of the soil at unsaturated conditions can be based on the change of moisture over time and the average moisture content at specific positions throughout the soil profile. This is given by the following:

$$\frac{\partial\theta}{dt} = D\frac{\partial^2\theta}{dx^2} \quad [48]$$

Where $\partial\theta/dt$ is the change in moisture content over time, $\partial^2\theta/dx^2$ is the second derivative of the moisture change at specified positions throughout the soil profile, and D is the diffusivity of the soil. $\partial^2\theta/dx^2$ is given by:

$$\frac{\partial^2\theta}{dx^2} = \frac{\theta_R + \theta_l - 2\theta}{x} \quad [49]$$

Where, θ_R is the moisture content of the right moisture sensor, θ_L is the moisture content of the left moisture sensor, θ is the moisture content of the middle sensor, and x is the difference between the right and middle sensors. The combination of equations 48 and 49 would then provide the diffusivity of the soil at moisture contents throughout the soil saturation range. These equations are applicable for the diffusivity of water in a horizontal direction. For determining the redistribution of water in y-directions (vertical), the following is necessary

$$\frac{\partial\theta}{dt} = D\frac{\partial^2\theta}{dx^2} + K\frac{dl}{dz} \quad [50]$$

Where K is the hydraulic conductivity and dl/dz is the change in length over the change in elevation between two points. For flow in strictly the vertical direction, dl/dz becomes 1. Equation 50 would account for flow of water in any combination of x and y directions.

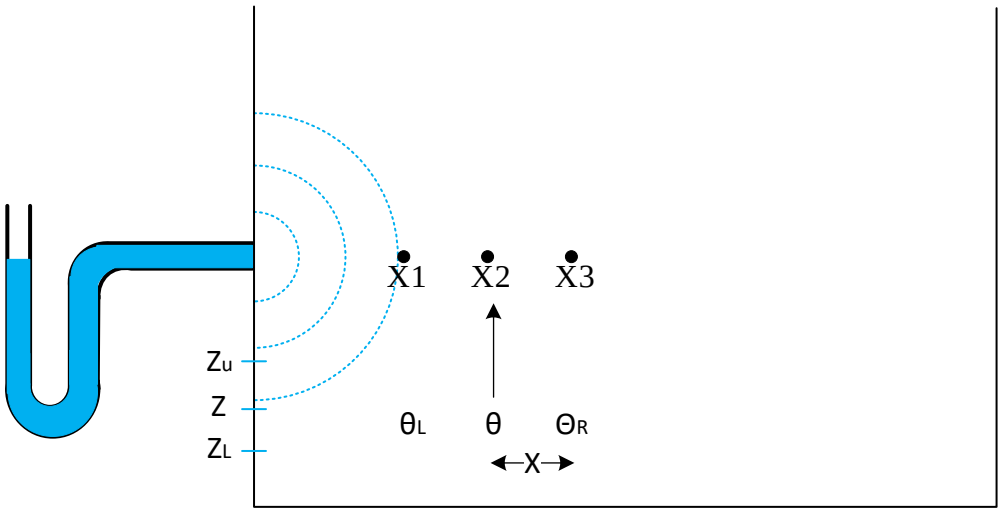

Figure 19: Early-stage design for the experimental setup. This drawing, while rudimental, provides a good visualization for the methods and potential sensor placement throughout the soil profile.

Therefore, the following experimental setup was developed to determine the parameters found in equations 48, 49, and 50. The thought process is displayed visually in Figure 19. The first attempt at measuring D was an approach that measured the change in moisture over time at specific positions in a soil profile. Figure 19 displays the initial setup for the first iteration of experimentation of measuring moisture content over time to acquire D. For measuring the soil water content over time, 5TM soil moisture (SM) sensor from METER Group (formerly Decagon Devices) in Pullman, Washington. Calibration curves were generated for each of the 5TM moisture sensors. Calibration of the sensors was determined by creating soil samples with known volumetric water content and then taking readings from the SM sensors for each of the different soil samples. The known values were then plotted against the measured values, and curves + equations were generated, allowing for adequate adjustment of the measured values. The 5TM sensor can log at regular intervals ranging from 1 min to 1 time per day. These sensors are commonly used in the field and have since been upgraded to newer products developed by METER Group. These moisture sensors are roughly 5 cm long and 0.693 cm in width. The

sensors are attached to a data logger through a jack connection. The sensors required spacing of 2.54 cm in order to not interfere with the readings of adjacent sensors. This requirement is consistent in both vertical and horizontal directions. The size of these moisture sensors and the placement requirements were design constraints when manufacturing the soil box or profile. It was desirable to obtain the flow of moisture throughout a soil profile in multiple directions. This leads to sensors needing to be placed in x, y, and z directions. Water would then need to be introduced into a central point in the soil profile, which could then account for flow above, below, and out from the point where water was introduced. This allowed for sensor placement in all directions, which was desired. Refer to Figure 19 for the basic experimental setup. To account for the initial design constraints and multiple sensors scattered throughout the soil profile, a box was chosen as the soil profile. Water would be introduced into the soil profile in a central location, and the sensors were placed evenly throughout the soil profile. The box was constructed out of wood and plexiglass. The plexiglass allowed for visual inspection of water entering the soil profile. The wood and plexiglass were laser cut and glued together. Waterproof silicon was used to ensure that there were not any leaks out of the box. Multiple coats of

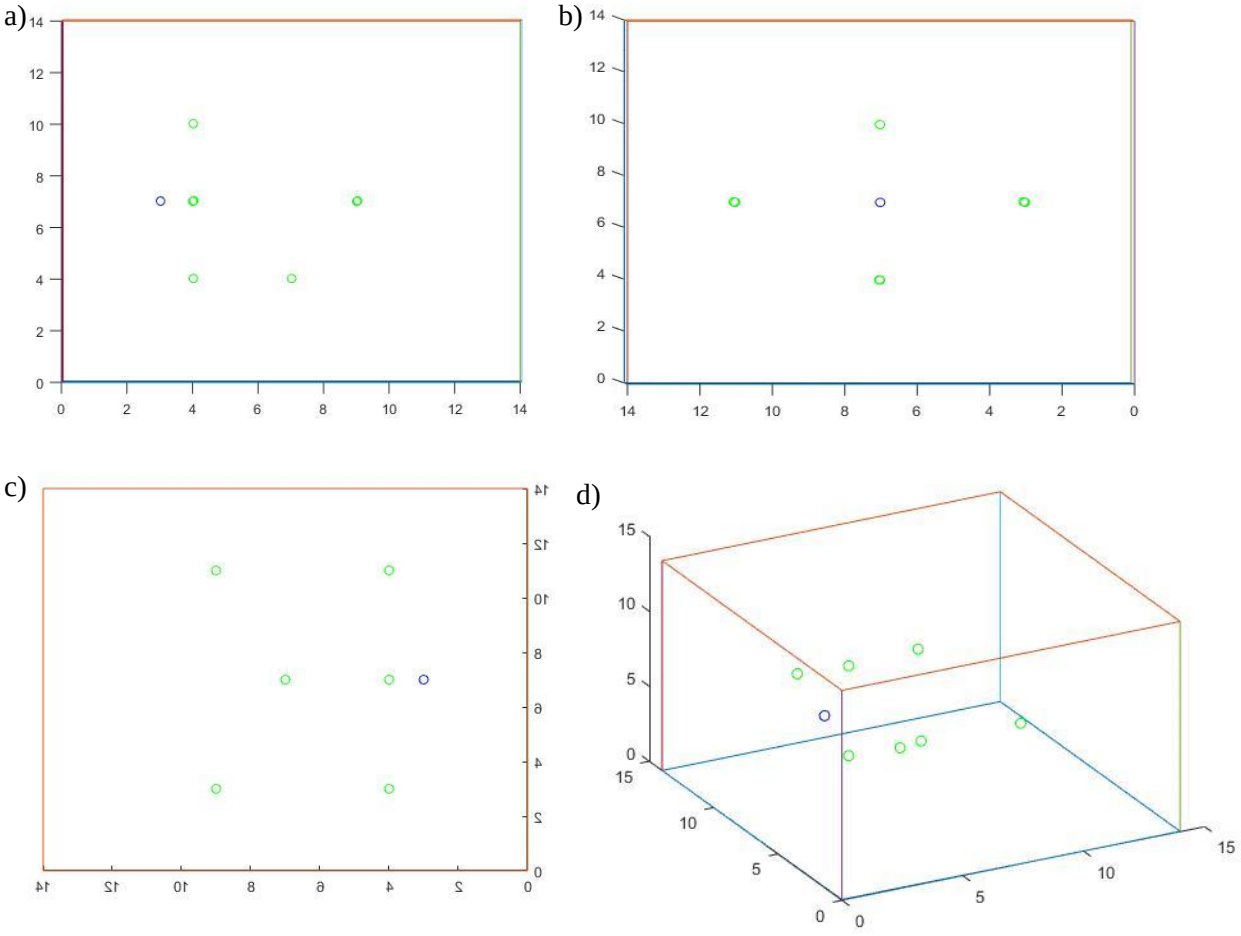

Figure 20: Layout of the Diffusivity box and sensor placement evenly distributed throughout the box, a) Side view. b) Rear view. c) Top View. d) Angled view. The blue circle indicates the point where water was introduced into the soil profile, and green circles indicate the presence of a soil moisture sensor.

polyethylene wood finish were applied to the wood portions of the box to ensure the wood was water-resistant. These portions were A concern in designing the setup was that introducing the water directly on the side of the box would create boundary effects between the opening of the water outlet, the walls of the box, and the soil directly in front of the box. This concern led to shifting the outlet pipe for water further into the soil profile, approximately 5.08 cm in front of the wall of the box. Furthermore, there was concern regarding the backflow of soil particles into the water outlet, which was solved by adding mesh to across the opening of the pipe. This would restrict particle backflow without restricting water entering the soil. The last major design constraint involved the need for constant head pressure (referred to as constant head from this point on) throughout the experimentation. Additionally, it was desired that head was not a driving force for water movement through the soil (only the soil hydraulic properties in question and gravity). Therefore, the construction of the experiment should be built with minimal head pressure in mind. Therefore, the design required float sensors to ensure that the flux of water into the system was constant and therefore not a factor in the rate in which water moved throughout the system. Small float sensors for an aquarium were used to the water level in a reservoir at roughly the same level (the sensor had roughly 1 cm difference in the height of water from the time the sensor was triggered to fill the water reservoir and filling stopped). This error in the water level was deemed to be

Figure 21: Constructed experimental setup. Box filled with soil and sensors dispersed throughout the box according to figure 19. Water reservoir filled and float sensor inserted at depth for minimal constant head pressure. Saturation zone on right picture is isolated to the level of the water pipe and below indicating that gravity is primarily driving water down into the soil

insignificant and therefore was ignored. In the derivations of the equations, the osmotic potential was deemed negligible and therefore was ignored. To saturate the soil DI water was used to ensure that, in fact, osmotic potential could be neglected from the calculations. The first sensor was placed 1 cm from the water outlet spout. Based on the placement of the first sensor and the sensor specifications, the sensors were placed based on the outline presented in Figure 20. This figure displays soil moisture sensors evenly distributed throughout the soil profile which would record the change in moisture over time. It is important to note that the sensors will monitor the change in soil moisture in various directions, which was desired. The completed experimental setup and a test run of the experiment is shown in Figure 21.

The experiment was tested for multiple runs of the same sample and then re-assessed for effectiveness and feasibility. During the re-assessment of feasibility limitations and concerns regarding the design setup would require addressing prior to complete experimentation. Firstly, the sensor placement was rigid in theory (every sensor had a precise spot it was supposed to be placed) but in practice ensuring correct placement of each sensor to minimize error was difficult. The sensors are most effective when inserted into the soil profile tangentially to the soil, ensuring the sensor is held in place and does not move from the original placement. With a box designed with rigid sides without holes, there was no effective way to consistently insert the SM sensors each trial run. This forced the sensors to be placed when the box was being filled and placed on top of the soil service or inserted to an approximate depth when filling. This created significant potential for error to occur between each of the runs affecting the output from equation 50. In the experiment's current state, the error would be difficult to minimize and potentially cast significant doubt or error in the results that could be obtained from the experiment.

Another limitation of this experimental design was in the packing of the soil when setting up the experiment, which would further create error in the data. The amount of soil required to create an adequate volume for the sensors to be placed lead to a significant amount of soil and consequentially packing. It was necessary to pack the soil placed into the box due to the role bulk density plays in soil hydraulic properties and soil-water relationships. It was desired to be as representative as possible to the field environments despite being in a laboratory setting. One method of achieving this is to attempt to pack the soil in such a manner that it achieves a desired bulk density that mimics, or is close to, the bulk density that is measured and reported from the field. This would reduce some of the inconsistencies that a varied bulk density would have on water movement. The volume of the box and the design constraints from the sensors required a significant volume of soil to be used for each run of the experiment. With a large volume of soil, it was difficult to achieve consistent packing throughout the soil profile and between each run. Even with a consistent packing procedure, the time it would take to ensure that the soil in the box was evenly packed was extensive (adding small amounts of soil at a time and packing the soil together). While, in nature, the bulk density of a soil may vary throughout the profile due to earthworm holes, rocks, and other aggregates, the overall bulk density of the soil will primarily be consistent. In the soil box, the inconsistencies created during packing would create pockets of loose soil and pockets of dense

soil, which would drastically impact where water would move through the profile. Water would move slower through denser areas of the soil, while it would move faster through loosely packed areas. Therefore, the sensors would have different readings between replicates of the same sample due to the variation in packing between runs. Additionally, there were boundary effect concerns regarding backflow of water towards the rear wall (behind and beneath the water inlet to the soil). It was difficult to pack the soil around the pipe to a similar bulk density as the rest of the sample. This would further increase the variability in bulk density throughout the profile, creating inconsistent flow patterns throughout the profile. The inconsistencies in flow would create variation in the measurements between runs, which was not ideal. This phenomenon was consistent for areas of soil near the corners of the box.

The final limitation that was documented with this approach was knowing when the experimentation was completed. Given the volume of soil used, placement of the sensors (in the soil profile), and the variation in the bulk density it was difficult to visually inspect when each of the sensors were saturated and the experiment was completed. An obvious counter to this would be to simply let the entire box saturate; however, this would extend the duration of experimentation by days and create significant clean-up, which was not ideal. The issues together created measurement uncertainty that was difficult to ignore, leading to the investigation of other experimental setups to determine the diffusivity of different soil samples.

Diffusivity Experiment 2: 1-dimensional soil column

The second experimental design was also based on equations 48, 49, and 50. Experiment 2 was a simpler design that analyzed the change in moisture over time in one direction, which utilized a 1-dimensional soil column and monitored the flow through said soil column. This experiment primarily relied upon work by Villarreal et al. 2016, which analyzed water flow through a horizontal soil column to measure diffusivity (Villarreal et al., 2016). Water flow through a soil profile in a horizontal direction is determined by Richard's equation. According to Villarreal et al., 2016 Richard's equation for horizontal water where the gravitational component of Richard's equation can be neglected, with space coordinate x and time t is given by:

$$\frac{\partial \theta}{\partial t} = \frac{\partial}{\partial x}\left[D(\theta)\left(\frac{\partial \theta}{\partial x}\right)\right] \quad [51]$$

Where $\partial\theta/\partial t$ is the change in moisture content over time, $\partial\theta/\partial x$ is the change in moisture content based on the change in position, and $D(\theta)$ is the soil water diffusivity as a function of water content (Villarreal et al., 2016). Further, Villarreal et al., showed that using a Boltzmann transformation of $l = l(q)$, the partial differential equation of diffusivity can be transformed into an ordinary differential equation given by:

$$\lambda = x t^{-\frac{1}{2}} \quad [52]$$

Where l is a function of q moisture content, x is position, and t is time. The Boltzmann transformation of equation 52 assumes that moisture content is a single-valued function of l only. Assuming diffusivity agrees with Darcy's law for unsaturated flow, combining equations 51 and 52 yields the following:

$$D(\theta) = \left(\frac{1}{4}\right)\left(\frac{x_i^2}{t^{\frac{3}{2}}}\right)\left(\frac{dt}{d\theta}\right)\int_{\theta_i}^{\theta}\left(\frac{1}{\sqrt{t}}d\theta\right) \quad [53]$$

Where is θ_i the initial water content, x_i is the fixed position at which water content is being measured, and all other variables are the same as previously presented. A more complete derivation of diffusivity from Richard's equation, the derivation displayed above, is found in "Soil water diffusivity: A simple laboratory method for its determination" by Villarreal et al, 2016 (Villarreal et al., 2016). Theoretically, equation 53 will be valid for most conditions where significant solute-water particle interactions do not exist. The conditions in which our experimentation occurred was determined to be sufficient conditions for equation 53 to be applied.

Figure 22: Completed setup of 1-dimensional soil column experiment. Sensors are inserted and float sensor maintains constant head pressure

The 1-dimensional soil column was constructed using 6 in. clear plastic pipe. One end of the device was capped with a 6 in. PVC solid endcap. A threaded adapter was attached to the other end of the column, allowing for an end cap to be screwed on tightly. This allowed for access into the soil column on one end. The screwed endcap is slightly curved, which created issues with packing the soil. Therefore, a plexiglass circle was plasma cut (holes were drilled into it) and attached to the inside of the cap. This mitigated the issues of packing the soil into the column. To ensure that water would be able to horizontally infiltrate into the soil evenly across the whole cross-section of the soil profile, circular pieces of felt were added to both ends. These felt pieces would absorb water initially and create differences in potential between the wet felt and the dry soil. Water could then move into the soil across the entire cross-section, evenly distributing water across the cross-section. In the side of the clear tubing, 3 holes were cut for sensors to be inserted. Sensors were spaced 3.81 cm apart (nearest edge of one sensor to nearest edge of the other sensor). Lastly, the flexible tubing was attached to both ends of the soil column, which allowed for water to enter the system from a reservoir container and exit the system in a catch basin. The finished setup for the 1-dimensional soil column is displayed in Figure 22.

Akin to the previous experimental design, DI water would be used. Water would be introduced into the soil laterally with minimal head pressure. It was desired that water would not be forced into the soil and would rather diffuse naturally, with matric potential being the primary driving force. The same float sensor as the

previous experimental setup was used to maintain constant head pressure. Water content over time was measured at three fixed positions in the soil sample by 5TM moisture sensors (from METER group in Pullman, Washington). The experiment occurred until the moisture contents in each of the sensors reached equilibrium. This was determined through visual inspection of the wetting front through the clear plastic tubing. If someone were concerned enough and time of experimentation was not a primary factor, researchers could leave the system to saturate completely, in which case water would steadily leave the system into the catch basin, indicating saturation. This would be analogous to the constant head permeameter experimental design for measuring the saturated hydraulic conductivity (K_{sat}) of soil samples (Reddy, 2021).

Comparing to the previous method, it was much more functional and sufficient for determining the diffusivity of soils. The system required less soil sample, water, and less time. The duration of the experiment remained roughly a day for saturation to occur. Additionally, there were minimal design constraints regarding the experimental setup that hindered functionality. Sensors could be placed in the same location in the soil profile, reducing variability. Consistency in procedure and testing were increased greatly with this experimental setup. Determining an equation that incorporated a head component would have been helpful in shortening the testing duration, making this setup more feasible. This testing method and data manipulation worked adequately and was in the long-term plans for measuring the diffusivity of different soils with and without biochar amendment until other more complete methods came into the fold. As briefly discussed in the theory section, the measurement of the WRC and using Van Genuchten equations and Darcy's law were deemed more appropriate for determining when the methods were known at this stage in the research.

Hydraulic Conductivity Experiment 1: Constant head permeability

At this stage in the research pathway, it is important to touch on measuring the hydraulic conductivity of soil. The 1-dimensional soil column was at a stopping point due to receiving information regarding the desired method for experimentation from another professor. Prior to this knowledge being acquired, measuring the hydraulic conductivity of soils with and without biochar was required for the redistribution model. A common laboratory experiment in soil labs, constant head permeability test or constant head test, was determined to be the first experimental setup for measuring the hydraulic conductivity of soil samples. The constant head permeability test relies on Darcy's law for the flow of water through porous media, which can be simplified to the following:

$$K = I * V \quad [54]$$

Where K is the coefficient of permeability or hydraulic conductivity, I is the hydraulic gradient, and V is the volume of fluid through the profile. The constant head permeability test relies on this equation to solve for K. The constant head permeability test is primarily for coarse-textured soils that contain significant of sand or resemble sand. Generally, the soil sample is held in a column, and water is introduced through the soil profile from the top. Eventually, the system will reach equilibrium, and water will be flowing through the soil profile at a constant rate. The rate is recorded, and then equation 54 can be solved. It is important to note that the hydraulic gradient or hydraulic head pressure and the water supply in this experiment needs to remain constant

throughout. This method provides the measurement of K in saturated conditions for coarse-textured soils and is an important parameter in soils. For more information regarding this method, refer to (Maupin Jr., 2000a) or (Tech limited, 2021a).

Hydraulic Conductivity Experiment 2: Falling head method

The falling head method is similar to the constant head permeability test, but it is for finer textured soils. It relies on a similar theory to acquire similar measurements, however, in this test, the head pressure from the water is not constant and will diminish over time. Water is introduced to the top of the soil column, and the volume of water passing through the cell is measured. For more information regarding this specific test, refer to (Maupin Jr., 2000b; Tech limited, 2021b).

Chosen Approach – HYPROP from METER Group

The previously mentioned experiments were all discussed and/or potential options for the measurement of the necessary parameters for modeling. These experiments were at various stages up until the final method was determined (ranging from completed/tested to theoretical and not yet constructed). However, new information was acquired that proved instrumental, which was then chosen as the method for the duration of the data collection portion of the thesis. The method that was primarily used was the HYPROP from METER Group in Pullman, Washington. As previously mentioned, measuring the water retention curve is one approach that would lead to the desired measurements for different soil samples. This approach was not known until knowledge regarding the HYPROP became known. The HYPROP was chosen for the benefit of being able to measure key points along the water retention curve. For comprehensive documentation of the HYPROP and methods for use, refer to previous chapters of this thesis or the Hyprop manuals (METER group, 2015). The HYPROP operates under the theory proposed by Dr. Schindler for simple evaporation from a confined soil sample. The evaporation method is commonly used to measure hydraulic functions in unsaturated soils (Schindler et al., 2010). This method provides measurements of the water retention curve and the hydraulic conductivity functions. The HYPROP measures these functions and then allows for the fitting of different soil hydraulic models along the measured values to provide an estimate of the water retention curve along all tensions. The HYPROP allows for fitting the measured values with Brooks-Corey, Fredlund-Xing, Kosugi, or the Van Genuchten-Mualem ($m = 1 – 1/n$). For this thesis, the traditional constrained Van Genuchten-Mualem ($m = 1 – 1/n$) model, which is frequently used throughout research, was chosen to fit the data, which fit the measured values adequately.

Lessons learned from the HYPROP

Despite the flexibility of the HYPROP (being able to fit measured values with multiple models), the device has a learning curve regarding setup procedures. An important aspect of the device is ensuring that the device is degassed adequately, which can take 24 hours. If the device (HYPROP base and tensiometers) is not degassed properly, the measurements that the system makes may be off. However, it appeared that the device is robust in handling poorly degassed components, and the measured values did not show the need for re-evaluation. An important consideration when using the HYPROP was that it is primarily used to measure points on the water

retention curve where there is a significant release of water from the soil (the middle of the curve). Pairing the HYPROP with a WP4 dew point potentiometer which allows for measurement on the dryer sections of the WRC (near PWP), generates measurements with a higher degree of resolution. Another important consideration regarding the HYPROP regards the measurement of hydraulic conductivity from the device. When determining the hydraulic conductivity of the soil sample, the HYPROP does not have direct measurements for the conductivity. This leads to an estimation of the conductivity of the soil rather than a direct measurement. Therefore, it will only catch the general trend of how the hydraulic conductivity changes with water content and tension and not the actual values. If measured K_{sat} values were determined externally, then inputting those values for the soil samples would act as an anchor point for the conductivity. This would increase the accuracy of the values obtained from the HYPROP.

The direct measurement of hydraulic conductivity was discussed in the previous section. This discrepancy between the measurements has two options for determining the Ksat values: pedotransfer functions (PTF's) and direct measurement. Pedotransfer functions are equations or sets of equations that utilize soil properties to estimate soil hydraulic properties or other characteristics about soils. These functions often rely on soil texture characteristics (%silt, %clay, %sand), organic matter, bulk density, field capacity, and permanent wilting point. The United States Department of Agriculture (USDA) has developed a program to estimate desired soil hydraulic properties using PTF's. This program is found as a neural network called Rosetta, which can be found in HYDRUS 1-D, which is another USDA program. This neural network was used for estimating the K_{sat} values from different soil properties in a hierarchical approach (Schaap et al., 2001).

Literature Cited

Hillel, D. (1998). *Environmental Soil Physics* (A. . Warrick, R. S. Baker, & C. Rosenzweig (eds.); First). Academic Press.

Maupin Jr., G. W. (2000). *Investigation of Test Methods, Pavements, and Laboratory Design Related to Ashphalt Permeability* (Issue 1645). http://www.virginiadot.org/vtrc/main/online_reports/pdf/Microsoft Word - 00R24.pdf

Mcmillan, M. (2012). *Water movement and retention: Effects of soil on water movement and retention* (Issue April). http://www.missouricareereducation.org/doc/soilsci/SRLesson10.pdf

METER group. (2015). *Operation Manual for HYPROP*. http://library.metergroup.com/Manuals/UMS/Hyprop_Manual.pdf

Mualem, Y. (1976). *A New Model for Predicting the Hydraulic Conductivity of Unsaturated Porous Media*. *12*(3). https://agupubs.onlinelibrary.wiley.com/doi/epdf/10.1029/WR012i003p00513

Or, D., Tuller, M., & Wraith, J. M. (2009). *Agricultural and Environmental SOIL PHYSICS*.

Reddy, K. (2021). *Experiment 10 Permeability (Hydraulic Conductivity) Test Constant Head Method*. http://www.uic.edu/classes/cemm/cemmlab/Experiment 10-Permeability.pdf

Schaap, M. G., Leij, F. J., & Van Genuchten, M. T. (2001). Rosetta: A computer program for estimating soil hydraulic parameters with hierarchical pedotransfer functions. *Journal of Hydrology*, *251*(3–4), 163–176. https://doi.org/10.1016/S0022-1694(01)00466-8

Schindler, U., Durner, W., von Unold, G., & Muller, L. (2010). *Evaporation Method for Measuring Unsaturated Hydraulic Properties of Soils : Extending the Measurement Range*. *74*(4), 1071–1083. https://doi.org/10.2136/sssaj2008.0358

Tech limited, V. (2021). *Introduction to Permeability Testing*. https://www.vjtech.co.uk/blog/introduction-to-permeability-testing

Van Genuchten, M. T. (1980). A Closed-form Equation for Predicting the Hydraulic Conductivity of Unsaturated Soils. *Soil Science Society of America Journal*, *May*. https://doi.org/10.2136/sssaj1980.03615995004400050002x

Villarreal, R., Lozano, L. A., Soracco, C. G., Filgueira, R. R., & Sarli, G. O. (2016). Soil water diffusivity : A simple laboratory method for its determination. *Water Resources and Irrigation Management*, *3*, 15–21.